IDENTIFICATION AND QUANTIFICATION OF IMPURITIES IN ZIRCON, PDZ AND OTHER RELEVANT ZIRCONIUM PRODUCTS

by

Steven James Lötter

A thesis submitted in fulfillment of the requirements for the degree of

Magister Scientiae

Department of Chemistry, University of the Free State

November 2008

Supervisor: Prof. W. Purcell

Co-supervisors: Dr J.T. Nel and Dr I.M. Potgieter

CONTENTS

LIST OF FIGURES

LIST OF TABLES

ACKNOWLEDGMENTS

I would hereby like to thank all those people and entities involved in the research presented herein, these being:

Prof. W. Purcell, my supervisor, for his guidance and assistance.

Dr. J.T. Nel and Dr. I.M. Potgieter, my co-supervisors, for their valuable insight and knowledge of the field.

The South African Nuclear Energy Corporation Limited (Necsa) for their funding and assistance throughout the course of the project.

The Advanced Metals Initiative (AMI) for initiating this project.

The personnel of the Department of Chemistry at the University of the Free State for their support and help.

My mother, Mrs N.J. Lötter, for her excellent grammatical and language editing.

Steven Lötter

Key Words

Zircon

Mineral

Digestion

Zirconium

Hafnium

Analysis

Determination

Quantification

Trace

Impurities

Fusion

Microwave

SUMMARY

The purpose of this study was to develop suitable analytical methods for the analysis of zircon, plasma dissociated zircon and other zirconium compounds. ICP-OES was used as primary analytical technique. Due to the chemical inertness of these compounds, several dissolution techniques were investigated and their suitability tested in terms of percentage recovery with respect to a certified reference standard. The standard addition method, using a flux fusion sample preparation, was used to analyse for both major and minor elements with a zircon ore matrix. The method shows a high degree of linearity in its calibration curves as well as an acceptable level of precision for most elements considering the matrix involved. Accuracy was obtained for the zirconium (102%), hafnium (131%) and titanium (118%) with these results being within the ranges set out in the objectives. Other elements show lower levels of accuracy, especially for silicon, it being outside the 4-6% acceptable range, which illustrates the difficulty of analysing zirconium silicate samples. The deviations from the expected recovery for the minor components are less severe than they appear, as they are present only in minute amounts. The flux fusion method shows the most promise with regard to a viable analytical method, its major advantage being the complete digestion of the sample without the loss of silicon content; theoretically, it is also able to ignore all matrix effects.

An alternative method making use of microwave-assisted acid extraction was also investigated. The success of this method is highly dependent upon the digesting media, and the best results were obtained with fluoride-containing substances. This method has the potential of being a purifying step, capable of removing all silica from the zirconium and other metals by an iterative process of extractions and plasma dissociations. Further refinement in the microwave-assisted extraction method is recommended.

OPSOMMING

Die doel van hierdie ondersoek was om geskikte analitiese metodes vir die analise van sirkoon, plasmadissosieerde sirkoon en ander sirkoniumprodukte te ontwikkel. IGP-OES is gebruik as primêre analitiese tegniek. As gevolg van chemiese onaktiwiteit van sekere van hierdie verbindings is verskeie oplossings-tegnieke ondersoek, asook die geskiktheid daarvan ten opsigte van persentasie herwinning met betrekking tot 'n gesertifiseerde verwysingstandaard. 'n Standaard byvoegingsmetode, wat 'n vloeimiddelsmelting monstervoorbereiding behels het, is gebruik om vir beide makro- en mikro-elemente in 'n sirkoonertsmatrys te analiseer. Die metode openbaar 'n baie hoë graad van lineariteit van al sy kalibrasiekrommes, sowel as 'n aanvaarbare vlak van presisie vir alle elemente, veral as die betrokke matrys in ag geneem word. Akkuraatheidswaardes vir sirkonium (102%), hafnium (131%) en titaan (118%) is verkry, en hierdie waardes voldoen aan die bestek soos uiteengesit in die doelwitte. Ander elemente het laer waardes ten opsigte van akkuraatheid getoon, vir silika in die besonder, aangesien hierdie waardes buite die 4 – 6% aanvaarbare bestek geval het, wat die moelikheidsgraad om sirkoniumsilikaatmonsters te ontleed, illustreer. Die afwykings ten opsigte van die verwagte herwinningswaardes vir die mikro-elemente is minder drasties as wat op sig voorkom, aangesien hulle slegs in baie klein hoeveelhede voorkom. Die vloemiddelsmeltmetode hou meeste belofte in met betrekking tot 'n haalbare analitiese metode, met die voordele van totale vertering van die monster, sonder verlies van silikoninhoud, en die vermoë om teoreties alle matryseffekte te kan ignoreer.

'n Alternatiewe metode wat van mikrogolfondersteunde suurekstraksie gebruik maak, is ook ondersoek. Die sukses van hierdie metode is baie sterk afhanklik van die verteringsmedium, en die beste resultate is met fluoriedbevattende media verkry. Hierdie metode het die potensiaal om te dien as 'n suiweringstap wat in staat is om alle silika vanaf die sirkonium- en ander metale deur 'n iteratiewe proses van ekstraksies en plasmadissosiasies te verwyder. Verdere verfyning van die mikrogolfondersteunde ekstraksiemetode word aanbeveel.

Chapter 1: Introduction and Objectives of this Study

1.1. INTRODUCTION[1,2,3]

Zirconium and hafnium are group IV transition elements, below titanium in the periodic table. Zirconium was first discovered by M.H. Klaproth in 1789 in Berlin, Germany, and isolated by J.J. Berzelius in 1824 in Stockholm, Sweden, while hafnium was discovered in 1932 in Norway by D. Coster and G. von Hevesey, using X-ray spectroscopy. The existence of hafnium up to this time was only predicted by the Bohr Theory which indicated that it should be associated with zirconium. This was found to be the case as zirconium ore is invariably contaminated by 1-3% hafnium.

Zirconium occurs naturally in the minerals zircon ($ZrSiO_4$) and baddeleyite (ZrO_2). Baddeleyite, which is a naturally occurring form of zirconia (ZrO_2), was the primary source of zirconium products and was recovered from the mining of the Palaborwa carbonatite in South Africa. This production ceased in 2003, and only small amounts of baddeleyite are currently produced from Kola in Russia.

Electric arc furnace treatment of zircon produces fused zirconia which is used mainly in ceramic pigment and opacifier manufacturing, while other zirconium products obtained from the chemical treatment of zircon are commonly used in applications as varied as drying agents, fire retardants, advanced ceramics, electronics and catalysts. These zirconias are also a key component of solid oxide fuel cells, a developing and important source of “clean” electricity.

---

[1]Gambogi , J., U.S. Geological Survey, Mineral Commodity Summaries, January 2008

[2] Zircon: Zircon Mineral information and data, http://www.mindat.org/min-4421.html, accessed 21/04/2008

[3] Chambers, I, The Dubbo Zirconia Project, June 2007

Recently hafnium has found use in microprocessors as part of a new alloy used by the micro-chip manufacturer Intel to replace silicon dioxide in their transistors. Previously the metal was only used in filaments, electrodes and nuclear control rods.[4]

Figure 1-1: Zirconium metal[5]

Zircon is the primary starting material used when making zirconium metal (seen in **Figure 1-1**). Zirconium metal exhibits a low thermal neutron capture cross-section as well a high resistance to corrosion which makes it ideal for cladding on fuel rods in nuclear reactors. It is essential to determine which impurities are present and to what extent since small impurities of elements such as hafnium, boron or cadmium will cause the zirconium metal to become unusable without further purification due to their extremely high thermal neutron capture cross-section (see **Table 1-1** for specifications for impurities in zirconium sponge). The high thermal neutron capture cross-section of hafnium makes it ideal to be used as control rods in nuclear reactors as it shares almost all of zirconium's other chemical attributes, such as its resistance to corrosion, which make zirconium an ideal material in reactor design. Unfortunately due to their similarity these two elements specifically are extremely difficult to separate which creates practical problems when preparing pure zirconium or hafnium for nuclear applications. In order for

[4] Markoff, J., http://www.nytimes.com, Intel says chips will run faster, use less power, January 7, 2007

[5] http://chemistry.about.com/od/periodictableelements/ig/Element-Photo-Gallery.--98/Zirconium.htm accessed on 09/15/2008

zirconium to be of use in a reactor, however, it is necessary for it to be alloyed with other metals to increase its mechanical strength. These alloys, known as Zircaloys, can contain one or many of the elements tin, iron, nickel, chromium and niobium.

Table 1-1: Standard specification for zirconium and zirconium alloy ingots for Nuclear Application[6]

	Maximum Impurities (Mass %)				
Element	UNS R60001	UNS R60802	UNS R60804	UNS R60901	UNS60904
Al	0.0075	0.0075	0.0075	0.0075	0.0075
B	0.00005	0.00005	0.00005	0.00005	0.00005
Cd	0.00005	0.00005	0.00005	0.00005	0.00005
Ca	---	0.003	0.003	---	---
C	0.027	0.027	0.027	0.027	0.027
Cr	0.02	---	---	0.02	0.02
Co	0.002	0.002	0.002	0.002	0.002
Cu	0.005	0.005	0.005	0.005	0.005
Hf	0.01	0.01	0.01	0.01	0.01
H	0.0025	0.0025	0.0025	0.0025	0.0025
Fe	0.15	---	---	0.15	0.15
Mg	0.002	0.002	0.002	0.002	0.002
Mn	0.005	0.005	0.005	0.005	0.005
Mo	0.005	0.005	0.005	0.005	0.005
Ni	0.007	---	0.007	0.007	0.007
Nb	---	0.01	0.01	---	---
N	0.008	0.008	0.008	0.008	0.008
P	---	---	---	0.002	0.002
Si	0.012	0.12	0.12	0.012	0.012
Sn	0.005	---	---	0.01	0.01
W	0.01	0.01	0.01	0.01	0.01
Ti	0.005	0.005	0.005	0.005	0.005
U	0.00035	0.00035	0.00035	0.00035	0.00035

[6] Standard Specification for Zirconium and Zirconium Alloy Ingots for Nuclear Application, B350/B 350M, ASTM International, 2006

1.2. THE MINERAL ZIRCON[7]

In ancient times zircon was known only as a gemstone and its identification was often suspect. Thus many historical references to zircon may not have been to the same material we identify as zircon today. However, thanks to its extraordinary index of refraction and the striking birefringence exhibited by the mineral it is quite likely that it was more often than not identified correctly. Different names have been used to refer to varying colours of zircon gems, some of these being *Matara diamonds* for the rare, colourless variety, *jargons* for pale, smoky and yellow zircons and *hyacinths* for the reddish-brown examples.

The basic crystalline structure of zircon is tetragonal and it is made up of alternating, edge-sharing SiO_4 tetrahedra and ZrO_8 dodecahedra. This is demonstrated in **Figure 1-2** and **Figure 1-3**.

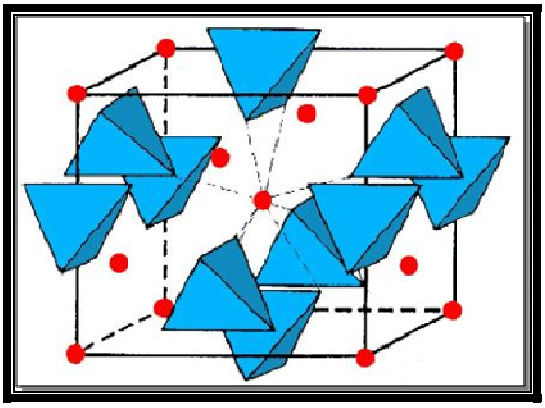

Figure 1-2: SiO_4 tetrahedra in zircon structure

[7] Blumenthal, W., B., The Chemical Behaviour of Zirconium, 1958

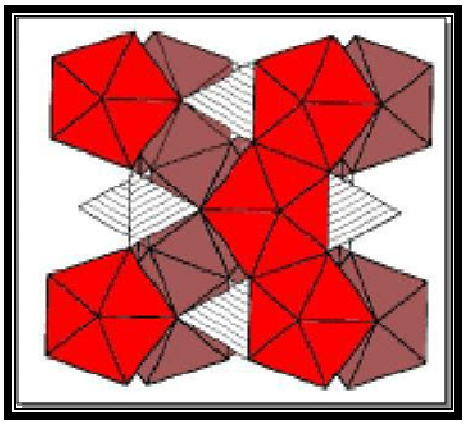

Figure 1-3: ZrO_8 dodecahedra in zircon structure

Today over 95% of world production of zirconia and zirconium chemicals comes from the processing of zircon. Zircon is generally a by-product of the mining of ilmenite and associated titanium minerals (from which it is magnetically separated), hence its availability is governed by the demand for titanium minerals. China currently dominates the world supply of processed zirconium products which is about 96,000 tons per year. The supply of hafnium is similarly linked to the titanium and zirconium industries as it is purified from zircon as starting material. The global production of zirconium concentrates has been steadily increasing over the past several years with prices for zircon concentrates increasing to record high levels in 2007. Global consumption of zircon has been forecast to increase by an average of 3% per year until 2015. As of 2007 several new mining operations have begun in Australia (Murray Basin, Tiwi Islands), Indonesia (Kalimantan), Mozambique (Moma) and The Gambia (Sanyang). Projects that are nearing completion include those in Australia (Keysbrook) and South Africa (Tormin). Projects are also being developed in Australia (Coburn Sands, Donald, Eucla Basin, and Murray Basin), Canada (Athabasca Oil Sands), India (Tamil Nadu), Kenya (Kwale), Madagascar (Fort Dauphin), Mozambique (Corridor Sands), Senegal (Grande Côte) and South Africa (Xolobeni). A breakdown of total worldwide production and reserves of both zirconium and hafnium can be seen in **Table 1-2**.

Table 1-2: Mine production and reserves of zirconium and hafnium[2]

	Zirconium				*Hafnium*	
	Mine Production		**Reserves**	**Reserve Base**	**Reserves**	**Reserve Base**
	(thousand metric tons)		**(million metric tons, ZrO_2)**		**(thousand metric tons, HfO_2)**	
	2006	2007				
United States	Withheld	Withheld	3.4	5.7	68	97
Australia	491	550	9.1	30	180	600
Brazil	26	26	2.2	4.6	44	91
China	170	170	0.5	3.7	NA	NA
India	21	21	3.4	3.8	42	46
South Africa	398	405	14	14	280	290
Ukraine	35	35	4	6	NA	NA
Other Countries	38	32	0.9	4.1	NA	NA
World Total (rounded)	1,180	1,240	38	72	610	1,100

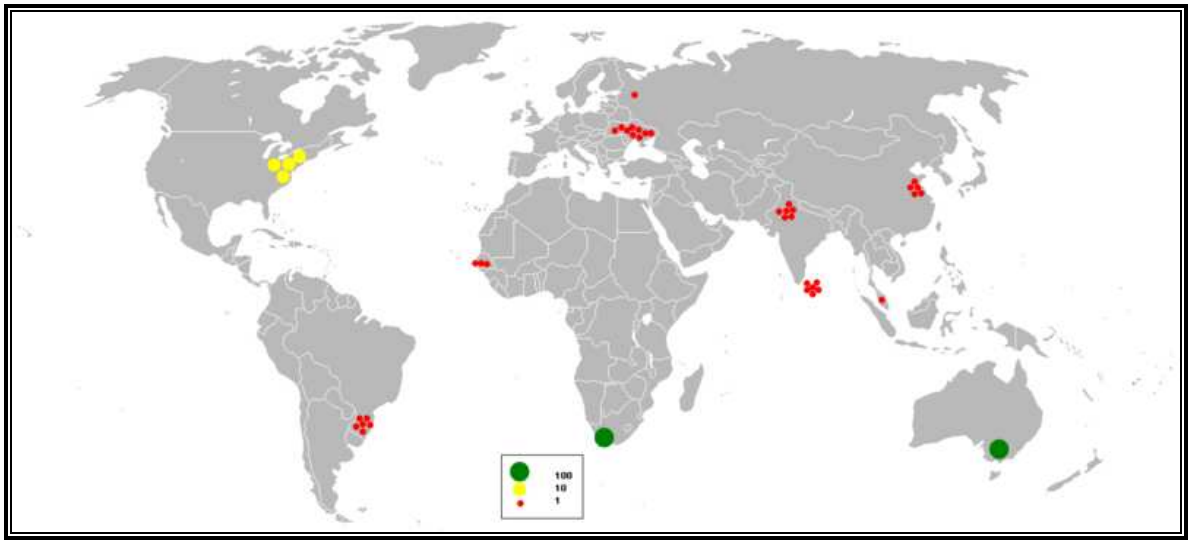

Figure 1-4: Map of active zircon mines with their output measured as a percentage of the top producer (Australia – 426,000 tons per year)[8]

[8] http://en.wikipedia.org/wiki/ Image:ZirconiumOutput.svg accessed on 16/05/2008

Figure 1-5: A cubic zirconia gemstone[9]

Zircon is a highly unreactive mineral and for this reason is often found as a constituent of some sands. Its colour can range from brown to reddish brown, colourless gray or green, and it has a prismatic or tabular crystalline form. It is found in most igneous rocks and some metamorphic rocks as small crystals or grains, usually widely distributed and rarely more than 1% of the total mass of the rock. It is also found as alluvial grains in some sedimentary rocks due to its high level of hardness. Due to its high index of refraction, crystals are also often used as gemstones (see **Figure 1-5**) when they are large enough. Zircon is also often found in the form of small crystals within diamonds and corundum.

1.3. CHEMISTRY OF ZIRCONIUM AND HAFNIUM[10,11,12,13]

One of the most important aspects of the chemistries of zirconium and hafnium is that they are more similar than any two other elements on the periodic table. It

---

[9] http://www.orleansjewels.com/cubic_zirconia_loose_stones.html accessed on 09/05/2008

[10] Wilkinson, G., Gillard, R.D., McClevery, J.A., Comprehensive Coordination Chemistry, Volume 3, 1987, pp. 364-440

[11] Cotton, F. A., Wilkinson, G., Advanced Inorganic Chemistry, 5th edition, 1988, pp. 776-787

[12] Monnahela, O. S., Advanced Metals Initiative (AMI) Project Literature Survey, Delta-F Department (Necsa), 22-11-2006

[13] McCleverty, J. A., meyer, T. J., Wedd, A. G., Comprehensive Coordination Chemistry II, Volume 4, 2004, pp. 105-175

was found that zirconium and hafnium do not form simple cationic species and their coordination chemistry is dominated by the 4+ oxidation state. Complexes with oxidation numbers of 0, 1+, 3+, 5+, 7+ and 8+ are known, but only a few complexes with the metals in oxidation states lower than 3+ have been isolated. The preference for the 4+ state is likely due to the ability of these elements to lose the 2 d and the 2 s electrons (four in total) to form the noble gas electron shell configurations for krypton and xenon respectively. According to valence electron theory atoms tend to gain or lose electrons in order to achieve the most stable outer electron shell with the least amount of gained or lost electrons. Zirconium and hafnium differ from titanium in that they appear to form more basic oxides, have a more extensive aqueous chemistry and more readily attain the 7+ and 8+ oxidation states. In spite of the fact that these metals have extremely limited chemistry in the 3+ oxidation state, this oxidation state is being dominated by MX_3 polymeric halide complexes (M = Zr or Hf and X = Cl^-, Br^- or I^-) which crystallizes in closely packed halide layers, with metal centres folded in between, in infinite succession. These structures are similar to those of the 4+ state as shown in **Figure 1-6**.

It is also interesting to note that, compared to other transition metals, relatively few zirconium and hafnium complexes have been characterised. The most well known and best characterised are the *tetrakis,* coordinated halides and ligands containing oxygen or nitrogen donor atoms. Research has shown that the known complexes of zirconium and hafnium show a great diversity in coordination geometries. Complexes with metal-oxygen bonds are the most commonly known with metal-halide and metal-nitrogen complexes following in that order. A very few complexes are known with arsenic, phosphorus or carbon bonding atoms. This similarity is attributed to the effect of lanthanide contraction resulting in bond lengths of similar complexes being almost identical. An example of this is given in **Figure 1-7** and **Table 1-4** where the structure and physical properties of the analogous zirconium and hafnium complexes with the structure of $[MCl\{N(SiMe_3)_2\}_3]$ are reported. Other zirconium and hafnium analogues, such as $[MCl_2\{N(SiMe_3)_2\}_2]$ and the $M_{4-y}X_y$ (where M = Zr/Hf and X = acetyl acetone)

series show much the same level of similarity. Due to this extreme similarity in the properties of the two metals, separation procedures must take advantage of small differences in solubility of the metal complexes in various solvents, such as methyl isobutyl ketone (MIBK)[14], to progressively separate these elements by repeated extractions. Thermo-chemical data seems to indicate that the hafnium bonds are slightly stronger in some cases than the corresponding zirconium bonds which allow for the successful separation of these two elements.

Table 1-3: Properties of zirconium and hafnium

Property	Zirconium	Hafnium
Atomic radius	1.45 Å	1.44 Å
Ionic radius	0.86 Å	0.85 Å
Melting Point	1855 ^{o}C ±15 ^{o}C	2222 ^{o}C ±30 ^{o}C
Standard atomic weight	91.224(2) g·mol^{-1}	178.49(2) g·mol^{-1}
Electron configuration	[Kr] 4d^{2} 5s^{2}	[Xe] 4f^{14} 5d^{2} 6s^{2}
Electronegativity (Pauling scale)	1.33	1.3
Ionization energies (kJ·mol^{-1})	1st: 640.1 kJ·mol^{-1}	1st: 658.5 kJ·mol^{-1}
	2nd: 1270 kJ·mol^{-1}	2nd: 1440 kJ·mol^{-1}
	3rd: 2218 kJ·mol^{-1}	3rd: 2250 kJ·mol^{-1}
Thermal Neutron Capture Cross Section	0.184 Barns (10^{-24}cm)	104 Barns (10^{-24}cm)

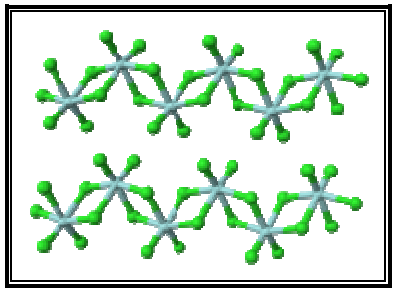

Figure 1-6: Polymeric structure of zirconium(IV) and hafnium(IV) chloride

[14] United States Patent 5176878

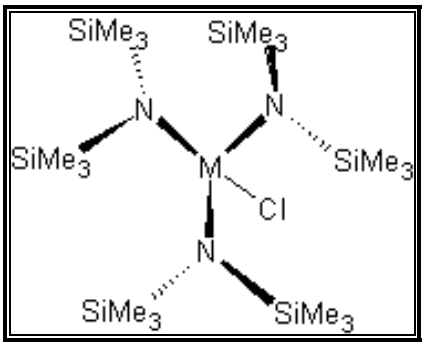

Figure 1-7: Structure of $[MCl\{N(SiMe_3)_2\}_3]$ where M = Zr/Hf

Table 1-4: Selected properties of $[MCl\{N(SiMe_3)_2\}_3]$ where M = Zr/Hf

M	M.P.(ºC)	ν(M-N) (cm^{-1})	ν(M-Cl) (cm^{-1})	^{1}H (NMR) (Hz)	^{13}C (NMR) (Hz)	M-Cl (Å)	M-N (Å)
Zr	182-183	408, 400	348	0.67	6.15	2.394(2)	2.070(3)
Hf	180-181	404, 388	338	0.62	6.38	2.436(5)	2.040(10)

Both zirconium and hafnium dissolve readily in hydrofluoric acid to form fluoro complexes in solution. Zirconium metal burns in air at sufficiently high temperatures but appears to react more rapidly with the nitrogen component than with the oxygen, giving a mixture of zirconium nitride, oxide and oxide nitride products.

Though they exhibit a greater range of aqueous chemistry than titanium, zirconium and hafnium's aqueous chemistry is not extensive due to the common 4+ oxidation state and is easily hydrolysed into polymeric compounds. Zirconium forms the $[Zr_4(OH)_8(H_2O)_{16}]^{8+}$ species[11] upon hydrolysis at high pH while the Zr(IV) species occurs at low pH and low zirconium concentrations only. As yet no ZrO_2^+ species has been convincingly identified. It also well-known that zirconium and hafnium form many basic salts including sulphates, chromates and perchlorates. Of these the sulphates are the most common, forming polymeric complexes with the sulphate acting as bridging bidentate, tridentate and tetradentate ligands. It was also found that the bidentate chelating ligands react with the zirconium and hafnium to form iso-structural complexes.

The most synthetically useful complexes of zirconium and hafnium are the tetrahalides. These act as precursors to the pure metal as well as starting material in most synthesis procedures. These compounds, MCl_4, MI_4 and MBr_4, exist as tetrahedral monomers in the gas phase but form polymeric solids with bridging halides. $ZrCl_4$ is a white solid which sublimes at 331^oC and has a structure similar to that of its titanium analogue, $TiCl_4$.

1.4. CHEMISTRY OF ZIRCON[15,16]

The most striking feature of zircon as mineral is its stability and lack of reactivity towards most reagents as illustrated by the fact that is present in sea sand which is mainly derived from the weathering of granitic and pegmatitic rocks. The inertness of the mineral and the difficulty of isolating zirconium with a high degree of purity are attributed to the resistance of the oxides to reduction, the high melting point of the metal and the ease with which the reduced metal reacts with other substances.

Extraction of the zirconium from the mineral is difficult and the first step in the process is the necessity to pulverize the mineral to a fine state of subdivision. The treating of the mineral with hot sulphuric acid, hydrochloric acid or aqua regia only succeeds in removing the iron from the mineral, with the zirconia remaining unaffected. One of the processes in which zirconium metal can be produced from zircon ore or baddeleyite is through a carbochlorination reaction process which is then followed by the reduction of the tetrachloride salt with magnesium.

$$ZrO_2 + 2Cl_2 + 2C \xrightarrow{\Delta} ZrCl_4 + 2CO \qquad (900^oC)$$

$$ZrCl_4 + 2Mg \xrightarrow{\Delta} 2MgCl_2 + Zr \qquad (1100^oC)$$

[15] Mellor, J. W., A Comprehensive Treatise on Inorganic and Theoretical Chemistry, Volume VII, pp.106-109

[16] The Economics of Zirconium, Roskill Information Services Ltd., ISBN 978 0 86214 538 5

A similar method can be employed for the extraction of zirconium from zircon ore instead of baddeleyite. Otherwise the steps are identical with the addition of a separation phase to remove the silicon tetrachloride.

$$ZrSiO_4 + 4Cl_2 + 4C \xrightarrow{\Delta} ZrCl_4 + SiCl_4 + 4CO \qquad (900^oC)$$

Another method of extracting zirconium from zircon ore is the caustic fusion of the zircon mineral and subsequent treatment with hydrochloric acid to form the oxychloride, which is then washed with water to remove silicates. This product can then be converted to the sulphate, the carbonate or other forms of the mineral.

The extremely chemically inactive zircon ore ($ZrSiO_4$) is also sometimes pre-treated in order to convert it to a chemically more amenable form. Such treatment greatly increases its reactivity towards more common reagents and the process increases the efficiency of raw ore processing. This can be achieved by heating the ore to more than 1500ºC in an arc plasma furnace or similar plasma heating method resulting in the separation of the zircon into a mixture of ZrO_2 (zirconia) and SiO_2 (silica).

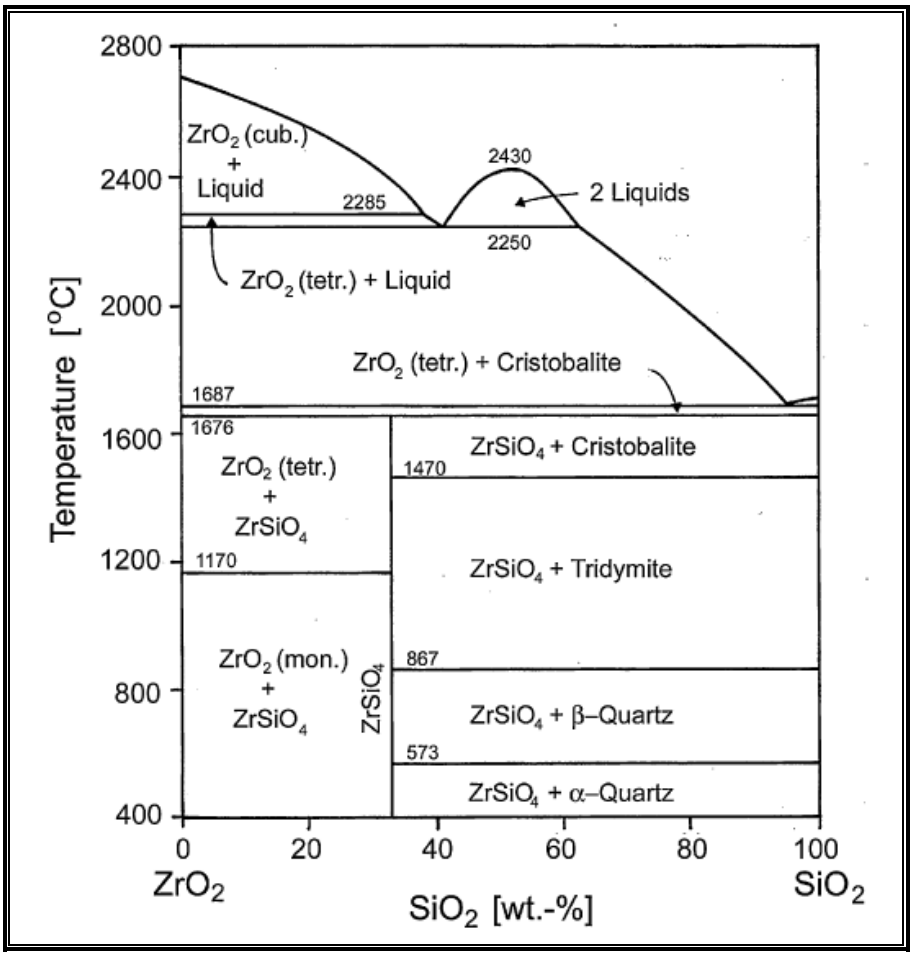

Figure 1-8: The ZrO_2–SiO_2 phase diagram[17]

$$ZrSiO_4\ (ZrO_2SiO_2) \xrightarrow{1800^oC\ Plasma} ZrO_2.SiO_2$$

(Zircon) (Plasma Dissociated Zircon)

During this heating process the zirconia's crystal structure changes from a dodechahedron (see **Figure 1-3**) to tetragonal and eventually it also melts which is illustrated by the phase diagram for zircon (see **Figure 1-8**). The liquefied product is

[17] Kaiser, A., Lobert, M., Telle, R., Thermal stability of zircon ($ZrSiO_4$), Journal of the European Ceramic Society, Volume 28, 2008, pp. 2199–2211

then rapidly cooled and the separated components solidify independently resulting in a mixture of crystalline zirconia bound together with amorphous silica. The crystal structure of the zirconia is dependant both on the rate of cooling and the constitution of the original feed stock. Slow cooling will result in the reformation of the zircon mineral without separation. This PDZ (plasma dissociated zircon) is then far more easily decomposed by the action of hydrofluoric acid (40%) than normal zircon.[12]

$$ZrO_2.SiO_2 + 12\ HF \longrightarrow H_2ZrF_6 + H_2SiF_6 + 4H_2O$$

The H_2ZrF_6 can act as a starting point in the purification process of the zirconium to nuclear reactor grade. It is however extremely dangerous to work with hydrofluoric acid in a laboratory environment (see **Paragraph 3.3.3**) and the use of other digestion methods on this scale is preferred. The ability of these alternative methods to digest the PDZ may result in a safer, more environmentally friendly industrial process.

Another method to convert the mineral to a more manageable form is the heating of the mineral with a flux. A number of different fluxes have been used to convert the zircon to a more reactive form. These include the use of alkali hydroxides or carbonates, the fusion with alkali metals or lead oxide, the fusion with pyrosulphate or hydrosulphate, the fusion with alkali hydrofluoride and finally the heating of the ore with carbon or calcium carbide.

It is crucial to be able to ascertain the exact condition and constitution/purity level at each phase during the various processing steps required to convert the raw zircon ore to nuclear grade zirconium metal sponge and alloys. If a purification step is not sufficiently efficient in removing an element such as hafnium or boron, the resulting sponge will be useless for nuclear application as indicated by the metal specifications for nuclear reactors as indicated in **Table 1-1**. Most zircon currently available in the country is supplied by Namakwa Sands, Richard's Bay Minerals or KZN Sands, with the

approximate chemical composition of these zircon minerals being given in **Table 1-5**. A comparison of these specifications with that needed for nuclear grade Zr shows that a large number of impurities are present in the mineral, some more serious than others. The Hf content is in the order of 1.3% while other impurities are below the 1% level. In order to convert the zircon to nuclear grade, most of these impurities need to be removed from the zirconium *via* different separation processes. In order to gauge the effectiveness of each purification step it is necessary to be able to quickly and accurately determine major and trace components at every step, starting with the raw ore, proceeding through all refinement steps and finishing with the final, pure product. From **Table 1-5** it can be seen that this ore contains a wide range of concentrations of elements, making simultaneous analysis of all components difficult.

The need for new zircon digestion procedures with the least amount of contamination, the quick and accurate determination of zirconium, and the determination of the type and quantity of all the associated impurities were the main driving forces behind this study. The objectives of the study are summarised in **Paragraph 1.5.**

Table 1-5: SARM62 zircon reference material certified constitution

Constituent	Certified Value	95% Confidence Interval	
		Low	High
ZrO_2 (Mass %)	64.2	63.8	65.4
SiO_2 (Mass %)	32.8	32.5	33.2
HfO_2 (Mass %)	1.31	1.01	1.36
TiO_2 (Mass %)	0.13	0.12	0.14
Al_2O_3 (Mass %)	0.88	0.62	1.06
Fe_2O_3 (Mass %)	0.07	0.06	0.07
P_2O_5 (Mass %)	0.12	0.11	0.13
CaO (Mass %) Uncertified	0.11		
MgO (Mass %) Uncertified	0.04		
U_3O_8 ($mg.kg^{-1}$)	354	324	382
ThO_2 ($mg.kg^{-1}$)	158	141	169
Cr ($mg.kg^{-1}$)	21-38		

1.5. OBJECTIVES

The objectives of this study are:

- to perform an in-depth literature study on all the available methods to analyse for zirconium and all its associated impurities obtained from the dissolution of a zircon matrix;
- to determine the usefulness of ICP-OES for this type of analysis;
- to examine the use of different flux agents for sample dissolution;
- to examine alternative digestion methods such as microwave digestion and their usefulness in comparison with existing methods;
- to develop a method for the simultaneous analysis of both major and minor components of zircon ore and PDZ within a relative margin for error of approximately 4-6% for the major components and 20-30% for the minor components, this being in keeping with the approximate size of the 95% confidence interval set out in the SARM62 certified reference material.

Chapter 2: The Spectrometric Analysis of Zirconium and Related Products - A Literature Survey

2.1. INTRODUCTION

Good results for the determination of zirconium have been obtained with a variety of chemical reagents using spectrophotometric methods as well as with the use of electrothermal vaporisation in graphite furnace atomic absorption spectroscopy (GFAAS). The use of GFAAS allows for the determination of impurities that may be present in high-purity materials, usually without the need for further treatment as no colouring reagents are required. Similarly ICP-OES has been employed to determine the trace impurities present in zirconium ores.[18]

The necessity of determining the level of trace impurities is paramount when preparing materials for the nuclear industry, where the presence of neutron absorbing species and other contaminants are very detrimental (see **Paragraph 1.1**), as well as for the glass optics industry, where the presence of colouring transition elements is similarly devastating to the transmitting efficiency of zirconium(IV) fluoride-based glasses.[19]

---

[18] Xiaoguo Ma, Yibing Li, Determination of trace impurities in high-purity zirconium dioxide by inductively coupled plasma atomic emission spectrometry using microwave-assisted digestion and wavelet transform-based correction procedure, Analytica Chimica Acta, 579, 2006, 47–52

[19] Nikitina, Z. A., Kuznetsova, N. M., Zharkova, I. P., Monakhova, N. G., Journal of Analytical Chemistry, Volume 50, No. 1, 1995, pp. 90-92

2.2. SPECTROMETRIC METHODS AND TECHNIQUES[20]

A wide selection of reagents and techniques has been studied for the spectrophotometric determination of trace zirconium concentration in a similarly wide array of sample media. Commonly used colouring reagents include Arsenazo III, phenyl fluorone, xylenol orange and 3-hydroxy-2-(2'-thienyl)-4H-chromon-4-one. Several chemically similar derivatives of these compounds are also known to give accurate, reproducible results.

Arsenazo III has been referred to as the preferred reagent for the determination of microgram (ppm) amounts of zirconium.[21] Analysis is carried out in a 2-10 M HCl solution in order to prevent polymerisation of the zirconium ions with the sensitivity of this method decreasing with an increase in pH. Arsenazo III is a highly selective reagent and determination is only interfered with by the presence of ions (of all oxidation states) of hafnium and thorium as well as specifically gallium(III), iron(III), lanthanum(III), cobalt(II), titanium(IV), and uranium(IV). Most of these interferences can be eliminated with the use of masking agents such as oxalate, or by chemical alteration, as in the case of iron(III) where reduction to iron(II) eliminates the interference. Procedures using Arsenazo III and its derivatives gave detection ranges, corresponding with the complexes' ability to obey Beer's law, of 0-16µg (Arsenazo III extracted in coordination with tetradecyl pyridium chloride[22]), 0-20µg/25ml (Arsenazo DBF[23]), 0-18µg/25ml (tribromocarboxy Arsenazo[24]), 0-30µg/25ml (dibromocarboxy Arsenazo[25]), 0-35µg/25ml

---

[20] Dalawat, D. S., Chauhan, R. S., Goswami, A. K., Review of Spectrophotometric Methods for Determination of Zirconium, Reviews in Analytical Chemistry, Volume 24, No. 2, 2005, pp. 75-102

[21] Kania, K., Buhl, F., Spectrophotometric Method for the Determination of Zirconium using 2,3,7-trihydroxyphenylfluorone and lauryldimethylammonium bromide, Chemia Analityczna, Volume 37, Issue 6, 1992, pp. 691-698

[22] Lei, L., Xiao, G., *Kuangye Gongcheng*, 11(1), 63, 1991

[23] Cheng, L., Luo, Q., Yu, X., Zeng, Y., *Huaxue Shiji*, 14(6), 325, 1992

[24] Yang, H., Zhang, H., *Yejin Fenxi*, 13,(2), 26, 1993

[25] Sun, J., Ma, J., Zhu, X., Yuan, R., Lihua, J., *Huaxue Fence*, 30(2), 95, 1994

(Arsenazo DBS[26]), 0-10µg/25ml (tribromoarsenazo[27]) and 0-30µg/25ml (DBM-carboxyarsenazo[28]).

The fluorone and phenyl fluorone have by far the largest number of analogues useful in the determination of zirconium. Fluorone itself forms a quaternary complex with zirconium(IV) ions in the presence of a surfactant known as BDMAF when the interference of high valence elements has effectively been removed by the addition of EDTA[29]. 3,5-dibromo-4-(8-hydroxy-5-quinolylazo)-phenyl-fluorone[30] undergoes a colour reaction with zirconium in the presence of cetyltrimethyl ammonium bromide, giving a detection range of 0-10µg/25ml. Common interferences with fluorone and phenyl fluorone include ions of all oxidation states of molybdenum, germanium and tungsten as well as specifically tin(II), antimony(III), vanadium(V), mercury(II) and chromium (IV).[21] All fluorone derivative colouring reagents reported in the literature require the presence of co-ligands, such as cetyltrimethyl ammonium bromide, in order to form stable complexes.

Xylenol orange has been reported as being useful for the determination of trace amounts of zirconium in geological ore samples, specifically for carbonate rock.[31] For this analysis the samples were first digested with a mineral acid mixture, consisting of 2ml nitric acid, 5ml perchloric acid and 5ml hydrofluoric acid. The residue was then fused, the melt dissolved and colouring reagents added. This method had a detection range of between 0 and 20µg/25ml and it gave results which were in good agreement with the certified values of the geological samples analysed. It was also found to be tolerant of several interferences, notably up to 500mg potassium and borate, 30mg

---

[26] Yin, J.J., Gansu, G., *Daxue Xuebao*, 23(4), 102, 1997

[27] Hao, T., Hao., P., Tang, N., Liu, Z., *Yejin Fenxi*, 20(4), 44, 2000

[28] Li, X., Jia, Z., Chen, Y., Lihua, J., *Huaxue Fence*, 37(9), 409, 2001

[29] Yang, D., Lu, H., Liang, L., Zhang, Y., *Yejin Fenxi*, 16(5), 1, 1996

[30] Li, X., Hung, Y.P., Zhang, H., *Fenxi Shiyanshi*, 12(6), 10, 1993

[31] Okai, T., *Geostandards Newsletter*, Volume 15, No. 2, 1991, pp. 187-189

calcium and magnesium, 20mg aluminium, 3mg titanium and 1mg manganese and phosphate. Quantities of fluorine in excess of 1µg will, however, suppress the colour development.

3-Hydroxy-2-(2'-thienyl)-4H-chromon-4-one has been found to be a highly specific and sensitive colouring reagent for use in zirconium determination.[32,33] In the presence of hydrochloric acid and the surfactant Triton X-100 it gave a 1:3 metal:ligand complex with a detection range of 0-2ppm and maximum absorption at 415nm. Interferences are listed in **Table 2-1**.

Table 2-1: Interferences in 3-Hydroxy-2-(2'-thienyl)-4H-Chromon-4-one determination of zirconium[33]

Anion	Tolerance limit mg/10ml	Cation	Tolerance limit µg/10ml
Chloride	7.4	Zn(II), Hg(II), Cu(II), Co(II), Cr(III), Mn(IV)	500
Iodide	3.32	Ni(II)	293
Nitrate	2.02	Bi(III)	10.5
Sulphate	1.33	Cr(VI)	2.59
Bromide	1.19	Pb(II)	1.06
Acetate	0.09	V(V)	0.509
Citrate	0.003	Fe(II), Fe(III)	0.279
Bromate	0.001	B(VI)	0.959
Nitrite	2		
Thiosulphate	1.2		
EDTA	0.003		

As stated earlier, while the use of spectrophotometric methods to analyse zirconium content in mineral samples is essential, it is also necessary to be able to analyse the trace components in high purity zirconium metal and other zirconium based chemicals.

[32] Nijhawan, M., Kakkar, L.R., *Chem. Anal. (Warsaw)*, 44(4), 711, 1999

[33] Sharma, V., Nijhawan, M., Malik, A. K., Rao, A. L. J., 3-Hydroxy-2-(2'-thienyl)-4H-Chromon-4-one as a Spectro-photometric reagent for the Trace Determination of Zirconium in Aqueous Phase, Journal of Analytical Chemistry, Volume 56, No. 9, 2001, pp. 830-832

Specifically analysing for the presence of hafnium in high purity metal sponge and iron in zirconium(IV) fluoride glasses, used in the manufacture of very long, repeaterless fibre communication links, poses challenges that spectrophotometric methods are ill-suited to resolve. For these analyses one must turn to the use of graphite furnace atomic absorption spectroscopy (GFAAS), inductively coupled plasma optical emission spectroscopy (ICP-OES) or inductively coupled plasma mass spectroscopy (ICP-MS) techniques.

As will be described in Chapter 3, GFAAS is a highly accurate instrumental detection method with extremely low detection limits, often in the parts per billion and even parts per trillion range[34]. Unfortunately this technique is not without problems. In the method reported for the analysis of trace copper and nickel[34] in zirconium fluoride it was necessary to compensate for matrix interferences with the addition of palladium nitrate and nitric acid as matrix modifiers. The role of a matrix modifier is to delay analyte atomization until the graphite tube has reached a stable temperature, thus facilitating volatilization of the complex matrices while keeping the analyte intact. In this case the nitric acid helped to reduce the background absorption while the palladium appears to form an alloy with some of the analyte species on the graphite surface, effectively increasing the thermal stability of the analyte during pyrolysis. This method gave good results with all results being in the 10-30ppb range with relative standard deviations of between 4 and 8 percent.

ICP-OES is becoming more and more popular and has largely replaced the use of atomic absorption spectroscopy, in spite of its slightly inferior detection limits, due to its rapid multi-element analysis capability without the need for consumable lamps. Matrix interferences are also minimal, while spectral interferences take a leading role in issues related to this technique.

---

[34] Jaganathan, J., Ewing, K. J., Buckley, E. A., Quantitative determination of Nickel and Copper in Zirconium Fluoride Using Graphite Furnace Atomic Absorption Spectroscopy, Microchemical Journal, Volume 41, 1990, pp. 106-112

As is seen in an article detailing the analysis of trace elements in high-purity zirconia[38] the spectrum of light emitted by excited zirconium was a concern when analysing trace and ultra trace elements due to its myriad emission lines. It was also shown to suppress the peak height of other analytes. However, these errors were corrected for using a mathematical technique called a wavelet-transform. The large linear dynamic range exhibited by ICP-OES allowed for the simultaneous analysis of several elements, these being iron, hafnium, manganese, sodium, silicon and titanium. In this method microwave digestion was used in order to completely dissolve spiked zirconia samples into aqueous medium. The detection limits for Fe, Hf, Mn, Na, Si and Ti were found to be 1.2, 13.3, 1.0, 4.5, 5.8 and 2.0 $\mu g.g^{-1}$, respectively.

In another study[35] zirconium and hafnium alone were analysed after undergoing cloud-point extraction. The extraction of analytes from aqueous samples was performed in the presence of quinalizarine as chelating agent and Triton X-114 as a non-ionic surfactant. The surfactant-rich phase was diluted with 30% (v/v) propanol solution containing 1 $mol.dm^{-3}$ HNO_3. The enriched analytes in the surfactant-rich phase were then determined by ICP-OES. The calibration graphs were linear in the range of 0.5–1000 μg dm^{-3} with detection limits of 0.26 and 0.31 $\mu g.dm^{-3}$ for Zr and Hf, respectively. No significant interference was observed from contaminating ions. The method was successfully utilized for the determination of these cations in water and alloy samples. In this study a Varian Vista-PRO ICP-OES apparatus coupled to a V-groove nebuliser and equipped with a charge-coupled device (CCD) detector was used for analysis.

2.3. CONCLUSION

It should be clear from the above discussion that the amount of work done on zircon and zirconium samples is somewhat limited. A larger amount of reference material is

[35] Shariati, S., Yamini, Y., Cloud point extraction and simultaneous determination of zirconium and hafnium using ICP-OES, Journal of Colloid and Interface Science, 298, 2006, pp. 419–425

available from Chinese journals but the translation of these is troublesome. The analysis of zirconium as a trace element is well documented and is a relatively simple procedure. The analysis of trace elements within high purity zirconium chemicals, ores and metal is more difficult and considerably less well documented. Very little published material deals with the accurate assay of zirconia and nothing whatsoever was found referring to quantitative analysis of the silicate ore, zircon, and its minor constituents. This leaves considerable scope for development into analytical methods for the analysis of said zircon and related materials, such as the PDZ referred to in **Paragraph 1.4**.

Chapter 3: Selection of Analytical Techniques

3.1. INTRODUCTION

Several spectrometric and digestion methods were investigated for use in the analysis of zircon prior to the beginning of this study. The advantages and disadvantages of each method were weighed in relation to each other before a specific method or instrument was chosen to perform the analysis. Only instrumental methods of analysis were considered due to the extremely low detection limits required for some of the trace elements as well as the need for rapid analysis. The silicate matrix of the analyte limited the number of digestion options available.

3.2. SPECTROMETRIC TECHNIQUES

3.2.1 INDUCTIVELY COUPLED PLASMA – OPTICAL EMISSION SPECTROSCOPY[36,37]

Inductively Coupled Plasma – Optical Emission Spectroscopy (ICP-OES) is an instrumental method utilising an inductively coupled plasma (approximately 6000^{o}C) to excite the atoms, ions and molecules present in a gas stream containing the nebulised analyte sample.

The plasma is generated by a radio frequency (RF) coil surrounding a quartz torch containing three concentric tubes (see **Figure 3-2**). The argon gas flow through the outermost tube is often called the plasma gas but for the sake of consistency will be called the coolant gas from this point. The auxiliary gas will in this case be called the plasma gas, and refers to the gas flowing through the middle of the three concentric

[36] Boss, C. B., Fredeen, K. J., Concepts, Instrumentation and Techniques in Inductively Coupled Plasma Optical Emission Spectrometry, 2004

[37] Skoog, D. A., Holler, F. J., Crouch, S. R., Fundamentals of Analytical Chemistry, 8th Edition, 2004, pp. 839-865

tubes. The central tube contains the sample gas flow and will be referred to as the nebuliser gas flow. The plasma and coolant gas flows function together to form a plasma in which the argon gas is ionised by the action of the high frequency and power of the RF generator. The RF coil generates an electro-magnetic field which causes the electrons in the plasma to move in one direction while the positively charged ions rotate in the other with respect to the direction of the field. The plasma is initiated with the use of a spark provided, in most cases, by an electric arc. The extremely high temperature of the plasma is produced by the friction created when the positively and negatively charged atoms pass each other.

A diagram of the components of an ICP-OES system is given in **Figure 3-1**. The sample is introduced into a nebuliser using a peristaltic pump to ensure minimal pulsing. The nebuliser feeds into the spray chamber where large droplets not sufficiently broken down by nebulisation are removed. The sample vapour is carried by the nebuliser gas into the plasma where the emissions of the different elements are detected by the optics of the spectrometer. These are then recorded and interpreted by a computer.

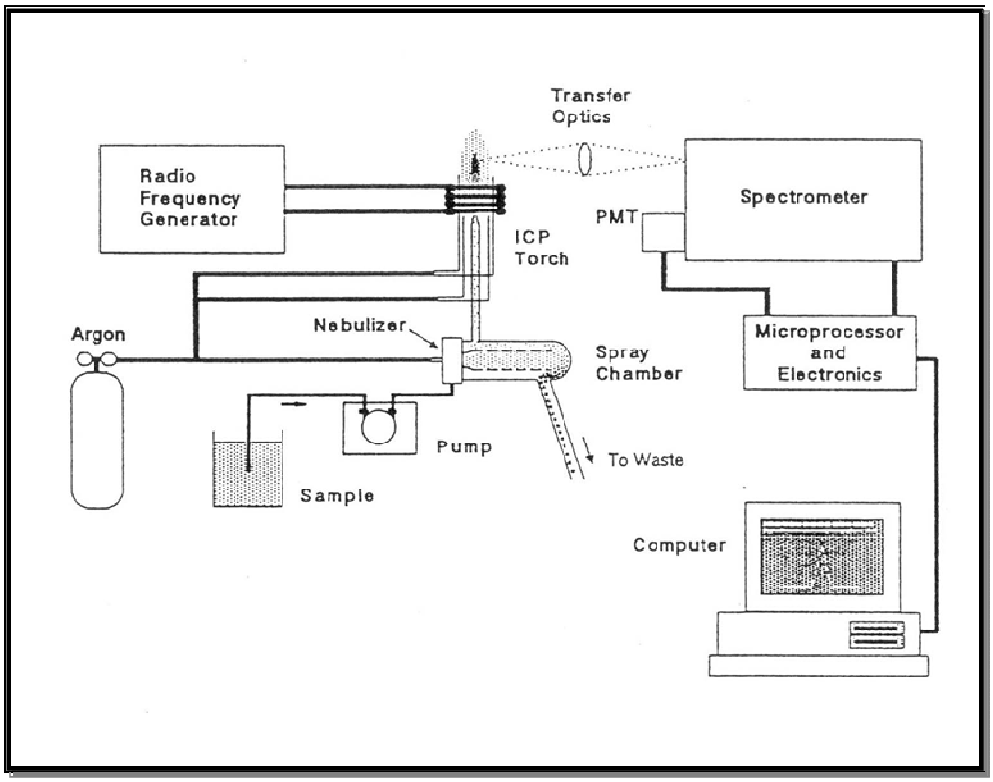

Figure 3-1: Diagrammatic representation of the main components of the ICP-OES system[36]

There is sufficient heat in the plasma (calculated at approximately 6000K – 10000K) to completely disintegrate almost any sample introduced into the plasma and to excite the constituent atoms and ions. These excited atoms and ions are unstable and will decay back to a less excited state. During this process, energy is lost in the form of electromagnetic radiation (photon). The wavelength of the emitted light is inversely proportional to the energy loss and is characteristic of the atom/ion. The amount of light emitted is directly proportional to the amount of analyte present in the sample and is measured by a set of spectrometer optics.

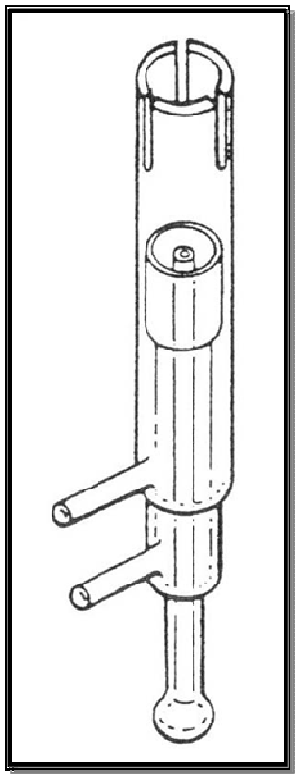

Figure 3-2: Diagram of a torch used in ICP-OES[36]

There are several types of optic configurations used in ICP-OES, currently the most common being the Echelle type grating system which splits the light emitted from the plasma into a two-dimensional grid which is collected by a CID (Charge Injection Device). Other methods exist which use CCD detectors and single dimensional dispersion. These methods result in a higher degree of accuracy, but at the cost of speed and some efficiency when reading a large number of elements. The spectrometer is typically situated separately from the plasma with the light from the latter being transferred to the former by means of a set of mirrors and optics.

The greatest advantages of the ICP-OES technique are the spectacular linear dynamic range, high sensitivity, low detection limits (ppb range) and multi-element detection

capacity.[38] As long as the sample does not dramatically change the conditions within the plasma, as easily ionisable elements like sodium can do, the calibration curve for an element can remain linear through up to seven orders of magnitude, making this method ideal for the measurement of both major, minor, trace and even ultra-trace components of a sample. The greatest disadvantage lies in the fact that the sample must be in solution, preferably aqueous solution, before it can be analysed. There are methods for introducing a solid sample to an ICP instrument, but these are difficult and sometimes unreliable.

ICP-OES does not suffer from chemical interference to the extent that other methods like AA spectrometry do, but it is affected by spectral interference due to the large number of emission lines of most elements. These interferences can manifest in several ways. A simple background shift where the entire background continuum intensity in a region may be increased, can be caused by a large concentration of another element present in solution. Another type is the sloping background shift where another element present in the sample has a significant peak near that of the analyte, affecting the background on one side of the analyte peak more than the other. Both of these effects can be compensated for by the use of a background correction, using points on one or both sides of the analyte peak respectively. A more difficult interference to detect and correct for is the direct spectral interference where another element present emits on the same wavelength as the analyte or so close to the same wavelength that the instrument cannot differentiate the between lines. This can be corrected for using an inter-element correction where another standard containing only a known concentration of the interfering element is used to determine the intensity per ppm (or other concentration measurement) at the analytes wavelength. The concentration of the interfering element in the analyte solution is then determined and, using the ratio obtained from the standard, the intensity of the interfering element is subtracted from the intensity of the analyte at its emission line. All of these can usually be avoided, however, by the selection of an interference-free line and this is indeed preferred if a complex

[38] Xiaoguo Ma, Yibing Li, Determination of trace impurities in high-purity zirconium dioxide by inductively coupled plasma atomic emission spectrometry using microwave-assisted digestion and wavelet transform-based correction procedure, Analytica Chimica Acta, 579, 2006, 47–52

background interference, where there are multiple interfering emissions in very close proximity to the analyte peak, is evident.

3.2.2 Atomic Absorption Spectroscopy[37,39]

Atomic absorption (AA) spectrometry functions similarly to ICP-OES except in that it does not detect the emissions of the excited elements but rather relies on their ability to absorb light of specific wavelengths. A sample in aqueous or organic solution is nebulised and passed into a flame (usually air/acetylene or nitrous oxide/acetylene) where it is atomized, or directly into the tube of a graphite furnace. Light from a lamp, made from the same element as the analyte, is passed through the flame and the percentage absorbance is measured using a set of optics similar to those used in ICP-OES. Until the emergence of ICP-OES, AA spectrometry was the industry standard for the analysis of cations and metals and is still an extremely useful method of analysis. Making use of a graphite furnace in this method can enable measurement a full order of magnitude lower than ICP-OES since the sample is atomised quantitatively and is also confined to the area through which the light to be absorbed is passed. However, AA does not have the linear dynamic range available to the ICP-OES. In the case of the ICP-OES technique the amount of light emitted is directly proportional to the concentration of analyte in solution. In the case of AA, on the other hand, the absorbance is governed by the equation $A = \log \frac{P_0}{P}$. This results in the absorbance of a medium increasing as the attenuation of the beam increases thus effectively limiting the linear dynamic range and causing significant deviation from Beer's law outside the linear dynamic range.

AA also suffers from various forms of interference which are mostly chemical in nature and must be corrected for. This can be difficult and expensive as additives must sometimes be used to make these adjustments as was mentioned in **Paragraph 2.2**. AA does suffer from spectral interference but not nearly to the extent that ICP-OES does, as each element has far less absorption than emission lines. The major disadvantage of

[39] Skoog, D. A., Holler, F. J., Nieman, T. A., Principles of Instrumental Analysis 5th Edition, 1998. pp. 206-225

this technique is that it is extremely slow when compared to multi-element detection methods like ICP-OES. This is due to the inherent limitation that only one element can be detected at a time because of the use of element specific cathode lamps. The temperature of the flame is also too low to completely atomise highly refractory elements like certain oxides and can thus severely under-read the true concentration of analyte present if the elements are not in the same chemical state in the sample as in the standard.

3.2.3 SPECTROPHOTOMETRIC METHODS[40]

UV/VIS spectrophotometric methods rely on either the absorbance or transmittance of a solution that is coloured either by the inherent colour of the analyte, by the colour produced by a complexing agent or by the colour of another species directly related to that of the analyte. UV/VIS methods usually have severely limited linear dynamic ranges when compared to other spectrometric methods due largely to concentration effects and the properties of the analytes being measured. These cause deviations to Beer's Law which states that the absorbance by a given sample is defined as $A = \varepsilon bc$ where A is the absorbance, ε is the molar extinction coefficient, b is the path length through the sample and c is the concentration of the sample. The variation of analyte concentration between completely clear to completely opaque may be less than an order of magnitude. The effect of this is clearly evidenced by the extremely short detection ranges given in Chapter 2 where the largest linear dynamic range was 0-35µg/25ml, while the average range was significantly shorter. This can easily be compensated for with the correct use of dilutions or preconcentration but can lead to delays in analysis.

Like AA spectrometry this method suffers from chemical interferences in that other species in solution may absorb at a similar wavelength or complex some of the colouring reagent, leading to false readings as seen in **Table 2-1**. The advantage of the UV/VIS spectrophotometer is that it is relatively simple compared to other methods of instrumental analysis and does not require the same amount of resources to operate.

[40] Skoog, D. A., Holler, F. J., Nieman, T. A., Principles of Instrumental Analysis 5th Edition, 1998, pp. 300-322

Due to limitations in the technique, however, it is very difficult, if not impossible, to perform simultaneous, or near simultaneous such as in the case of AA, multi-element determinations with this instrument, increasing the time necessary to perform a full analysis.

3.2.4 X-RAY FLUORESCENCE[41]

X-ray fluorescence makes use of the ability of high energy X-rays (10^{-6}nm to 10nm) (see **Figure 3-3**) to excite electrons in an atom to a higher energy state. In most cases, but not all, X-rays are produced by accelerating electrons through a vacuum tube from a heated tungsten cathode towards a metal anode, often molybdenum, chromium, rhodium, scandium, cobalt, silver, iron, copper, or tungsten, with a potential difference of up to 100kV. When these electrons strike the large anode plate, made of copper with the anode material imbedded in it, an X-ray continuum or line spectrum is produced. This method of generating X-rays is extremely inefficient with up to 99% of the energy used being given off as heat, the rest being released as X-ray radiation. The apparatus must thus be cooled very efficiently to avoid melting the anode. The X-ray radiation is then allowed to strike the sample which is thus electronically excited. When the sample returns to its ground state it fluoresces, emitting a photon which is lower in energy than the initial excitation photon. This is then transmitted through a collimator to a crystal, often lithium fluoride or sodium chloride, which is angled with respect to the incident beam. The X-ray beam is reflected by the crystal with the wavelength reflected being selectable by the application of Bragg's Law, wherein only certain wavelengths are reflected due to diffraction. The reflected beam of monochromatic radiation is detected by a transducer such as a Geiger counter, ionisation chamber or a scintillation counter. The output of the transducer is transferred to a signal processor, which converts the result to useable data.

Sample preparation for X-ray fluorescence is different from other methods in that the sample is in a powder or fused state. This greatly simplifies sample preparation as no

[41] Skoog, D. A., Holler, F. J., Nieman, T. A., Principles of Instrumental Analysis 5th Edition, 1998. pp. 272-296

solvation into a liquid medium need occur. It is also non-destructive so it can be used for the analysis of precious artifacts or jewellery without fear of destroying them. This method is used extensively in geochemistry as ore samples are often difficult to dissolve completely. This method is relatively free of interferences, but can be extremely time-consuming.

3.3. DIGESTION TECHNIQUES

3.3.1 FLUX FUSIONS[42,43]

The term flux fusion refers to the digestion of samples, usually ores, by means of a fusion with an inorganic salt at high temperature. This fusion, referred to as the melt, is then dissolved in dilute acid. Fluxes are generally used when a sample is insoluble or only partially soluble in acids. The high temperatures necessary to dissolve the alkali salt as well as the massive concentration of reagent which is in direct contact with the sample results in the dissolution of even the hardiest sample, such as alumina or silica.

Table 3-1 shows a list of some of the more commonly used fluxing agents. When digesting materials containing silica, anhydrous lithium metaborate is the preferred fluxing reagent. This is due to silica separating upon dissolution into acid medium in the case of a melt created using sodium carbonate. This separation does not occur in the case of lithium metaborate. Advantages claimed for lithium metaborate include:

- quicker fusion times at lower temperatures than other fluxes.
- no evolved gases, leading to less sample loss by volatilization.

---

[42] Jeffery, G.H., Bassett, J., Mendham, J., Denney, R.C., Vogel's Textbook of Quantitative Chemical Analysis 5th Edition,1991,pp. 112-113

[43] Skoog, D. A., West, D, M., Holler, F. J., Crouch, S. R., Fundamentals of Analytical Chemistry, 8th Edition, 2004, pp. 1049-1051

- direct determination can be performed for many elements in the acid solution without the need for separations.
- the loss of platinum from the crucible is less during a lithium metaborate fusion than with sodium carbonate.

Table 3-1: Table of commonly used fluxing agents

Flux	Sample type	Comments
Sodium Carbonate	Acidic materials	Used with sodium peroxide or potassium nitrate when an oxidising medium is needed.
Potassium Pyrosulphate	Basic materials	
Sodium Pyrosulphate	Basic materials	
Sodium Hydroxide	Acidic materials, silicates (leaves silica residue)	
Potassium Hydroxide	Acidic materials, silicates (leaves silica residue)	
Lithium Metaborate	Silicates, acidic materials	Fast dissolution at low temperatures, preferred for XRF as lithium does not give rise to interfering X-rays.
Lithium Tetraborate	Silicates, basic materials	Fast dissolution, preferred for XRF as lithium does not give rise to interfering X-rays.

Unfortunately the disadvantages of using a flux are quite significant. These include the possibility of severe contamination of the sample, both by impurities in the flux and by the flux itself due to the minimum tenfold excess required for dissolution. The high

temperatures necessary lead to the possibility of sample loss through volatilisation and the container itself is attacked by the flux, leading to further contamination.

Fluxing is carried out in a high temperature environment, usually an oven, in a crucible that is minimally attacked by the fluxing reagent. Platinum crucibles are used for lithium metaborate as well as sodium carbonate and potassium pyrosulphate while nickel, gold, silver or iron crucibles are used for sodium carbonate and sodium peroxide.

3.3.2 MICROWAVE DIGESTION[44]

Microwave radiation is a non-ionising radiation with a frequency range of between 300 to 300,000MHz (see **Figure 3-3)**. Most microwave systems, laboratory and domestic, function at specific wavelengths set out by the International Radio Regulations adopted at Geneva in 1959. They cause molecular motion by migration of ions and rotation of dipoles without causing changes in the molecular structure of a material.

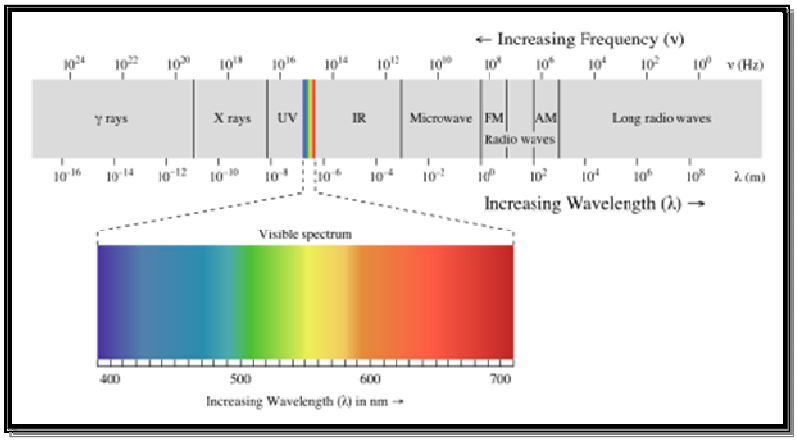

Figure 3-3: Diagram of wavelengths of electromagnetic radiation[45]

[44] Kingston, H. M., Jassie, L. B., Introduction to Microwave Sample Preparation Theory and Practice, 1988

[45] http://en.wikipedia.org/wiki/Microwave retrieved on 15/05/2008

Unlike traditional acid digestion of samples using conductive methods, such as hot plates and heating mantles, microwave heating provides thermal energy directly to the sample by means of the interaction of the microwave beam with dipoles in the sample. Water is especially susceptible to this type of heating in that it is a highly polar molecule which interacts easily with microwave energy.

Microwave heating results in significantly faster digestion times compared to conventional heating methods. The traditional methods rely on the ability of the reaction vessel to transfer heat from the heat source to the sample and most sample vessels are composed of materials particularly ill-suited for this purpose (e.g. glass). In the case of liquid samples this results in slow heating with only the contact surface of the sample being directly influenced while the rest of the sample is heated by means of convection. Microwaves have the distinct advantage of heating the entire sample homogenously, thus reaching maximum temperature far quicker than with conventional methods. This difference is illustrated in **Figure 3-4**. In a study[46] done to determine the efficacy of various methods of leaching, microwave heating achieved maximum extraction in a period of less than two minutes in all cases. Other methods, such as ultrasonic assistance and conventional stirring with heat, achieved this in a period of fifteen minutes and sixteen hours respectively. Almost all extractions gave comparable and approximately quantitative results with the exception of the nickel extraction which gave only 85% extraction.

[46] Arain, M. B., Kazi, T. G., Jamali, M. K., Speciation of heavy metals in sediment by conventional, ultrasound and microwave assisted single extraction methods: A comparison with modified sequential extraction procedure, Journal of Hazardous Materials, 154, 2008, pp. 998–1006

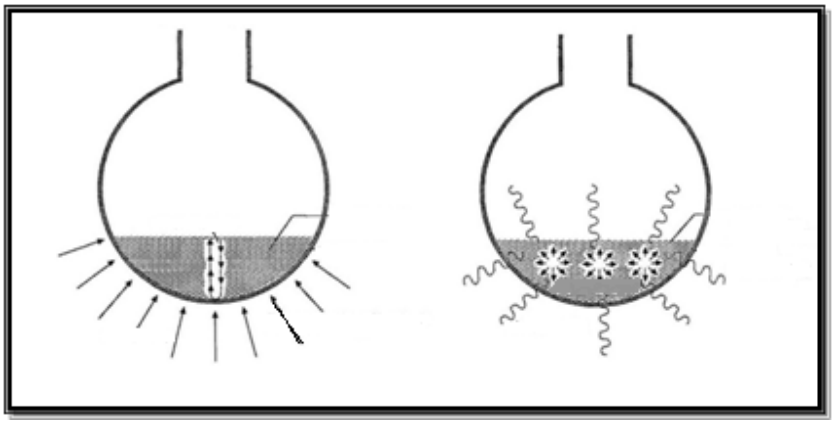

Figure 3-4: Diagram showing differences between conductive and microwave heating[44]

The microwave radiation is generated by a magnetron before being channeled along a wave guide into the microwave cavity wherein the microwaves are distributed by a combination of what is known as a mode stirrer, a circulator and a turntable in order to ensure the homogenous heating of the entire sample, as seen in **Figure 3-5**. The amount of microwave energy applied to the sample is controlled by cycling the magnetron in what is referred to as a duty cycle. This duty cycle results in the magnetron being on for only a certain percentage of the duty cycle, resulting in the average effective output of said percentage of the magnetron's maximum output. In modern microwave digesters the magnetron(s) can deliver unpulsed microwave power over its full power range. Precise regulation of energy is particularly important for fast and homogeneous heating, reduced spontaneous reactions or charring and increased reliability. Both the wave guide and the cavity are completely reflective of microwave radiation with the result that if there is not sufficient sample in the microwave cavity to absorb all the radiation the magnetron can be damaged, reducing its maximum output and reducing repeatability.

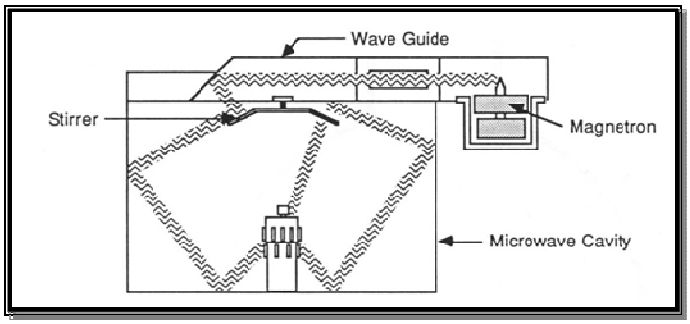

Figure 3-5: Diagrammatic representation of the components of a microwave digestion system[44]

Most, but certainly not all, microwave sample preparation devices make use of sealed, chemically inert reaction vessels (e.g. PTFE) which are transparent to microwave radiation and act as high pressure bombs inside of which samples are subjected to both high pressure and temperature conditions that are simply not possible or extremely difficult to obtain using other methods. This combination of high pressure and temperature allows for the speedy digestion of mineral samples using acids that normally take several hours to digest the sample or do not cause decomposition at all.

3.3.3 HYDROFLUORIC ACID DIGESTION[47,48]

The most commonly used method for the digestion of silicate ores is by treatment with dilute or concentrated hydrofluoric acid as this is the only acid capable of complete dissolution of silica. It is used only when the analysis of the other components of a material, not silica, is to be carried out as the fluoride ions form silicon tetrafluoride which volatilises readily. The excess fluoride must also be removed after digestion as it forms highly stable complexes with many cations, interfering with analysis. This can be achieved by boiling with sulphuric acid.

---

[47] http://www.fap.pdx.edu/safety/hydrofluoric_acid/ accessed on 19/05/2008

[48] Skoog, D. A., West, D, M., Holler, F. J., Crouch, S. R., Fundamentals of Analytical Chemistry, 8th Edition, 2004, p 1044

The use of hydrofluoric acid carries with it significant biological hazards due to its extremely corrosive nature. It is colourless in solution and relatively difficult to detect by smell at high concentrations as it destroys the nerves responsible for smell. Hydrofluoric acid is absorbed directly through the skin and attacks the bones due to their high calcium content and disrupts the body's electrolyte balance. It is easily the most dangerous mineral acid as only a small amount coming into contact with the skin can be fatal if left untreated, and the fumes emitted can cause severe respiratory problems, even death.

3.4. CONCLUSION

The use of ICP-OES as analytical method was decided upon for this study due to its high sample throughput rate, low level of interference, extensive linear dynamic range and multi-element detection capability. This was found to be preferable over the use of other methods which suffered either from extensive chemical interferences or overly long experimental time despite the simplified sample preparation of X-ray fluorescence. The advantages and disadvantages of the techniques are summarised in **Table 3-2.**

Different digestion techniques were also discussed and it was decided to investigate the usefulness of flux and microwave preparation methods and compare their results with respect to accuracy and precision for the same samples. The conclusion was reached that hydrofluoric acid digestion was too dangerous under current laboratory conditions due to the hazards involved in using and storing this acid.

Table 3-2: Table summarising advantages and disadvantages of instrumental methods

Technique	Advantages	Disadvantages
ICP-OES	Extremely fast, low level of interference, extensive linear dynamic range, multi element detection, accurate	Samples must be in aqueous solution, spectral interferences
AAS	Fast, accurate, well documented	Must have element specific lamps, short linear dynamic range, aqueous solution required
GFAAS	Fast, extremely accurate, well documented, extremely low detection limits	Must have element specific lamps, very short linear dynamic range, aqueous solution required
XRF	Relatively simple sample preparation, few interferences	Very slow

Chapter 4: Experimental Aspects and Troubleshooting in Relation to ICP-OES

4.1. INTRODUCTION

Like all analytical techniques, ICP-OES is not without experimental problems and issues. The instrument itself requires maintenance and careful attention to ensure that results obtained are useable and correct. In this study a Shimadzu ICPS-7510 was used and all experimental work and problems overcome are stated with respect to this machine.

4.2. RUNNING ASPECTS

Elements can emit on what are called atomic, ionic or molecular wavelengths depending on their electronic state. If an atom is in the ground state and is excited by the plasma it will form an unstable excited atom. After a short while this excited atom will fall back to a more stable state and the excess energy will be emitted as light at a characteristic wavelength known as an atomic line, while if it is already in an ionized state and is further excited it will form an unstable excited ion. After a short while this excited ion will also fall back to a more stable state and the excess energy will be emitted as an ionic line. At the tip of the plume the analyte may have cooled sufficiently to form a stable oxide or nitride which can also be excited and these emission lines are known as molecular lines. Each species is prevalent at a different height in the plasma. If the optics are not aligned correctly they may be focused away from the majority of the light being emitted on the analytical wavelength. In the case of the above-mentioned apparatus there are only two settings for the height at which a radial reading can be taken, making it difficult to ensure that the maximum amount of light at the analytical wavelength is being detected. This can cause the detection ability of the method to be

severely compromised. This problem can be avoided by taking all readings using the axial-read head supplied for use with this model. Advantages of using these settings are that the line of sight is directly down the centre of the plasma, resulting in all wavelengths, atomic, ionic and molecular, being detected equally without the danger of missing the optimum region. The problem with taking this approach is that the free atoms and oxides that are present in the cooler part of the plasma might absorb some of the emitted light (similar to the AA process) and cause a deviation in the linearity. It can also limit the maximum concentration that can be analysed. Unlike certain other ICP-OES models this instrument does not use a shear gas to protect the optics and read head from the heat of the plasma. The head is thus constructed of copper with a constant flow of chilled water passing through it in order to prevent damage. A problem arises if the chiller unit (Eyela CA-1112) is turned on well before the ICP instrument, resulting in condensation on the read head and water dripping down into the torch. Water present in the torch will prevent the plasma from igniting as it interferes with the flow of the argon gas.

It is necessary to ensure that sufficient argon gas is available as the plasma requires a gas pressure of 350 kPa and a flow rate of up to 22 litres per minute depending on settings. At this flow rate a 17.4kg mass of compressed argon (one cylinder) will be emptied within 8 hours. Unless sufficient care is taken to prepare a large number of samples per run a large amount of gas can also be wasted as the ICP instrument requires half an hour to achieve thermal stability. This state is necessary to avoid thermal drift, which can drastically affect the intensity of the readings taken.

The RF coil itself is cooled by water from an internal reservoir, making the use of an external chiller unnecessary when not using the axial read head. The water level must be monitored occasionally as, despite it being well sealed, some coolant does escape and the reservoir must be refilled from time to time.

Extraction of heat and gas from the plasma chamber is an absolute necessity. Not only does insufficient extraction cause heat to build up inside the machine, but argon acts as an asphyxiant in high concentrations and can be fatal if the excess is not removed from the laboratory working area. Toxic fumes can also form in the plasma and have to be removed as well. The use of an extraction fan attached to the machine with an outlet outside the lab is critical. Argon is present in the atmosphere at low levels and is chemically inert, thus this practice is environmentally sound.

Certain types of nebulizers are self-aspirating and can be used to move sample in an unpulsed way, rendering excellent precision. Under certain circumstances this might not be ideal, especially when one works with varying matrices. The viscosity of a sample has a large effect on the efficiency with which the sample is nebulised as well as the flow rate. Thus, if the sample matrix differs from the standard's matrix or different types of acid are used in the standards and samples (for example the highly viscous sulphuric acid) the results obtained can be heavily influenced. This problem is minimised by using a peristaltic pump to ensure a constant flow rate or by using internal standardisation.

The use of concentrated acids in the sample introduction system should be avoided. Though their affect on the glass and PTFE components is negligible they can seriously damage the elasticity of the tubing used for the peristaltic pump. This tubing must be removed from the pump after use, in order to preserve its elasticity. Once this is lost the efficiency of the tubing, and hence the pump, is greatly compromised and results in poor precision due to insufficient or inconsistent sample introduction.

The majority of the sample introduced into the spray chamber is drained off as waste and this is collected in a reservoir outside the machine. This reservoir must be checked regularly and emptied into a toxic waste disposal bucket as the samples are often high in toxic metals and acid.

The torch itself can undergo a process called devitrification in which it is damaged by the reaction of alkalis, especially sodium, with the quartz body of the torch. This process is slow but inevitable and the torch must eventually be replaced. Damage to the torch can be accelerated when it becomes dirty from sample depositing on the walls of the torch. These deposits can be removed by cleaning with dilute acid.

The optics of the spectrometer are extremely sensitive, due largely to the necessity for extreme precision in wavelength determination. For this reason the temperature (approximately 40^{o}C) of the machine and the degree of vacuum must be precisely controlled. This is done automatically by the apparatus although it can take several days from the moment it is turned on, for the optics and other components to reach a stable equilibrium. For this reason the ICP-OES spectrometer itself is rarely, if ever, turned off.

The software package provided with the apparatus reads peak intensity by measuring the height of the selected peak with respect to a baseline drawn between the two lowest points within a reasonable proximity of the peak. This eliminates the effects of both a simple and sloping background shift error. It is, however, unable to correct automatically for complex background shifts or direct spectral interferences. These must be removed either by selecting another line or, if this option is not viable, by other mathematical methods (see Chapter 3).

4.3. TROUBLESHOOTING

While the ICP apparatus is relatively reliable with regular maintenance, it can develop problems that need to be corrected to ensure reliable results. The nebuliser can become blocked and, while this is possibly the simplest problem that can occur, it can sometimes be the most difficult to fix. In this study a concentric nebuliser was used. This type of nebuliser consists of two concentric tubes (see **Figure 4-1**): the inner, extremely thin (less than 1mm diameter), tube carrying the sample, while the carrier gas flows through

the outer tube. The inner tube is easily blocked and difficult to clean if the blockage is not easily soluble. The simplest solution is to remove the nebuliser and place it in a dilute hydrochloric acid solution, allowing it to stand until the blockage is dissolved. If this is unsuccessful, the blockage may be forced out with compressed air. This, however, may also not work and replacement of the nebuliser may be the best solution. A clogged nebuliser can lead to very small amounts of sample being introduced into the spray chamber, resulting in greatly diminished detection limits. Clogging can also cause the tubing of the peristaltic pump to pull loose due to pressure build-up inside the tube. The simplest solution to this problem is to ensure that there are no solids in sample solutions and so avoiding clogging altogether.

The tubing on the peristaltic pump must be inspected regularly to ensure its elasticity and replaced if it has lost this. The elasticity of the tubing is critical in the consistent introduction of sample into the spray chamber. Tubing is a consumable, but its lifespan can be greatly extended by removing it from the pump when not analysing, where it is under tension, and not using samples with very high acidity.

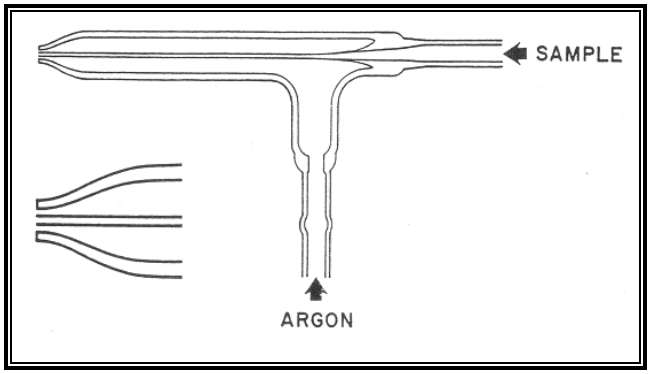

Figure 4-1: Diagram of a concentric nebuliser

The axial read head contains a small mirror which transfers the light from the plasma to the optics of the spectrometer. Both the read head itself and this mirror become dirty over time as they are in the direct path of the plasma. The head itself can be cleaned with steel wool, while the head must be disassembled in order to clean the mirror. This can be accomplished with a small amount of dilute acid on a cotton bud.

Occasionally the optics in the spectrometer can become misaligned and must be calibrated. This is a simple software-controlled procedure but neglecting to do this can cause severe errors in readings if the software is unable to locate the analytical line due to misaligned optics.

The selection of an appropriate analytical wavelength can be troublesome. One issue that can result in difficulties is the intensity of emission at a specific wavelength. The most intense peak may not be the best for analytical purposes. If the gradient of the calibration graph is too steep a very large standard deviation on the y-axis (emission intensity) may be observed but will relate only to a very small standard deviation on the x-axis (concentration). This can result in poor results if the phenomenon is too extreme. The ideal working line is one where the gradient is as near as possible to unity. Other factors such as interferences and matrix effects also influence the choice of analytical wavelength.

The amount of light emitted by the elements present in the analyte is influenced heavily by the temperature within the plasma. Unfortunately this temperature is not necessarily constant as matrix elements can affect it. Easily ionisable elements such as sodium and lithium lose electrons very easily to the plasma. As the temperature of the flame is partially dependent on the electron density in the plasma, a matrix with a large concentration of these elements can strongly influence conditions within the flame. This can be corrected for with some accuracy by matrix-matching the calibration standards to the analytical sample. A better and simpler method is to use a standard addition method where there is no chance of an unknown contaminant affecting readings. In this method the matrix of the analyte becomes part of the calibration standards. This effectively maintains conditions within the plasma with each sample being practically identical, other than small changes in the concentration of the analyte. Other ways to overcome this type of matrix effect is to use internal standardisation, use of robust plasma settings and the use of an ionization buffer. Internal standardisation is where an element that is

not present in your sample is added in identical concentrations to your blank, standards and samples. The suppression (or enhancement) of the signal of your internal standard element is then used by the software to calculate a correction factor for all analytes. Robust plasma conditions normally mean higher power and lower nebulizer gas flows. This ensures more energy and a hotter plasma and makes the residence time of the analyte in the plasma longer.

4.4. CONCLUSION

The simplicity and modularity of the ICP-OES system make it easy to work with and maintain. Troubleshooting is simple as there are only a limited number of possible problems. One simply needs to know what can go wrong to be able to quickly and easily rectify a problem. If one keeps a regular maintenance schedule and takes care with the samples introduced, very little can go wrong.

Chapter 5: ICP-OES Assay Method Development and Experimental Results

5.1. INTRODUCTION

Perhaps the most critical of all the steps required in the development of an analytical method is the digestion and preparation of one's sample. It is vital that the sample be converted from its raw form to a homogenous state that is compatible with the analytical technique used. The sample must also be representative of the body of the material analysed. This is achieved by ensuring that a large enough sample is used and that the original material from which it is derived is as homogenous as possible. In the case of ores this can be achieved by taking a large, representative sample and pulverizing or milling it using a non-contaminating medium, such as yttria-stabilised-zirconia (YSZ).

As discussed in earlier chapters, one of the digestion methods for zirconium-containing ores is the use of hydrofluoric acid. This can be dangerous on a laboratory scale and is not environmentally friendly on an industrial scale. It was therefore decided to avoid the use of this acid in the digestion of our samples as much as possible and the generation of *in situ* HF was performed in lieu of using the acid as is.

In this study two variations of the zircon ore were used. The first sample was the SARM62 certified reference standard which has a chemical composition as given in **Table 1-5**. All analytical results obtained in the course of this study were evaluated with respect to this standard to measure the success of the digestion and analytical method. The second sample was the first stage refinement product known as plasma dissociated zircon (PDZ) described in **Paragraph 1.4**. This refinement step converts the zircon to a chemically more amenable form. These samples were subsequently digested using different techniques in order to obtain homogenous solutions and then analysed for their individual component elements. These results were then compared to the values known

for the SARM62. It was decided that initially only the major (Zr, Si) and minor (Hf, Al, Fe, Ti) elements would be analysed for in order to properly develop the method before attempting the trace and ultra trace components like Ca, Mg, Cr, U and Th.

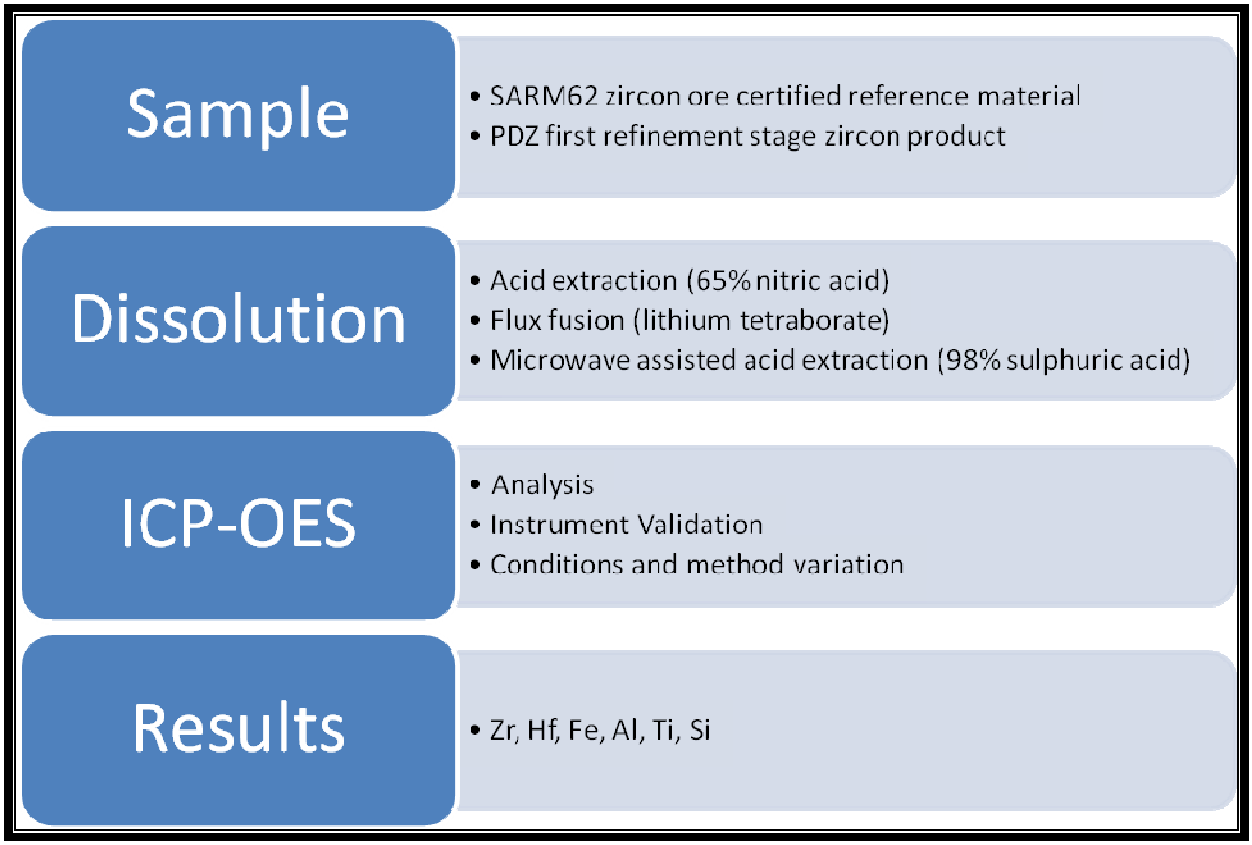

Figure 5-1:Brief outline of analytical procedures followed in this study

5.2. EQUIPMENT AND REAGENTS

A Shimadzu ICPS-7510 ICP-OES sequential plasma spectrometer was used for all analytical determinations. Flux fusions were performed in a high temperature oven supplied by Labequip. All element standards were bought from Merck and included a 1000ppm Hf standard, both 1000ppm and 10000ppm Zr standards, a 1000ppm Ti standard, a 1000ppm Si standard as well as the Merck XXVI multi standard containing

1000ppm each of Al, Fe, Cr, Ca, Mg, B, Li and several other elements not used in this study. Lithium tetraborate was bought from Johnson Matthey Materials Technology. Analytical grade sulphuric acid 95-98% A.C.S. reagent was obtained from Sigma-Aldrich while analytical grade 65% nitric acid and 32% hydrochloric acid were provided by Merck. The SARM62 certified reference material was sourced from Industrial Analytical while the PDZ was supplied by the South African Nuclear Energy Corporation Limited (Necsa). An Anton Paar Multiwave 3000 was used for microwave-assisted acid extractions. The water used during this study was distilled and checked for impurities before use by the ICP-OES apparatus. Results obtained indicated the absence of any foreign metals. Grade B volumetric flasks and glassware were used in all cases and these were obtained from Merck.

All ICP-OES results given are the average of three replicate readings taken sequentially. These readings were accepted only if the standard deviation of the set was less than two orders of magnitude smaller than the average of the readings. Results not following this requirement were discarded and the reading repeated.

All results were treated using the statistics given in **Paragraph 8.1**. The presence of all elements was checked by scanning at the three most intense analytical wavelengths. If the element was not present at all three of these lines it was taken to be absent entirely.[36,49] The lines used are given in **Table 8-23**. Interferences were checked for and ruled out by analysing for each element individually on the analytical lines for all elements. No interferences were noted.

[49] Winge, R. K., Fassel, V. A., Peterson, V. J., Floyd, M. A., Inductively Coupled Plasma-Atomic Emission Spectroscopy – An Atlas of Spectral Information, 6th Impression, 1993

5.3. INSTRUMENT VALIDATION

At the beginning of every analytical determination the instrument was checked for blockages in the sample introduction system. The piping attached to the peristaltic pump was checked to ensure elasticity and replaced if necessary.

The ICP-OES plasma conditions used in all measurements can be found in **Table 5-1**.

Table 5-1: ICP-OES plasma conditions used in all experiments

Condition	Setting
RF Power (kW)	1.2
Coolant Gas Flow Rate (L/min)	14
Plasma Gas Flow Rate (L/min)	1.2
Carrier Gas Flow Rate (L/min)	0.7

5.3.1 DETECTION LIMITS WITH 5ML HNO_3 AS MATRIX

Five 100ml samples containing 0.4, 1, 2, 5 and 10ppm of each element respectively, except for Zr which concentrations were 10, 20, 30, 40 and 50ppm, were made up, along with a blank, using 5ml 65% HNO_3 as matrix. The calibration curve was drawn and the detection limits were calculated as shown in **Paragraph 9.1** of the Appendix**.** Readings were taken in axial mode. Results are given in **Table 5-2.**

Table 5-2: Detection limits for elements analysed for in HNO_3 sample matrix using the axial read-head

Element	LLOD (ppm)	LLOQ (ppm)
Zr	0.0004406	0.004406
Hf	0.005798	0.05798
Al	0.002838	0.028382
Ca	0.001333	0.013326
Cr	0.003095	0.030952
Mn	0.000357	0.003568
Fe	0.000916	0.009162

5.3.2 Detection limits with 10ml H_2SO_4 as matrix

Five 100ml samples containing 0.4, 1, 2, 5 and 10ppm of each element respectively were made up, along with a blank, using 10ml 98% H_2SO_4 as matrix. The calibration curve was drawn and the detection limits were calculated as shown in **Paragraph 8.1.** Readings were taken in axial mode. Results are given in **Table 5-3.**

Table 5-3: Detection limits for elements analysed for in H_2SO_4 sample matrix using the axial read-head

Element	LLOD (ppm)	LLOQ (ppm)
Zr	0.00166	0.01663
Hf	0.002	0.01995
Mg	0.0008	0.00801
Al	0.00297	0.0297
Si	0.00126	0.01258
Ca	0.00117	0.01172
Ti	8.9E-05	0.00089
Cr	0.00164	0.01635
Fe	0.00109	0.01094

5.4. SAMPLE PREPARATION METHODS AND RESULTS

In the case of ICP-OES it is required that the sample be in aqueous solution with no solid particles present. This in turn requires that the sample be either completely digested or that the residue be removed. In the latter case it is necessary that the incomplete digestion be consistent, and that the extraction of the analytically interesting species be as quantitative as possible.

5.4.1 ACID EXTRACTION

The first method investigated was a simple acid extraction using concentrated nitric acid. 50.1g of zircon ore was placed in a round-bottomed flask along with 50ml of analytically pure 65% nitric acid. This was then attached to a reflux apparatus and boiled for 72 hours. The sample was removed from the reflux apparatus and transferred quantitatively to a 200ml volumetric flask, which was then filled to the mark. 5ml of this solution was transferred with filtering into a 100ml volumetric flask and this was then filled to the mark with distilled water. The samples were analysed using an external calibration curve with the ICP-OES instrument. Readings were taken in axial mode. Results are given in **Table 5-4.**

Table 5-4:Table of results for acid extraction using nitric acid

Element	Zr	Hf	Al	Fe
% Recovery	1.15	0.65	38.76	316.06

5.4.2 INITIAL FLUX FUSION DIGESTION

Approximately 0.2g of zircon ore (in the form of SARM62 certified reference material) was placed in a platinum crucible. To this was added approximately 2g of lithium tetraborate fluxing reagent and this was placed in the high temperature oven set to 1100^{o}C for not less than 4 hours. Digestion was considered complete when no solid sample was visible within the transparent melt. The crucible was allowed to cool to room

temperature and then half-filled with 3.25% nitric acid and allowed to stir overnight. More 3.25% nitric acid was then added to the top of the crust formed by the insoluble $H_2B_4O_7$. This solution was transferred quantitatively to a 100ml flask and the previous step was repeated. This second quantity of sample was added to the first in the 100ml flask, which was then filled to the mark with distilled water. The solution was allowed to stand overnight to ensure complete dissolution of the $Li_2B_4O_7$. This solution was analysed using an external calibration curve without matrix matching. Readings were taken in axial mode. The results can be seen in **Table 5-5** and the raw data can be seen in **Table 8-3**. The data for a typical external calibration curve can be seen in **Table 8-4**.

Table 5-5: Table of results from direct reading of flux fusion mother solution

Metal	% Recovery	Recovery (Mass %)	SARM62 Certified Value (Mass %)	Literature 95% Confidence Limits of SARM62	
				Low	High
Zr	83.86	53.84	64.2	63.8	65.4
Hf	88.63	1.16	1.31	1.01	1.36
Al	134.96	1.19	0.88	0.62	1.06
Fe	129.36	0.09	0.07	0.06	0.07

5.4.3 Determination of the Effect of the Amount of Flux on Analytical Results

Five 100ml samples were prepared, each containing 20ppm Zr, 2ppm Fe, Al, and Hf, 5ml 65% nitric acid as well as 0, 0.1, 0.5, 1 and 2g of lithium tetraborate respectively. These were analysed using an external calibration curve. This was done in triplicate. The results are the average of nine replicate readings. Graphs of these results can be seen in **Figures 5-2 – 5-5** and the recovery percentages can be seen in **Table 8-24.** Readings were taken in axial mode.

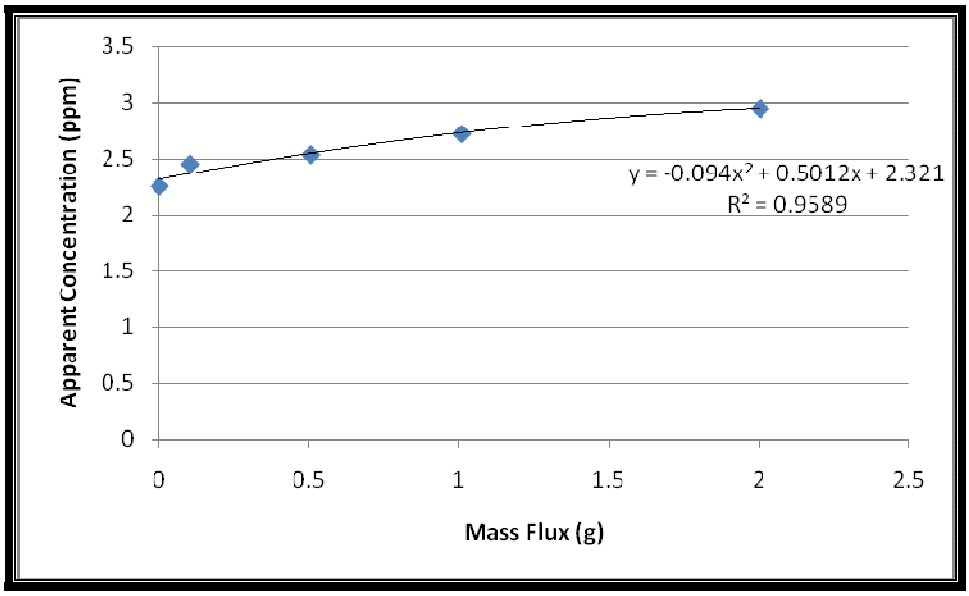

Figure 5-2: Influence of flux on the aluminium results – 2ppm Al, 5ml HNO_3, varying mass of $Li_2B_4O_7$

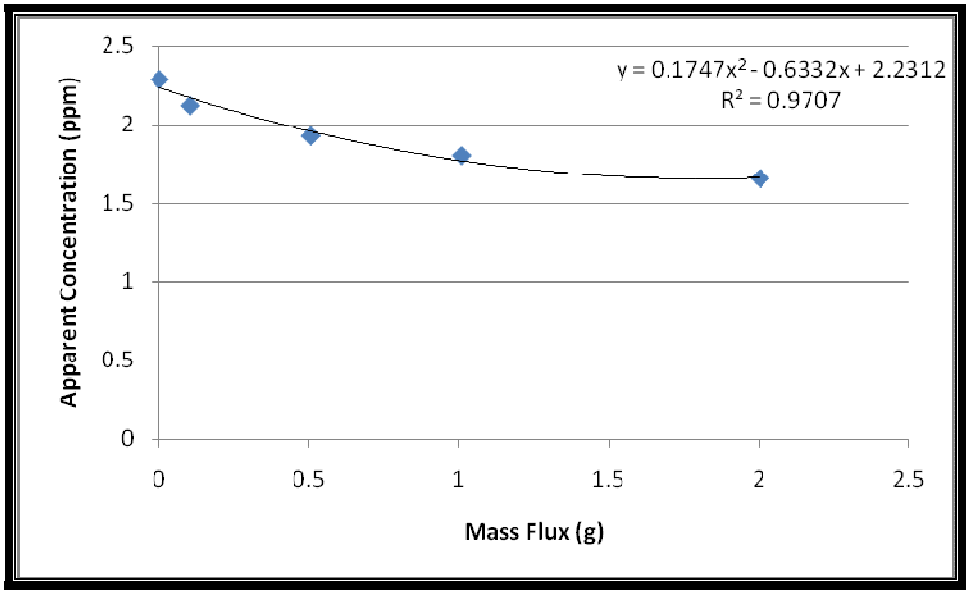

Figure 5-3: Influence of flux on the iron results – 2ppm Fe, 5ml HNO_3, varying mass of $Li_2B_4O_7$

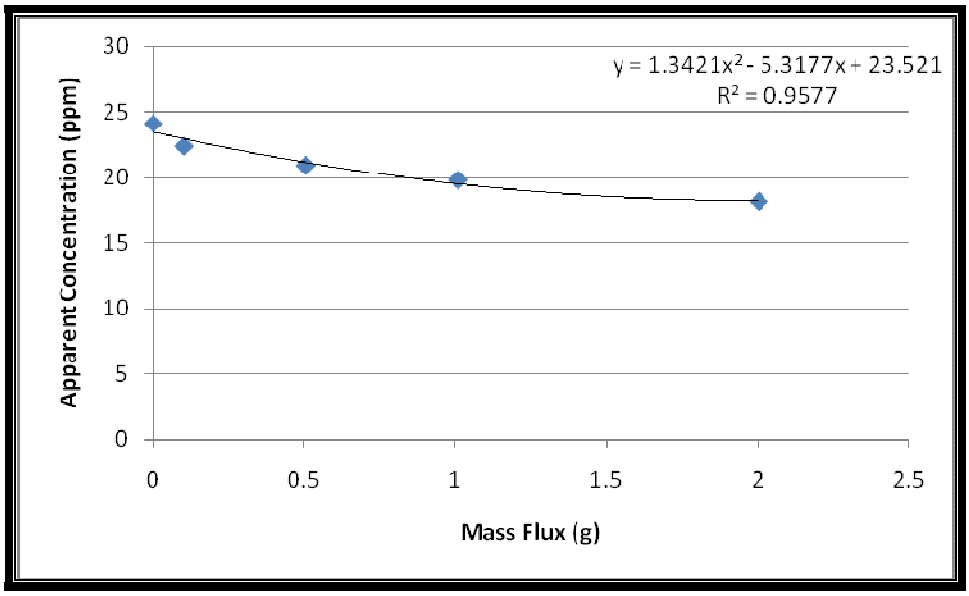

Figure 5-4: Influence of flux on the zirconium results – 20ppm Zr, 5ml HNO_3, varying mass of $Li_2B_4O_7$

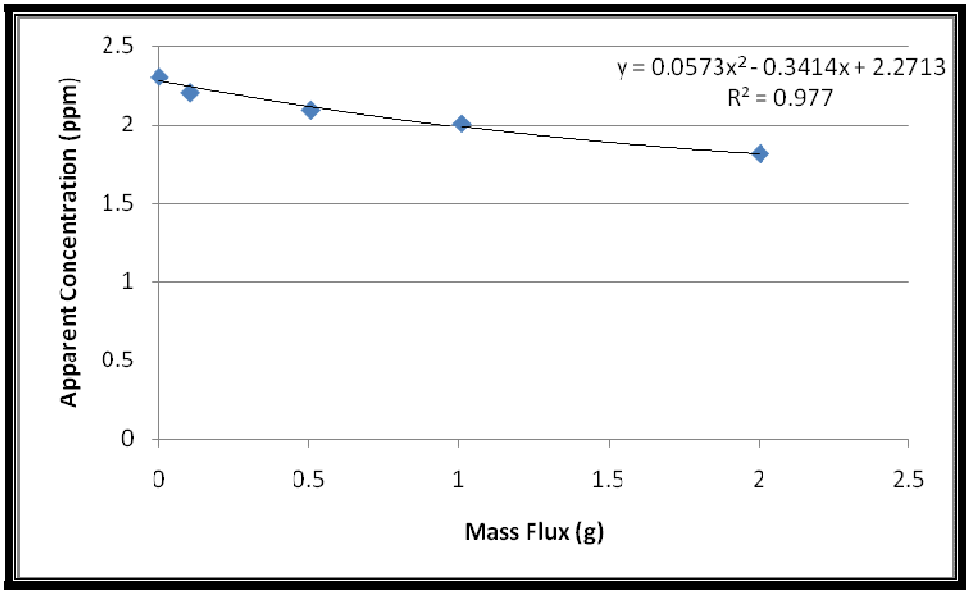

Figure 5-5: Influence of flux on the hafnium results – 2ppm Hf, 5ml HNO_3, varying mass of $Li_2B_4O_7$

5.4.4 INITIAL FLUX FUSION STANDARD ADDITION METHOD

Approximately 0.2g of zircon ore (in the form of SARM62 certified reference material) was weighed accurately and placed in a platinum crucible. To this was added approximately 2g of lithium tetraborate fluxing reagent and this was placed in the high temperature oven set to 1100^{o}C for 4 hours. Digestion was considered complete when no solid sample was visible within the transparent melt. The crucible was allowed to cool to room temperature and then half-filled with 3.25% nitric acid and allowed to stir overnight. More 3.25% nitric acid was then added to the top of the crust formed by the insoluble $H_2B_4O_7$. This solution was transferred quantitatively to a 100ml flask and the previous step was repeated. This second quantity of sample was added to the first in the 100ml flask, which was then filled to the mark with distilled water. The solution was allowed to stand overnight to ensure complete dissolution of the $H_2B_4O_7$. 5ml 65% nitric acid and 5ml of sample solution were added to each of 5 100ml volumetric flasks. Standard solutions were added to each of these flasks to yield concentrations of 1, 2, 3, 4 and 5 ppm respectively of Hf, Al, Fe, Mg, Ca, Cr and volumes of Zr standard were added to make concentrations of 10, 20, 30, 40 and 50 ppm. A dark yellow colour (see **Figure 8-1**) was observed in the solution at this point. The flasks were filled to the mark and allowed to stand overnight before ICP-OES analysis. The yellow colour disappeared immediately upon the addition of water. This was done in triplicate. Readings were taken in axial mode. These results can be seen in **Table 5-6**.

Initially the solutions were analysed immediately upon being filled. A typical set of results for this can be seen in **Figures 5-6** – **5-9**. The raw data is provided in **Table 8-6**.

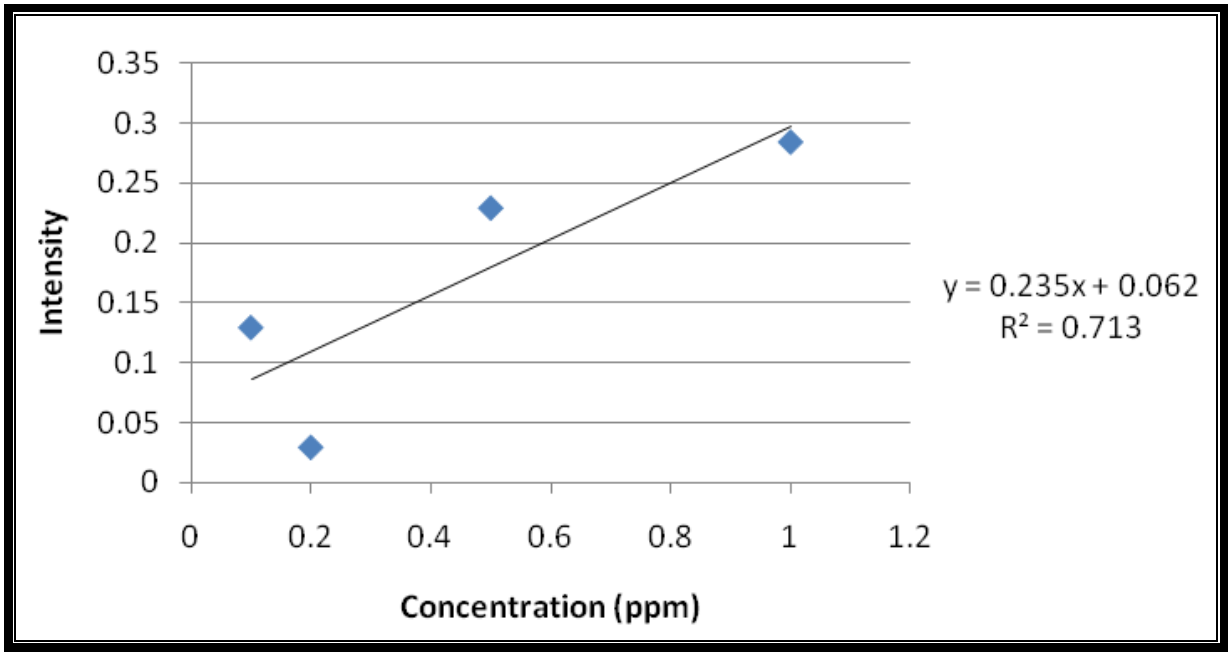

Figure 5-6: Calibration curve for aluminium immediately after preparation – 5ml mother solution, 5ml HNO_3, varying concentrations of standards

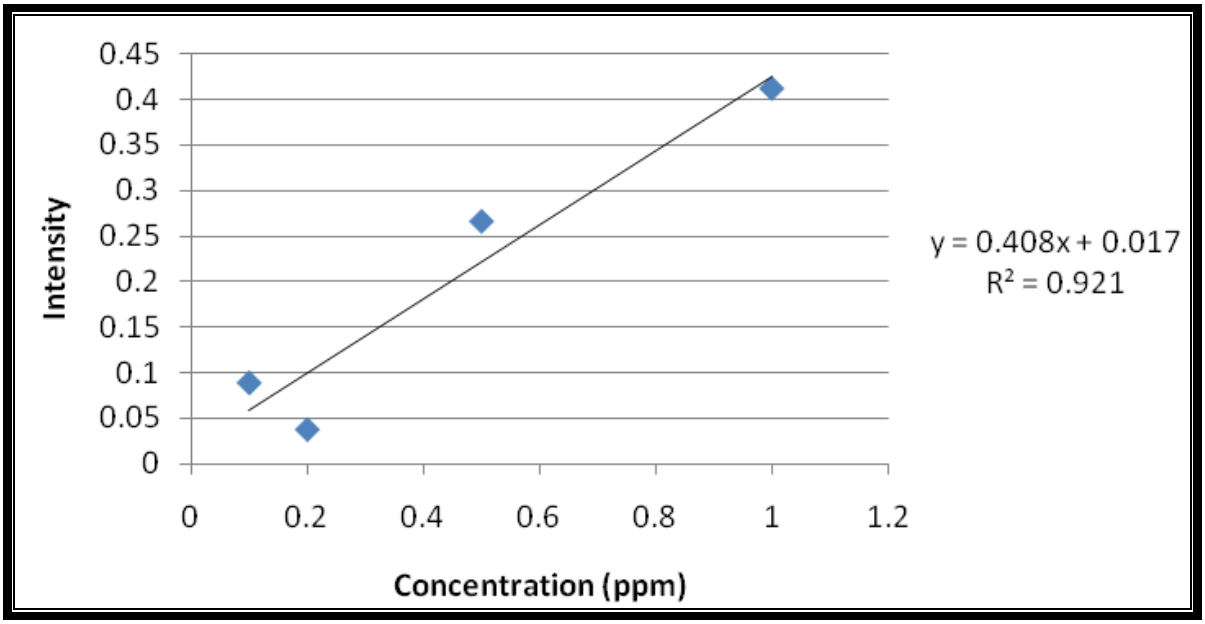

Figure 5-7: Calibration curve for iron immediately after preparation – 5ml mother solution, 5ml HNO_3, varying concentrations of standards

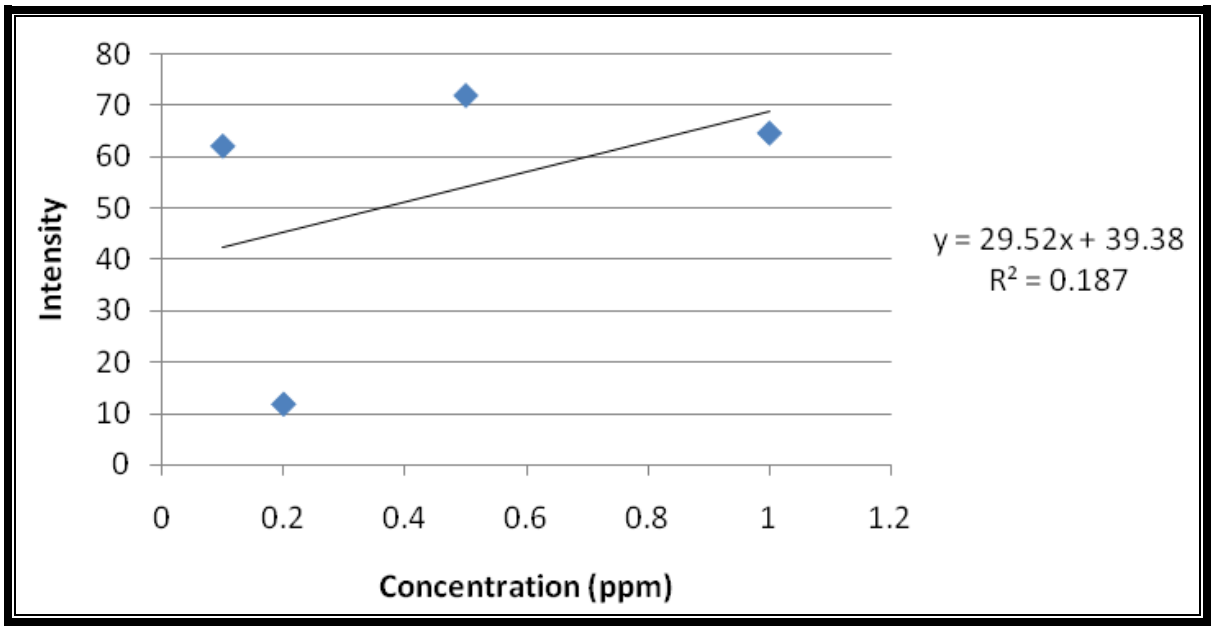

Figure 5-8: Calibration curve for zirconium immediately after preparation – 5ml mother solution, 5ml HNO_3, varying concentrations of standards

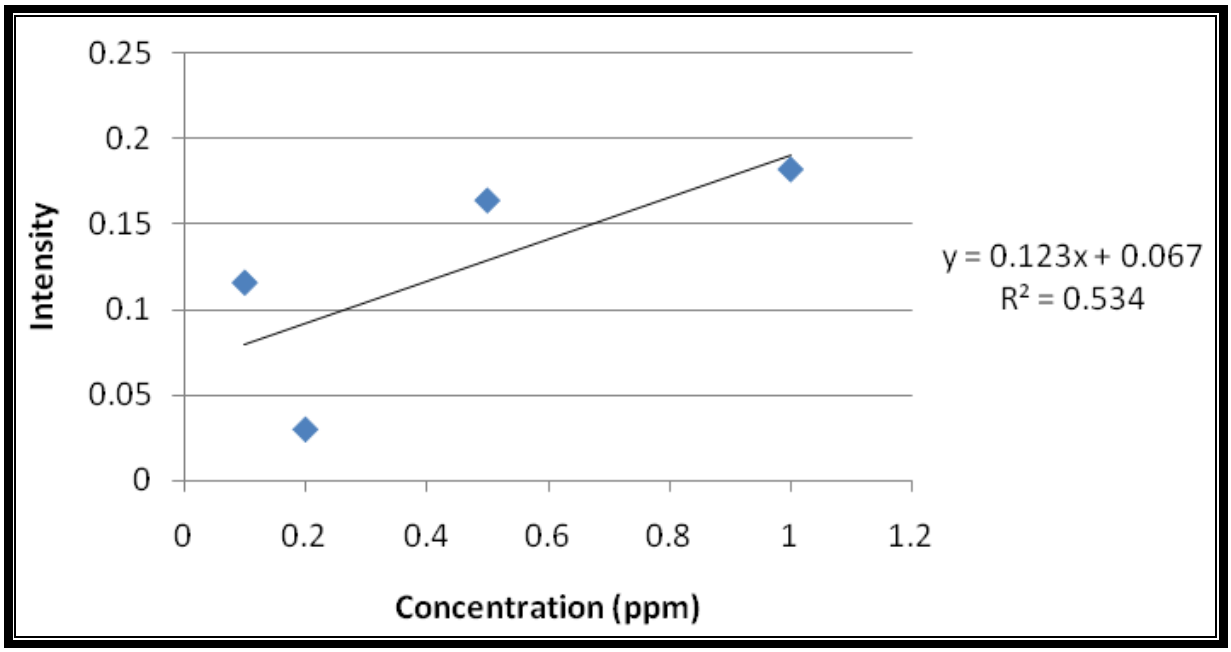

Figure 5-9: Calibration curve for hafnium immediately after preparation – 5ml mother solution, 5ml HNO_3, varying concentrations of standards

The calibration curves improved greatly after the standard solutions were allowed to stabilise overnight, a typical example of which can be seen in **Figures 5-10 – 5-13**. **Figures 5-6 - 5-9** as well as **Figures 5-10 - 5-13** were chosen as representative examples and are not consecutive readings of the same samples.

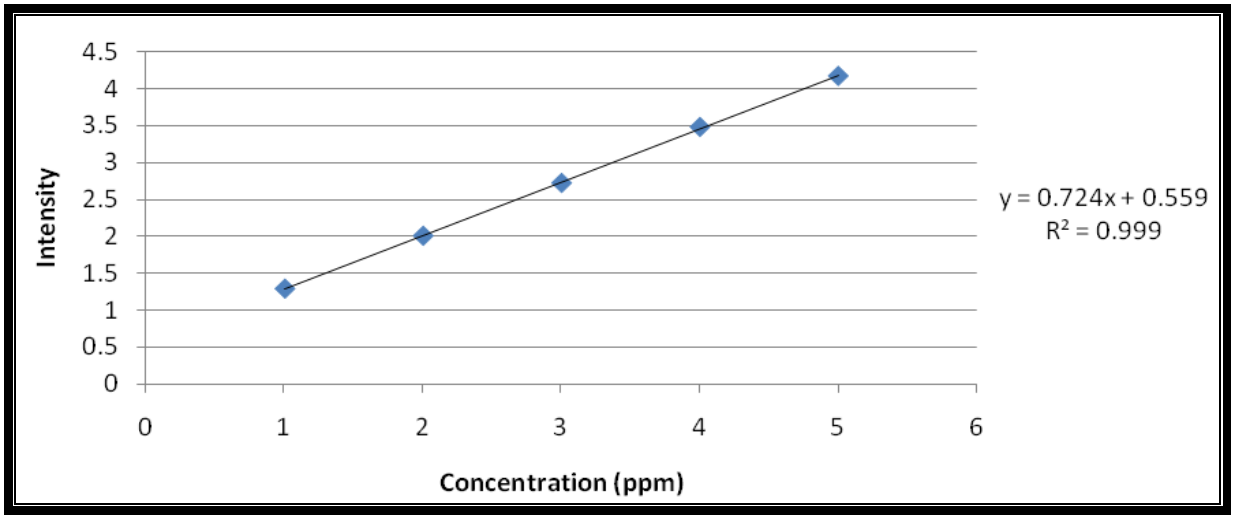

Figure 5-10: Aluminium calibration curve after standing overnight - 5ml mother solution, 5ml HNO_3, varying concentrations of standards

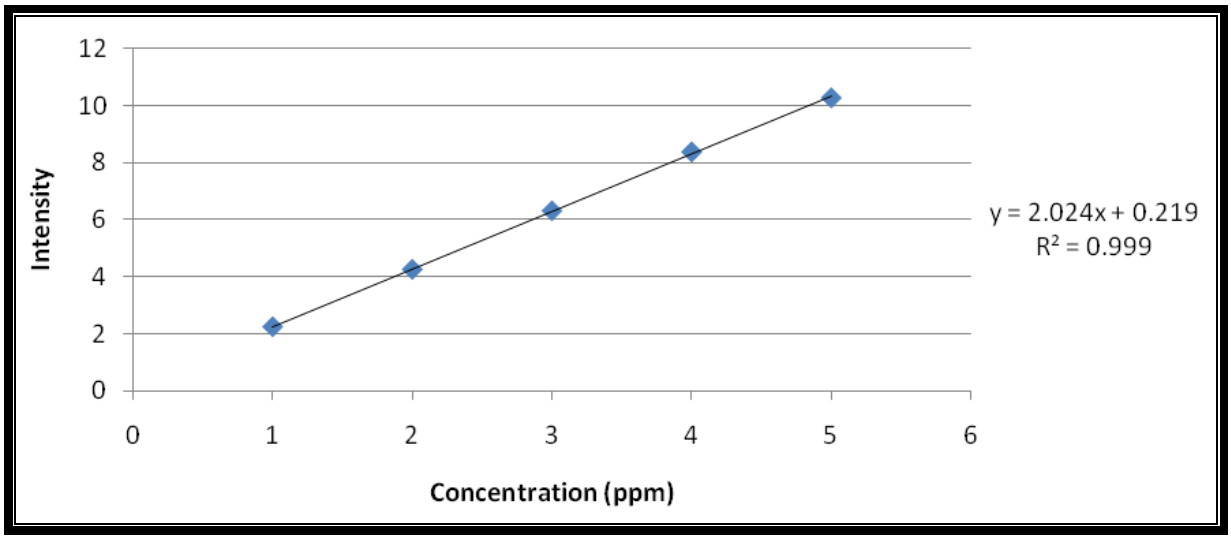

Figure 5-11: Iron calibration curve after standing overnight - 5ml mother solution, 5ml HNO_3, varying concentrations of standards

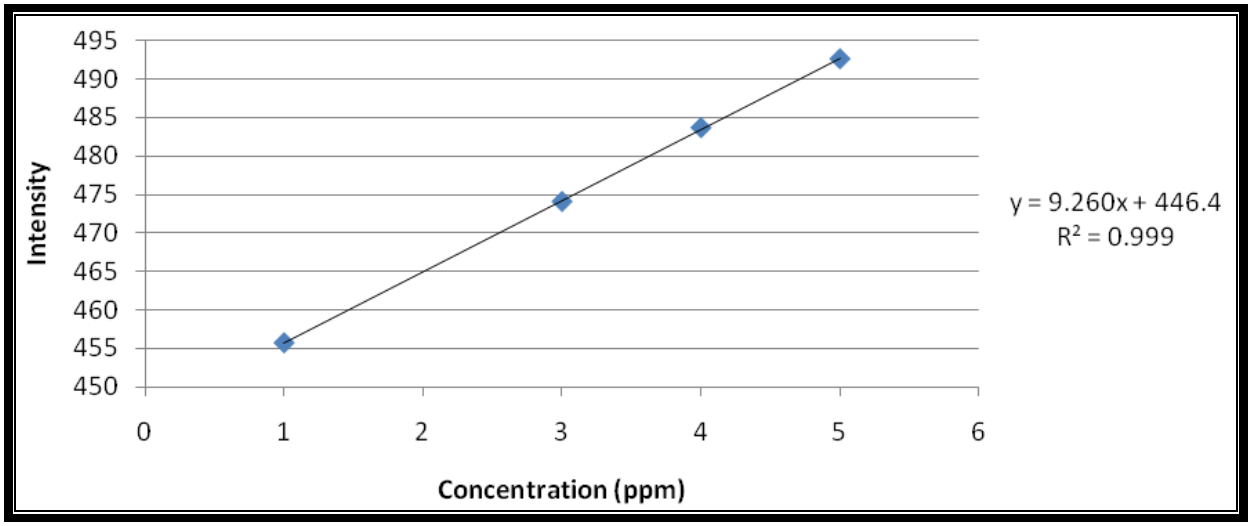

Figure 5-12: Zirconium calibration curve after standing overnight - 5ml mother solution, 5ml HNO_3, varying concentrations of standards

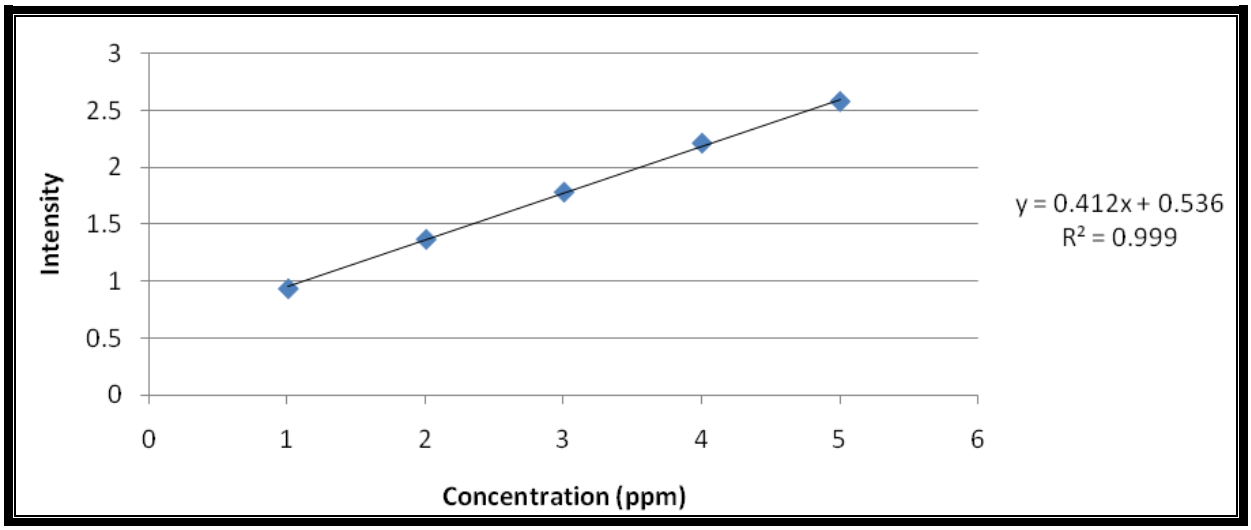

Figure 5-13: Hafnium calibration curve after standing overnight - 5ml mother solution, 5ml HNO_3, varying concentrations of standards

Table 5-6: Initial results for flux fusion standard addition method.

Metal	Average %	Percentage Recovery	SARM62 Certified Value %	Literature 95% Confidence Limits of SARM62	
				Low	High
Zr	67.65 ± 3.19	105.37	64.2	63.8	65.4
Hf	1.26 ± 0.06	96.18	1.31	1.01	1.36
Al	1.00 ± 0.01	113.64	0.88	0.62	1.06
Fe	0.10 ± 0.07	142.86	0.07	0.06	0.07

5.4.5 First modified Flux Fusion Standard Addition Method Digestion (modifications in bold)

Approximately 0.2g of zircon ore (in the form of SARM62 certified reference material) was weighed accurately and placed in a platinum crucible. To this was added approximately 2g of lithium tetraborate fluxing reagent and this was placed in a Labequip high temperature oven set to 1100^{o}C for not less than 4 hours. Digestion was

considered complete when no solid sample was visible within the transparent melt. **The crucible was immediately upon removal from the oven placed in a plastic container filled with 200ml 3.25% nitric acid solution and allowed to stir until complete dissolution of the sample was achieved. This solution was transferred quantitatively to a 250ml plastic volumetric flask and filled to the mark with distilled water.** 5ml 65% nitric acid and **12.5ml** of sample solution was added to each of 5 **plastic** 100ml volumetric flasks. Standard solutions were added to each of these flasks to make concentrations of 1, 2, 3, 4 and 5 ppm respectively of Hf, Al, Fe, Ti and volumes of Zr standard were added to make concentrations of 10, 20, 30, 40 and 50 ppm. A dark yellow colour (see **Figure 8-1**) was observed in the solution at this point. The flasks were filled to the mark and allowed to stand overnight before ICP-OES analysis. The yellow colour disappeared immediately upon the addition of water. Readings were taken in axial mode. The results using this method can be seen in **Table 5-7.**

Table 5-7: Recovery of elements after the introduction of larger volumes of dilute acid solvent and using plastic (polyethylene) containers.

Sample No.	Zr (Mass %)	Zr % Recovery	Hf (Mass %)	Hf % Recovery	Al (Mass %)	Al % Recovery	Fe (Mass %)	Fe % Recovery	Ti (Mass %)	Ti % Recovery
1	34.75	54.12	2.74	209.50	0.94	106.43	0.03	37.04	0.02	15.29
2	61.48	95.76	3.28	250.71	0.47	52.89	0.12	164.76	0.11	88.09
3	134.72	209.85	3.56	272.01	1.25	141.78	0.17	247.69	0.13	100.18
4	108.77	169.43	3.77	288.08	0.53	60.33	0.19	264.82	0.23	178.07
5	62.91	97.99	3.42	261.12	1.17	133.37	0.13	188.59	0.16	119.44
6	72.65	113.17	3.58	273.07	0.44	49.73	0.08	107.50	0.11	86.88
Average	80.53	**125.43**	3.36	**256.28**	0.87	**98.96**	0.13	**180.58**	0.13	**100.21**
Standard Deviation	40.32	62.81	0.39	29.59	0.36	40.89	0.06	90.16	0.08	58.76
Relative Standard Deviation	50.08	50.08	11.54	11.54	41.32	41.32	49.93	49.93	58.59	58.59

The entire procedure was repeated six times on six different days.

5.4.6 Second modified Flux Fusion Standard Addition Method Digestion (modifications in bold)

Approximately 0.2g of zircon ore (in the form of SARM62 certified reference material) was weighed accurately and placed in a platinum crucible. To this was added approximately 2g of lithium tetraborate fluxing reagent and this was placed in a

Labequip high temperature oven set to 1100^{o}C for not less than 4 hours. Digestion was considered complete when no solid sample was visible within the transparent melt. **Upon complete digestion the platinum crucible was removed from the high temperature oven and immediately cooled by direct contact with water in a water bath, in order to crack the melt, facilitating faster dissolution times.** The crucible was placed in a plastic container filled with **150ml** 3.25% nitric acid solution and allowed to stir until complete dissolution of the sample was achieved. This solution was transferred quantitatively to a **200ml glass** volumetric flask and filled to the mark with distilled water. 5ml 65% nitric acid and **10ml** of sample solution was added to each of 5 **glass** 100ml volumetric flasks. Standard solutions were added to each of these flasks to make concentrations of 1, 2, 3, 4 and 5 ppm respectively of Hf, Al, Si, Ti and Fe and volumes of Zr standard were added to make concentrations of 10, 20, 30, 40 and 50 ppm. A dark yellow colour (see **Figure 8-1**) was observed in the solution at this point. The flasks were filled to the mark and allowed to stand overnight before ICP-OES analysis. The yellow colour disappeared immediately upon the addition of water. Results are shown in **Table 5-8**. **Readings were taken without the use of the axial read head of the ICP-OES apparatus, that is to say, radial readings were taken.**

Table 5-8: Recovery of the elements after the introduction of the sample into cold water immediately upon digestion

	Zr % Extraction	Hf % Extraction	Al % Extraction	Fe % Extraction	Ti % Extraction	Si % Extraction
1	98.6	124.08	130.60	90.88	---	---
2	122.43	127.21	172.82	333.12	109.37	135.29
3	107.02	123.02	179.61	238.24	---	---
4	102.79	155.32	174.37	225.16	115.11	138.94
5	98.06	127.92	158.52	197.43	---	---
6	89.98	142.55	159.03	165.06	128.90	174.86
7	97.67	116.97	165.56	220.94	120.93	82.54
Average	**102.37**	**131.01**	**162.93**	**210.12**	**118.58**	**132.91**
Standard Deviation	10.27	13.27	16.30	73.79	8.34	38.03
Relative Standard Deviation	10.03	10.13	10.00	35.12	7.04	28.62

The entire procedure was repeated six times on six different days.

5.4.7 Results of Inter-Lab Analysis using Internal Standard Method

A sample of both SARM62 and PDZ was sent to Analytical Services laboratories in order to obtain an external result confirming the validity of the digestion method. The sample was digested using lithium tetraborate flux and analysed with an external calibration curve using cobalt as an internal standard. These results can be seen in **Table 5-9**.

Table 5-9: Table showing results of inter-lab analysis

Metal	SARM62 (Mass %)	SARM62 (% Recovery)	PDZ (Mass %)	PDZ (% Recovery)
Zr	64.5	100.47	64.3	100.16
Hf	1.33	101.6	1.30	99.54
Fe	0.05	74.29	0.04	51.43
Al	0.82	92.73	1.14	129.89
Si	32.6	99.39	32.1	97.87
Ti	0.05	39.23	0.05	35.38

5.4.8 Results of Intra-Lab Analysis using the Second Modified Flux Fusion Standard Addition Method

An intra-lab confirmation of results was carried out by supplying another Master's level student (Mr M. Nete) with a SARM62 sample and the method given in **Paragraph 5.4.6**. The results were as shown in **Table 5-10**.

Table 5-10: Table showing results of intra-lab analysis

Metal	% Recovery	Recovery (Mass %)	SARM62 Certified Value (Mass %)	Literature 95% Confidence Limits of SARM62	
				Low	High
Zr	105.33	67.62	64.2	63.8	65.4
Hf	100.76	1.32	1.31	1.01	1.36
Al	69.32	0.61	0.88	0.62	1.06
Fe	114.29	0.08	0.07	0.06	0.07
Ti	15.38	0.02	0.13	0.12	0.14
Si	66.55	21.83	32.8	32.5	33.2

5.4.9 Initial Microwave Assisted Acid Extraction[38]

All reagents and the sample were placed within the reaction vessels which were then tightly sealed and subjected to a set microwave program. Unless otherwise stated 10ml sulphuric acid was used as digestion medium. Approximately 15 minutes at 1200 Watts was required for the samples to reach maximum temperature. Upon completion of the microwave program the samples were diluted with approximately 20ml of distilled water and then quantitatively transferred with filtering into 100ml volumetric flasks. The samples were filled to the mark, shaken, allowed to cool and again filled to the mark. All samples were analysed using ICP-OES and an external calibration curve that was matrix matched as far as possible.

An initial experiment was conducted to determine which conditions might prove to be most favourable for digestion. 0.4g of either SARM62 or PDZ was weighed off in each case and to each was added a different digestion reagent with the reagents and results

for this experiment seen in **Table 5-11**. $(NH_4)_2SO_4$, a variety of acids as well as alkali were tested to determine their effect on the microwave digestion. The conditions of the experiment were 315 Watts for 15 minutes then 630 Watts for 30 minutes at 60 bar. The maximum temperature reached by each individual sample was dependent upon which reagents were present and the boiling points of the various components and additives in the sample. Readings were taken in axial mode.

Table 5-11:Table showing initial microwave experiment results using various reagents

No.	Sample	Reagents	Max Temperature Reached	Zr % Recovery	Hf % Recovery	Al % Recovery	Fe % Recovery
1	SARM62	4g $(NH_4)_2SO_4$, 10ml H_2SO_4	±240 ℃	4.58	4.01	51.05	73.14
2	SARM62	4g $(NH_4)_2SO_4$, 10ml H_2SO_4, 10ml H_2O	±140 ℃	2.43	2.20	49.81	90.00
3	SARM62	10ml H_2SO_4	±240 ℃	6.41	7.17	72.53	68.86
4	PDZ	10ml H_2SO_4	±240 ℃	14.58	18.31	7.18	15.14
5	PDZ	4g $(NH_4)_2SO_4$, 10ml H_2SO_4	±240 ℃	1.53	1.63	2.89	8.43
6	PDZ	4g $(NH_4)_2SO_4$, 10ml H_2SO_4, 10ml H_2O	±140 ℃	0.13	0.12	3.08	8.00
7	PDZ	2ml HNO_3, 8ml HCl	±140 ℃	0.03	0.26	2.82	8.14
8	PDZ	10ml 8M NaOH	±140 ℃	0.20	0.24	18.82	17.00

5.4.10 Microwave Assisted Extraction with Varying Quantities of Ammonium Sulphate

0.4g of either SARM62 or PDZ was weighed off in each case and to each was added a different quantity of ammonium sulphate as seen in **Table 5-12**. To each was added 10ml H_2SO_4. The conditions of the experiment were 1200 Watts for **30 minutes**, ±240℃ and 60 bar pressure. Upon completion of the microwave program the samples were

diluted with approximately 20ml of distilled water and then quantitatively transferred with filtering into 100ml volumetric flasks. The samples were filled to the mark, shaken, allowed to cool and again filled to the mark. All samples were analysed using ICP-OES and an external calibration curve that was matrix matched as far as possible. Readings were taken in axial mode. A graph showing the effect of the ammonium sulphate can be seen in **Figure 5-14**.

Table 5-12: Table showing the effect of varying amounts of ammonium sulphate on % recovery of different elements

No.	Sample	Mass $(NH_4)_2SO_4$ (g)	Zr % Recovery	Hf % Recovery	Al % Recovery	Fe % Recovery
1	SARM62	0	10.44	10.51	94.19	99.52
2	SARM62	1.0596	9.57	10.23	145.58	140.94
3	SARM62	2.0449	12.21	12.88	158.20	149.26
4	SARM62	3.0507	10.64	10.71	140.33	142.69
5	SARM62	3.9895	11.30	11.94	130.20	140.47
6	SARM62	5.0484	14.31	15.36	145.03	153.57
7	SARM62	6.0737	17.36	19.88	141.81	138.73
8	PDZ	0	57.79	83.77	28.17	46.74

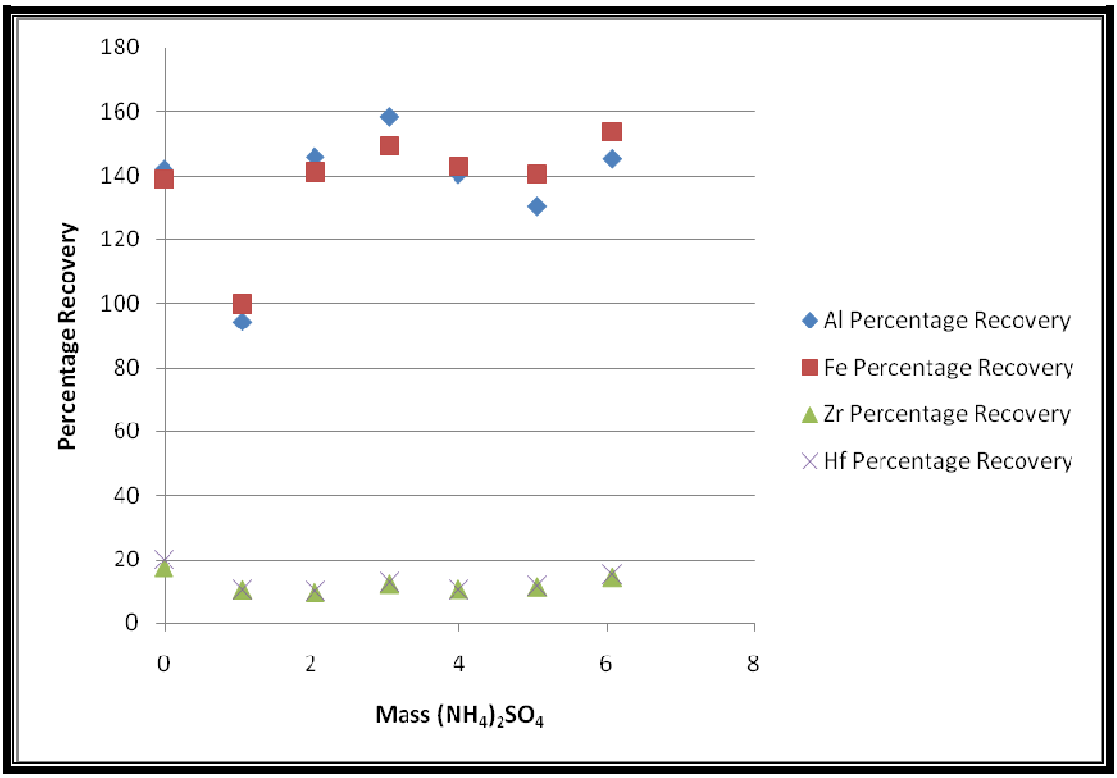

Figure 5-14: The relationship between mass $(NH_4)_2SO_4$ and percentage extraction of Zr and Hf from SARM62 using microwave assisted digestion - 1200 Watts for **30 minutes**, ±240 ℃ and 60 bar pressure

5.4.11 Microwave Assisted Extraction with Varying Ratio of Sample Mass to Digestion Medium

Different weights (0.1 to 0.4g) of SARM62 and PDZ samples were weighed off accurately in each case. To each was added 10ml H_2SO_4. The conditions of the experiment were 1200 Watts for **3 hours**, ±240℃ and 60 bar pressure. Upon completion of the microwave program the samples were diluted with approximately 20ml of distilled water and then quantitatively transferred with filtering into 100ml volumetric flasks. The samples were filled to the mark, shaken, allowed to cool and again filled to the mark. All samples were analysed using ICP-OES and an external calibration curve that was matrix matched as far as possible. Readings were taken in axial mode. These results can be seen in **Table 5-13** and **Figure 5-10**.

Table 5-13:Table showing differences in percentage extraction with differing ratio of sample mass to digesting medium for SARM62 and PDZ.

No.	Sample	Mass Sample (g)	Zr % Recovery	Hf % Recovery	Al % Recovery	Fe % Recovery
1	SARM62	0.1050	9.66	10.32	74.45	77.95
2	SARM62	0.2002	9.61	10.28	71.84	72.80
3	SARM62	0.2987	11.10	11.77	78.31	71.56
4	SARM62	0.4082	12.27	11.87	76.41	62.48
5	PDZ	0.1000	44.39	49.75	17.79	41.25
6	PDZ	0.2055	37.86	48.49	16.01	28.11
7	PDZ	0.3112	34.51	45.70	16.88	22.91
8	PDZ	0.4273	28.97	40.94	14.93	20.90

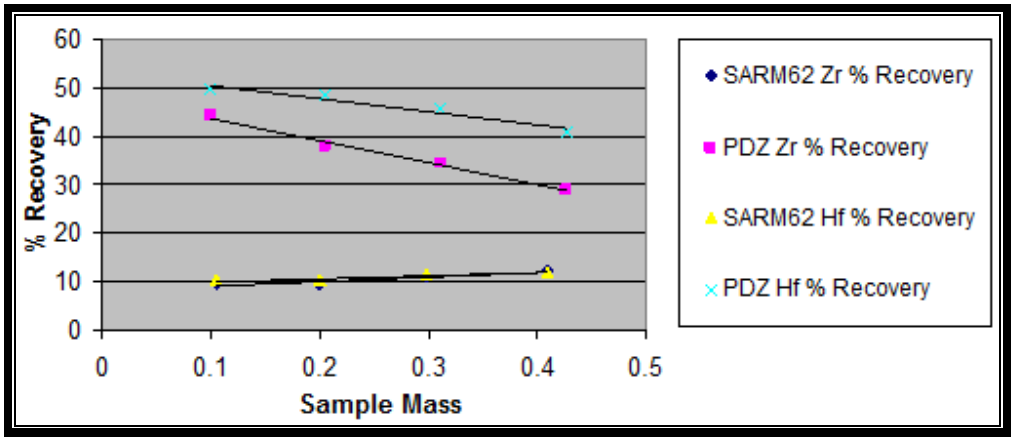

Figure 5-15:Change in percentage extraction with increasing sample mass to digestion medium ratio - 1200 Watts for **3 hours**, ±240 ℃ and 60 bar pressure

This experiment was repeated using only PDZ and without additives such as ammonium sulphate, with the conditions being the same for all but the duration of the extraction.

The samples were subjected to 1200 watts of microwave energy for only 30 minutes, instead of the previous 3 hours. In all other aspects the conditions were identical to those in **Paragraph 5.4.10**. The results can be seen in **Table 5-14** and **Figure 5-16**.

Table 5-14: Table showing differences in percentage extraction with differing ratio of sample mass to digesting medium for PDZ only.

No.	Mass Sample (g)	Zr % Recovery	Hf % Recovery	Al % Recovery	Fe % Recovery	Si % Recovery	Ti % Recovery
1	0.1022	1.75	1.41	1.05	0.00	0.34	24.48
2	0.201	1.59	1.44	1.29	0.00	0.17	18.32
3	0.3076	2.29	2.30	1.86	1.73	0.12	25.39
4	0.4005	2.80	2.87	2.53	4.19	0.10	27.19
5	0.5016	3.99	4.20	7.04	23.61	0.08	36.25
6	0.6018	3.86	4.07	3.32	5.12	0.06	28.54
7	0.7282	4.31	4.56	3.61	6.10	0.06	35.44
8	0.8012	4.14	4.49	3.41	4.56	0.07	24.31

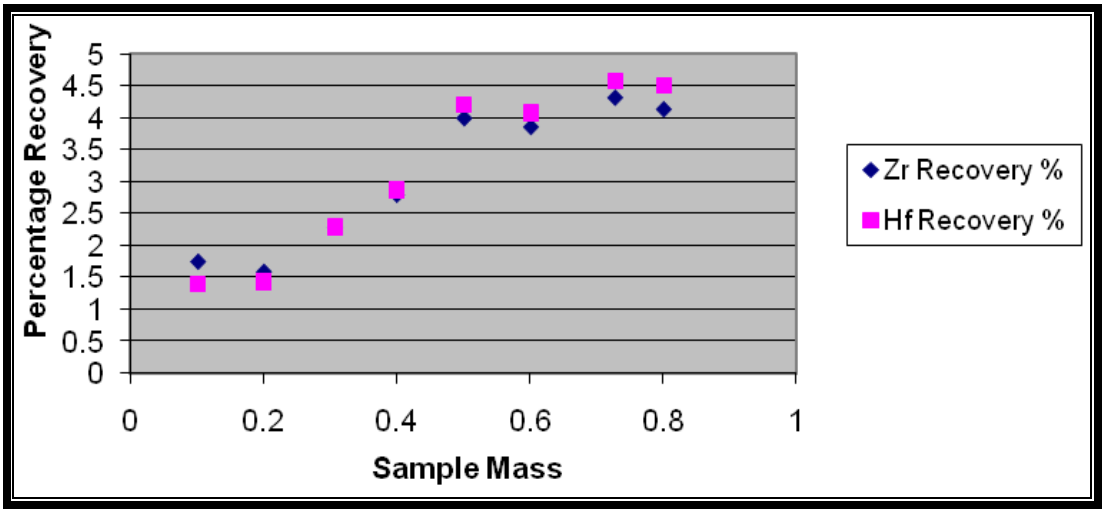

Figure 5-16: Difference in percentage extraction between Zr and Hf with increasing sample mass to digestion medium ratio - 1200 Watts for **30 minutes**, ±240℃ and 60 bar pressure

5.4.12 Microwave Assisted Extraction with Fluoride Containing Additives

Samples of approximately 0.5g of PDZ were weighed off accurately in each case as seen **Table 5-15**. To each was added 10ml H_2SO_4 as well as a fluoride containing additive, such as potassium fluoride or ammonium bifluoride, in some cases. The conditions of the experiment were 1200 Watts for 30 minutes, ±240℃ and 60 bar pressure. Upon completion of the microwave program the samples were diluted with approximately 20ml of distilled water and then quantitatively transferred with filtering into 100ml volumetric flasks. The samples were filled to the mark, shaken, allowed to cool and again filled to the mark. All samples were analysed using ICP-OES and an external calibration curve that was matrix matched as far as possible. Readings were taken in axial mode.

Table 5-15: Percentage recovery with and without fluoride containing additives

No.	Sample	Additive	Zr % Recovery	Hf % Recovery	Al % Recovery	Fe % Recovery
1	PDZ	none	15.37	16.96	11.58	12.93
2	PDZ	none	9.15	10.26	7.14	9.29
3	PDZ	none	15.29	16.87	11.89	12.07
4	PDZ	0.4573g $NH_4F.HF$	36.37	40.60	34.9	55.26
5	PDZ	0.4219g $NH_4F.HF$	34.18	37.43	32.70	83.51
6	PDZ	0.4701g $NH_4F.HF$	37.10	40.98	34.63	54.87
7	PDZ	0.4202g KF	28.41	31.93	27.75	46.86
8	PDZ	0.4499g KF	28.04	31.22	26.57	46.04

5.5. CONCLUSION

The effect of the lithium tetraborate as well as the other matrix elements, as seen in **Figures 5-2 - 5-5** and **Table 8-24** where it can be seen that the simple presence of these elements causes noticeable errors in recovery, clearly indicates the necessity for a matrix correcting method, such as the standard addition method used. Matrix matching was not used in the case of the flux fusion method as attempting to match the standards closely enough to the samples, in terms of flux concentration, was deemed to be more labour intensive and would allow for a greater degree of error than the standard addition method. This was due to the large degree of error seen with even a slight alteration in the quantity of flux in solution.

PDZ was more heavily used in the microwave assisted acid extraction procedure, due to its greater chemical amenability to acid digestion, in the hopes of gaining more quantitative extractions.

Chapter 6: Discussion and Conclusion

6.1. INTRODUCTION

Two main digestion and analytical procedures were investigated for their ability to analyse for the major and minor components of zircon ore and PDZ. Various method modifications and conditions were investigated with varying degrees of success. The results obtained were compared to the known values of each element present in the certified reference material and the effectiveness of each method and modification was measured with respect to this.

6.2. INSTRUMENT VALIDATION

The detection limits as determined in **Paragraph 5.2 and 5.3** were used to ensure that the results obtained from instrumental analysis were valid. Quantification limits as low as 0.0044ppm for Zr and 0.058ppm for Hf were obtained, these being well below the levels at which the elements were present. Quantification limits for Al and Fe were not much lower than the concentrations present which may be a contributing factor in the errors observed. Instrument responses were monitored throughout the study in order to ensure that the detection limit was not affected. This was of particular concern when the axial read head of the instrument was used as the mirror inside became progressively dirtier, requiring regular cleaning to ensure maintained low detection limits.

6.3. METHOD VALIDATION[50]

In essence, all work done on the flux fusion standard addition method constitutes an attempt to validate the method used. The SARM62 certified reference material was used in all determinations as it provided a known quantity against which any and all results could be judged. The method was at all times scrutinised for linearity of calibration curves, accuracy, precision, robustness and specificity.

With respect to linearity all calibration curves demonstrated R^2 values of better than 0.999 (see **Figures 5-10** to **5-13**) which is greater than the lowest acceptable value of 0.997.[50] At least 5 concentrations of standard were used in all calibrations. Accuracy was determined by the closeness of the average of a data set to the accepted true value of the SARM62 certified reference material. In the beginning of the study it was decided that, due to the complexity of the matrix, a deviation of 4-6% for the major components would be acceptable, rather than the usual 2%. The minor components were judged acceptable if within a 20-30% envelope as this coincided with the concentrations range of the certified values in the reference material. Precision was gauged using the standard deviation of the results averaged. The greater the standard deviation, the less precision achieved. Robustness was evaluated by considering the difference in analytical results after applying small, deliberate changes to the method, and specificity was achieved by selecting analytical lines free of interference. Analytical lines evaluated are seen in **Table 8-23.** The first order lines were found to be acceptable in all cases.

[50] Chan, C. C., Lee, Y. C., Zhang, X-M, Analytical Method Validation and Instrument Performance Verification, Wiley-Interscience, 2004

6.4. ACID EXTRACTION

An acid extraction was initially attempted as this has been a tried and true method of analysing various elements in ores. Nitric acid was used because of its strong oxidizing properties. The extremely low extractions (see **Table 5-4)** of zirconium and hafnium were expected due to the inert nature of the ore. A higher degree of extraction was obtained for aluminium and iron, with the iron over-reading significantly. The extremely low levels of aluminium and iron present in the samples allows for a significant percentage deviation without a large difference in actual recovery. The 200% over-recovery corresponds to a reading of 0.21% mass instead of 0.07%. However Al and Fe are ubiquitous and contamination must also be considered as a possibility, especially when using concentrated acids as was the case here. This may explain the surprisingly high levels of iron apparently present. This high level of extraction for Al and Fe, as opposed to that of the Zr and Hf, may allow for a pre-extraction process of the majority of these impurities before the plasma dissociation step of the refinement procedure. This would remove the necessity of separating these impurities later in the purification process.

6.5. FLUX FUSION STANDARD ADDITION METHOD[42]

Due to the expected failure of the acid extraction it became necessary to find other methods to digest the ore. A common method for the quantitative digestion of zircon ore is the use of a flux fusion (discussed in **Paragraph 3.3.1**). Lithium tetraborate was chosen to perform the fusions due to its availability and ability to completely dissolve silicate matrices. No literature was found relating to the dissolution of zircon or PDZ-like substances using the tetraborate flux and this method is, to our knowledge, unique. Other fluxes known to be capable of digesting zircon are the alkali hydroxide and carbonate fluxes. These, however, cause the silica to precipitate out upon dissolution with dilute acid making quantitative analysis of the silicon content impossible. A

decrease in temperature of 100^{o}C from the 1100^{o}C specified in the method caused the dissolution to take upwards of 2 days, while increasing the sample content resulted in digestion time increasing by approximately 1 day for every 0.2g.

It is theorised that the high temperature, oxygen rich atmosphere and abundance of bound oxygen present in the fusion process create a highly oxidizing, or at the very least not a reducing, environment. At these temperatures the flux will act as an ionic liquid with free tetraborate ions attacking the oxides and other compounds of the various elements in the zircon ore. The zirconium, hafnium and silicon are all in the +4 oxidation state in the mineral. In this environment the zirconium and hafnium are possibly oxidized to a higher state although this is highly unlikely. Tetraborate ions could then coordinate as these metals are known to form complexes with valences of higher than +4 as stated in **Paragraph 1.3**. Another possibility is that as the crystal structure of the zircon is broken down the oxygen atoms are replaced by tetraborate ions in an ion exchange reaction. Zirconium tetraborate is a known compound which may be produced in this method.[51] Upon dissolution in dilute nitric acid it is likely that either of the products suggested would undergo dissociation of the tetraborate to form the tetraboric acid that was seen to form after dissolution (see **Paragraph 5.4.2)**. The open coordination site would then be occupied by either a nitrate group or water, making the resulting compound soluble in water, where the original oxide was not.

It was decided to focus on the major elements as well as some of the more abundant minor ones as these were clearly certified in the reference material. Elements such as calcium, magnesium, chromium, uranium and thorium will be investigated once the more abundant constituents are quantifiable. Due to the differences in the matrices of the silicon and titanium standards' (which were basic and pH neutral respectively) from those of the samples it was feared that these standards might precipitate from the

[51] Afanasev Y. A., Ryabinin A. I., Eremin V. P., Synthesis and Investigation of zirconium tetraborate, Doklady Akademiil NAUK SSSR, Volume 215, 1974, pp. 97-100

solution with the risk of removing other analytes by co-precipitation. To avoid this, initial tests were performed and the method evaluated without these elements.

The initial analysis (**Table 5-5)** using the flux fusion resulted in the expected large errors of approximately 10–20% in recovery possibly due to the high levels of lithium (an easily ionisable element) present in the sample affecting the conditions of the plasma. The level of this effect was gauged by varying the amount of flux with a constant amount of standard as seen in **Figures 5-2 - 5-5.** As can clearly be seen in these graphs even a small addition of this flux causes significant errors in the results obtained with the error increasing with the amount of flux added. At 2g of flux the errors were well in excess of 25%. The apparent increase in aluminium concentrations as opposed to the apparent decrease in other elements may be attributable to the fact that the wavelength used to analyse for it was an atomic line while the other elements used ionic lines. This is possibly an indication that the flux causes a decrease in ionization of elements within the plasma. Whether this is a chemical effect or related to the effect of the lithium on the plasma temperature has not yet been determined. It was then decided to proceed with a standard addition method in an attempt to remove the effect of the matrix from the analysis without the need of an internal standard.

The decision not to use an internal standard was a result of the fact that different elements ionise differently in the plasma. In theory an internal standard may work for one or two elements but is not likely to ionise in the exact same ratios as all elements of the matrix. This is evident in **Table 5-9** where an internal standard was used. This method gave excellent results for some elements (Zr, Hf and Si), acceptable results for others (Al and Fe) but poor results for Ti, although this may have been due to precipitation of the titanium. In theory a problem associated with internal standards stems from the fact that results obtained using an internal standard are adjusted in a fixed ratio with the change in apparent intensity of a constant amount of reference standard. If the reference standard reacts to the flame in a different way than the analyte the results will be significantly skewed. The standard addition method avoids this

problem but investigation into the use of an internal standard method is definitely warranted due to the excellent results obtained.

The first attempt to analyse the SARM62 certified reference material using a standard addition method (see **Table 5-6**) resulted in acceptable accuracy with a relatively high level of precision for both zirconium and hafnium, results for these elements both lying within the 6% deviation envelope. The results for aluminium and iron were not as good, with errors of approximately 13% and 40% respectively, but were deemed to be acceptable, considering the relatively large degree of uncertainty in even the SARM62 certification where relative errors of upwards of 20% are seen for these elements within the 95% confidence interval. The method was slow however, taking several days to perform a single analysis due to the long periods required for digestion and dissolution. The requirement of leaving the final solution to stand overnight in order for the calibration curves to be linear is one of the major contributors to this fact. The reason for the calibration standards being unusable without a stabilisation period is not yet understood. The appearance of colour (seen in **Figure 8-1** where a broad absorption peak at 300nm is observed) in the early stages of preparing these samples and the later disappearance thereof indicates that complexes may be forming between the metals and the high initial excess of nitrate ions with these complexes stabilising at different rates, depending on slight variations in the speed of dissolution when the sample is filled to volume. The possibility that these complexes may be highly refractory and thus resistant, to an extent, to the high temperatures of the plasma may cause slight variations in ionisation, resulting in poor readings. Zirconium and hafnium are known to form highly refractory compounds.[52,53,54]

[52] United States Patent 3804649

[53] Latastea, E., Erauwb, J. P., Olagnona, C., Fantozzia, G., Microstructural and mechanical consequences of thermal cycles on a high zirconia fuse-cast refractory, Journal of the European Ceramic Society, 2008, pp. 1-8

[54] Opeka, M. M., Talmy, I. G., Wuchina, E. J., Mechanical, Thermal, and Oxidation Properties of Refractory Hafnium and Zirconium Compounds, Journal of the European Ceramic Society, 19, 1999, pp. 2405-2414

The results seen in **Table 5-7** demonstrate an attempt to increase the speed of the analysis. Greater quantities of solvent were used to speed dissolution of the melt and correspondingly more sample was added per standard to compensate for this (see modifications in **Paragraph 5.4.5**). Plastic containers were used in an attempt to avoid contamination from elements leaching from the borosilicate glass used in previous experiments. This modification however proved to be a step backwards with standard deviations being between 40 and 90% and errors ranging between 25% for zirconium to 156% for hafnium. The averages obtained for the aluminium and titanium were very close to agreement with the certified values, but with the standard deviations so high that the results could not be trusted.

Table 5-8 shows the results of a further revision to the method. Glass containers and equipment were once again used and the sample was rapidly cooled to ensure that the melt cracked, further speeding dissolution time. Significantly improved precision was achieved with standard deviations ranging from 11% for zirconium to 38% for silicon. The 80% standard deviation for iron was still problematic however. While the precision was significantly improved for almost all elements the averages determined showed little improvement. In the case of zirconium the result of 102% recovery is most satisfactory. The other elements however are still showing recoveries higher than expected. This is not catastrophic, however, as the very low level of these elements present results in even a slight error appearing as a relatively large error in percentage recovery. The consistently extremely high iron readings may be due to a systematic error that has not yet come to light while the high silicon readings may be a result of contamination from the glass volumetric flasks that the samples were stored in. The improvement in accuracy may be attributable to not using the axial read-head for the ICP-OES machine. This attachment is meant to increase the sensitivity of the equipment but in this case seems to decrease the accuracy of the results.

The inter-lab analysis performed showed extremely good results for zirconium, hafnium and silicon, but with less satisfactory readings for the iron, aluminium and titanium. The

iron and aluminium showed errors consistent in range with those seen in the standard addition method while the titanium results were significantly worse.

The inter-lab analysis performed (results shown in **Table 5-9**) showed extremely good results for zirconium, hafnium and silicon, but with less satisfactory readings for the iron (74.3% recovery - single determination), aluminium (93.2% recovery - single determination) and titanium (38.5% recovery - single determination). The iron and aluminium showed errors consistent in range with those seen in the standard addition method provided in **Table 5-8** where iron gave 210.12% recovery (average of 7 determinations) and aluminium gave 162.93% recovery (average of 7 determinations), while the titanium results were significantly worse with 118% recovery (average of 4 determinations).

The final flux fusion standard addition method (see **Table 5-8**) shows a high degree of linearity in its calibration curves as well as an acceptable level of precision for most elements considering the matrix involved. The robustness of the method is highly questionable as large errors were obtained in the first modified method which was only slightly different from the others. Accuracy was obtained for the zirconium (102%), hafnium (131%) and titanium (118%) components with these results being within the ranges set out in the objectives. Other elements show much lower levels of accuracy, especially the silicon, it being far outside the 4-6% acceptable range with 132% recovery, this likely being due to contamination.

6.6. MICROWAVE ASSISTED ACID EXTRACTION

In literature[38] it was found that sulphuric acid is capable of dissolving zirconia with ammonium sulphate as additive and microwave assistance. In the initial microwave experiment (see **Table 5-11**) the conditions set out in literature as well as some other possibilities were examined. The use of pure sulphuric acid showed the most promise in

these results despite the extremely low recovery percentages of 6.41% Zr and 7.17% Hf for the SARM62 and 14.58% Zr and 18.31% Hf for the PDZ. As expected the PDZ was more amenable to chemical extraction than the unaltered zircon ore. Interestingly, significantly greater extractions were achieved for aluminium and iron from the SARM62 than from the PDZ. This suggests the possibility of an initial purification step wherein the aluminium and iron may be significantly removed, prior to any further refinement, with minimal loss of zirconium and hafnium. The ability of the sulphuric acid to extract far greater quantities of zirconium and hafnium than other acids may lie in the strong tendency of these elements to form sulphate compounds.[10,11,13] Under the harsh conditions of the microwave reaction system these compounds may form in preference to the silicate materials allowing for the dissolution of the sulphates into aqueous solution.

From these results it appears that the addition of the ammonium sulphate used in literature has a minimal impact on extraction of both the zirconium and hafnium from the zircon mineral. The impact of this additive was studied with the results being reported in **Table 5-12** and the results for the SARM62 being seen in **Figure 5-9**. There is a general upward trend in the percentage recovery of Zr (from 9.57% to 17.36%) and Hf (from 10.23% to 19.88%) as the mass $(NH_4)_2SO_4$ increased except at the lowest quantity of additive. The extraction achieved in this instance for the PDZ was impressive and highly encouraging but could not be repeated at this stage. It is not clear why such a high extraction was achieved in only one instance.

It was decided to attempt to determine whether the ratio of sample to digesting medium would have any effect on the extraction percentage. The results from this experiment can be seen in **Table 5-13** and **Figure 5-15**. In the case of the unaltered zircon ore a slight increase in extraction was seen with increasing amounts of sample while the opposite trend was true of the PDZ. This may have been due to a saturation effect caused by the significantly larger quantity of analyte extracted. The graph shows a slightly greater extraction for hafnium than zirconium.

The experiment was repeated using only PDZ and less time, to confirm whether the decreasing trend seen was due to saturation. These results continued to show the slight preference for extracting hafnium, but to a far smaller degree. Here the trend is not as well defined as in the first experiment, possibly being due to random “clumps” of PDZ forming in the digestion vessels, increasing the difficulty for the sulphuric acid to make contact with the entire sample. The increasing trend seen in **Figure 5-16** shows that a saturation point has not yet been reached with the percentage extractions being well below what was seen in the previous experiment.

A possible reason for the significantly better extraction from the PDZ than the SARM62 may lie in their physical structures.

$$\underset{\text{(Zircon)}}{ZrSiO_4\ (ZrO_2SiO_2)} \xrightarrow[\text{Plasma}]{1800^oC} \underset{\text{(Plasma Dissociated Zircon)}}{ZrO_2.SiO_2}$$

As stated in **Paragraph 1.4** the zircon mineral structure consists of zirconium dioxide dodecahedra interlaced by silica tetrahedra. In this case the analyte elements are bound in the inert crystal structure of the zircon ore which appears as red and grey particles in our samples but may vary depending on their source. In the PDZ however the analytes have formed pockets of zirconia and hafnia tetrahedra surrounded by amorphous silica, this having a uniformly beige colour. The harsh conditions in the microwave digestion vessels may be sufficient for the heated sulphuric acid to enter some of these pockets and affect dissolution of the analytes.

As it is known that silica is completely insoluble in sulphuric acid, the method was tested on the silica matrix using fluoride-containing additives, such as ammonium bifluoride and potassium fluoride, to facilitate the dissolution thereof. It was hoped that this would allow

for the formation of *in situ* hydrofluoric acid which could allow more of the zirconia crystallites to come into contact with the digesting medium of the sulphuric acid. These results are shown in **Table 5-15**. The presence of hydrofluoric acid was confirmed by the etching apparent on the surface of the quartz sample digestion vessels used. Comparing the results to those without additives it showed an enormous difference. For all elements the recoveries more than doubled. Iron achieved more than 50% recovery with the ammonium bifluoride additive with zirconium and hafnium recoveries ranging between 34.18% and 40.98%. Extraction increases appear to correlate with the quantity of additive, whether directly or inversely, depending on the element.

6.7. CONCLUSION

Both methods of digestion and analysis explored show interesting results, if for different reasons. The flux fusion method shows the most promise with regard to a viable analytical method, its advantages being the complete digestion of the sample without the loss of silicon content and theoretically it is able to ignore all matrix effects. The results obtained so far show a high degree of deviation, being between 10% and 20% for even the best ones, which is problematic. The 102% average recovery for zirconium in the last set of results and consistently excellent recoveries for titanium indicate that the method has merit. The time taken from beginning of the digestion to the final result is significantly longer than what would be hoped for in a rapid, high throughput method but, as has been demonstrated, it may be possible to further accelerate the digestion process and with further understanding of the chemistry involved in the dissolution, the stabilisation time may be decreased.

The microwave-assisted acid extraction shows less promise of being a viable analytical method to date, with no extractions consistently exceeding 50% other than for iron. The method could be modified to be the basis for an effective extractive procedure. With an iterative approach involving multiple extractions taking place between plasma dissociation runs to redistribute zirconia crystallites within the amorphous silica, near

complete extraction of the desired metals could be achieved while completely removing the silica component. The use of various additives in order to accelerate the process may improve extraction at the expense of purity.

When these digestion methods are compared to those using hydrofluoric acid we can see several advantages as well as disadvantages. The use of hydrofluoric acid greatly simplifies the digestion of PDZ as it is capable of completely dissolving all components of this product and converting them to the synthetically useful fluoride complexes. It makes analysis of silicon impossible, however, due to volatilization. The additives used in the microwave-assisted digestion suffer from this drawback as well. The advantage of the flux fusion method lies in that it achieves complete digestion without the use of the environmentally unfriendly hydrofluoric acid but it does introduce massive quantities of contaminant and necessitates a standard addition method to compensate for the matrix.

Neither method that was investigated in this study currently shows the desired level of accuracy and precision set out to be obtained for all elements at the beginning of this study. The standard addition method does show good accuracy and precision for elements such as zirconium and titanium with acceptable levels of precision for the others. Elements that have yet to be quantified with these methods include magnesium, calcium, chromium, uranium and thorium.

Chapter 7: Evaluation of the Research

7.1. CURRENT RESEARCH

In terms of the objectives laid out at the beginning of this study it has been mostly successful. The literature study revealed that few methods exist for the analysis of zirconium as a major component and none have the ability to quantify all components of the matrix. In addition, no methods were found dealing specifically with zircon, the most similar being zirconia, the method for which was ineffective when applied to zircon and only partially effective when applied to the PDZ.

The usefulness of the ICP-OES instrument was investigated and proved to be an acceptable tool for this analysis. With its advantage of high throughput rate and large linear dynamic range it is the most robust instrument available short of an XRF, which suffers from extremely long data collection times. Spectral interference was not observed due to the excellent resolution of the equipment used, and the almost complete lack of chemical interferences makes for a very useful analytical tool.

The use of large quantities of hydrofluoric acid was successfully avoided by using alternate digestion methods. This was done due to the significant dangers posed in working with HF and in an attempt to find a more environmentally friendly analysis procedure.

Different fluxing agents were considered to perform the dissolution, including lithium metaborate, sodium pyrosulphate, sodium carbonate and sodium hydroxide. Lithium tetraborate was decided upon due to its availability and ability to completely digest a silica matrix without said silica precipitating out upon acid dissolution.

The use of microwave assisted digestion was investigated, showing limited ability to digest the sample matrix but a far superior sample preparation time, typically taking hours instead of days to prepare a sample. Further advantages of this method are that the samples undergo far less contamination from reagents, as opposed to the flux fusion method, while also providing a simpler sample matrix. As it is as yet impossible to obtain complete extraction of the analyte species using this method, it is not yet as useful as the flux fusion digestion method.

A standard addition method has been developed that, in part, complies with the objectives. Not all elements are within the ranges set out in the beginning of the study and the standard deviations are larger than would be liked, owing to the complexity of the matrix involved. It is however capable of analysing zirconium and titanium to a high degree of accuracy and other elements to an acceptable level of precision.

7.2. FUTURE RESEARCH

Further refinement of the standard addition method is necessary to make it an acceptable analytical tool. The use of other fluxing agents in conjunction with the one already used may allow for faster digestion and dissolution times. Further understanding of the chemistry involved in the sample preparation process may allow for speedier digestion times and more accurate analyses.

An internal standard method should be developed as an alternative to the standard addition method, as a possible complementary technique. The one may succeed where the other fails, and vice-versa.

Other additives and conditions, including the use of hydrofluoric acid, may make the microwave-assisted acid extraction a more viable analytical route. The possibility of using a similar approach to separate the desired metals from the silica matrix will also be investigated.

Chapter 8: Appendix

8.1. STATISTICS AND CALCULATIONS

The statistical treatment of data in this study was performed using the following calculations.

The average of a set of results was calculated using the formula $\bar{x} = \frac{\sum x_i}{N}$ where $\bar{x}$ is the mean, $\sum x_i$ the sum of all the results and N the number of results.

The sample standard deviation was determined using the equation $SD = \sqrt{\frac{\sum_{I=1}^{N}(x_i - \bar{x})^2}{N-1}}$ where SD is the standard deviation, $\sum_{I=1}^{N}(x_i - \bar{x})^2$ the sum of the deviations and N the number of data points.

Relative standard deviation was determined by the equation $RSD = \frac{SD}{\bar{x}} \times 100$ where RSD is the relative standard deviation, SD the standard deviation and $\bar{x}$ the mean.

Determination of the slope and intercept of a line were determined using Microsoft Excel and checked using a Least-Squares regression[55].

[55] Skoog, D. A., West, D. M., Holler, F. J., Crouch, S. R., Fundamentals of Analytical Chemistry, 8th Edition, 2004, pp. 196-197

The detection limit of the instrument is defined as the minimum concentration necessary for the instrument to be able to clearly distinguish between the analytes' emission and the background.[36] This is critical in determining whether it is in fact possible to determine quantitatively the concentration of an analyte. The detection limits of the instrument for a normal calibration curve were determined by the equation $DL = \frac{3 \times SD_b}{m}$ where DL is the detection limit in ppm, m is the gradient of the calibration graph and SD_b is the standard deviation of the blank. The quantification limit is defined as 10 times the detection limit.

Standard addition results were calculated using the following equations.

$$x\ intercept = \frac{-y\ intercept}{slope}$$

$$Concentration\ in\ solution\ (ppm) = -x\ intercept \times dilution\ factor$$

$$Mass\ in\ solution\ (mg) = Concentration\ in\ solution \times volume\ of\ mother\ solution$$

$$Mass\ \%\ in\ sample = \frac{Mass\ in\ solution \times Molar\ mass\ of\ oxide \times 1g}{Molar\ mass\ of\ metal \times Mass\ of\ sample\ digested \times 1000mg} \times 100\%$$

$$\%\ recovery = \frac{Mass\ \%\ in\ sample}{True\ \%\ in\ sample} \times 100\%$$

The results for the microwave analysis were calculated as follows.

$$Mass\ in\ solution = Measured\ concentration\ in\ solution\ (ppm) \times volume$$

$$Mass\ \%\ in\ sample = \frac{Mass\ in\ solution \times Molar\ mass\ of\ oxide \times 1g}{Molar\ mass\ of\ metal \times Mass\ of\ sample\ digested \times 1000mg} \times 100\%$$

$$\%\ recovery = \frac{Mass\ \%\ in\ sample}{True\ \%\ in\ sample} \times 100\%$$

8.2. RESULTS FOR DETECTION LIMITS

Table 8-1: Raw data for HNO_3 detection limit determination

[] (ppm)	Intensity readings for each element given						[] (ppm)	Zr intensity readings
	Na	Mg	Al	Ca	Cr	Hf		Zr
0.4	0.269893	3.39654	0.074504	16.4594	0.101995	0.036459	4	12.3449
1	0.714119	8.39266	0.188587	42.3212	0.263045	0.09237	10	26.7336
2	1.5897	16.6891	0.395009	84.5009	0.519732	0.178898	20	64.413
5	4.37188	38.9945	1.00788	192.668	1.28171	0.457507	50	228.614
10	9.63595	71.0245	2.02929	335.967	2.52528	0.919954		
Std Dev Blank	0.00034	0.000791	0.000193	0.014712	0.00026	0.000178		0.000711
m=	0.9800	7.0247	0.2040	33.1200	0.2520	0.09210		4.84142181
DL=	0.001041	0.000338	0.002838	0.001333	0.003095	0.005798		0.00044057
QL=	0.010408	0.003378	0.028382	0.013326	0.030952	0.05798		0.00440573

Table 8-2: Raw data for H_2SO_4 detection limit determination

[] (ppm)	Intensity readings for each element given								
	Mg	Al	Si	Ca	Ti	Cr	Fe	Zr	Hf
0.4	21.6881	0.255689	0.286033	80.8362	6.49089	0.407755	0.690134	3.94065	0.157422
1	55.5188	0.650046	0.675788	267.029	16.1833	1.03648	1.74866	10.4425	0.397267
2	108.931	1.30978	1.42158	541.227	32.0956	2.0406	3.45868	20.5473	0.795922
5	266.455	3.23808	3.14081	1373.65	80.856	5.06198	8.59513	51.0966	1.95399
10	519.046	6.40744	9.22763	2716.96	159.407	9.85192	16.8832	101.279	3.88704
Std Dev Blank	0.013803	0.000634	0.000385	0.10695	0.000472	0.000536	0.000615	0.005611	0.000258
m=	51.70958	0.640342	0.917995	273.7376	15.94287	0.983259	1.685991	10.12202	0.387958
DL=	0.000801	0.00297	0.001258	0.001172	8.88E-05	0.001635	0.001094	0.001663	0.001995
QL=	0.008008	0.029703	0.012582	0.011721	0.000888	0.016354	0.010943	0.01663	0.019951

8.3. RESULTS FOR INITIAL FLUX DATA

Table 8-3: Raw data for readings of unaltered flux fusion solution

<Intensity>				
Element	Zr	Hf	Al	Fe
No. 1	470.267	0.79005	1.54537	0.255088
No. 2	469.421	0.792671	1.55214	0.256648
No. 3	468.078	0.786742	1.55333	0.252858
Average	469.256	0.789821	1.55028	0.254864
R	2.18857	0.005928	0.00796	0.00379
S	1.10366	0.002971	0.004293	0.001905
CV	0.235194	0.37613	0.276896	0.747443
<Conc.>				
Element	Zr	Hf	Al	Fe
No. 1	453.74	11.188	7.11829	0.720171
No. 2	452.912	11.225	7.14908	0.725033
No. 3	451.596	11.1413	7.15451	0.71322
Average	452.749	11.1847	7.14063	0.719475
R	2.14444	0.083726	0.03622	0.011813
S	1.08141	0.041957	0.019533	0.005937
CV	0.238853	0.375125	0.273549	0.825201
Mass extracted (mg)	45.2749	1.11847	0.714063	0.071948
Mass %	53.83508	1.161084	1.187684	0.090553
% Recovery	83.85526	88.63236	134.9641	129.3608

Table 8-4: Example of the raw data for a typical external calibration curve

Concentration (ppm)	**Al**	**Fe**	**Zr**	**Hf**
0	0.144088	0.136007	0.437331	0.035084
0.4	0.255689	0.690134	3.94065	0.157422
1	0.650046	1.74866	10.4425	0.397267
2	1.30978	3.45868	20.5473	0.795922
5	3.23808	8.59513	51.0966	1.95399
10	6.40744	16.8832	101.279	3.88704
Gradient	0.635004	1.683275	10.11266	0.386941
Intercept	0.053508	0.089924	0.278412	0.017834
R^2	0.999574	0.999916	0.999966	0.999945

Table 8-5: Table of raw data for failed standard addition curves

Concentration (ppm)	Al (Intensity)	Fe (Intensity)	Zr (Intensity)	Hf (Intensity)
0.1	0.129643	0.088545	62.1487	0.115661
0.2	0.029634	0.037196	11.8411	0.029491
0.5	0.229563	0.266376	72.0185	0.163873
1	0.284643	0.41259	64.6918	0.182082

Table 8-6: Table of the raw data showing the effect of mass flux on ICP-OES readings

Mass Flux	Al	Fe	Zr	Hf
Run 1	**Apparent Concentration (ppm)**			
0	2.13515	2.19141	23.02	2.19526
0.1009	2.4379	2.14905	22.2963	2.20377
0.4976	2.52667	1.91744	20.817	2.09978
0.9969	2.66115	1.81565	19.7558	1.99416
1.9996	2.90708	1.67302	18.3013	1.81811
Run 2				
0	2.14328	2.14939	22.9883	2.14706
0.0994	2.47815	2.15827	22.7411	2.2391
0.5204	2.46984	1.93107	21.0191	2.11118
1.0179	2.78087	1.81509	19.9887	2.0363
2.0085	2.94829	1.66361	18.3261	1.80485
Run 3				
0	2.48479	2.51406	26.3694	2.58025
0.1018	2.44511	2.04965	22.1692	2.16709
0.4958	2.61703	1.93307	20.9359	2.07279
1.0046	2.72829	1.77629	19.7601	1.98927
1.9933	2.99361	1.63602	17.9542	1.81806
Average				
0	2.254407	2.284953	24.1259	2.307523
0.1007	2.45372	2.11899	22.4022	2.20332
0.5046	2.537847	1.927193	20.924	2.094583
1.0064667	2.723437	1.802343	19.83487	2.006577
2.0004667	2.94966	1.65755	18.19387	1.813673

8.4. RESULTS FOR STANDARD ADDITION METHODS

8.4.1 INITIAL STANDARD ADDITION METHOD

Table 8-7:Initial standard addition result 1

Al					**x-int**	**-0.54335**	**Mass (g)**	**0.2075**
Concentration (ppm)	Intensity					0.543347		
1	0.321388	Slope / Intercept	0.201815	0.109655	ppm Osol=	10.86694		
2	0.51721	SD Slope / SD Intercept	0.001611	0.008497	mass (mg)	1.086694		
3	0.707119	R2 / SD Regression	0.999809	0.011486		2.053288		
5	1.10577	Fstat / Degrees Freedom	15683.71	3		0.002053		
10	2.1349	Sum Squares Regression/Residual	2.069043	0.000396	mass %	0.989537		
					% Recovery	112.4473		
Fe								
Concentration (ppm)	Intensity				x-int	-0.12124		
1	0.16418	Slope - Intercept	0.147802	0.01792		0.121244		
2	0.311863	SD Slope - SD Intercept	0.00033	0.001738	ppm Osol=	2.424877		
3	0.46392	R2 - SD Regression	0.999985	0.002349	mass (mg)	0.242488		
5	0.758738	Fstat - Degrees Freedom	201158.2	3		0.346699		
10	1.49475	Sum Squares Regression/residual	1.109754	1.66E-05		0.000347		
					mass %	0.167084		
					% Recovery	238.6915		
Zr								
Concentration (ppm)	Intensity				x-int	-61.1836		
10	57.2644	Slope - Intercept	0.825693	50.5189		61.18362		
20	66.7285	SD Slope - SD Intercept	0.021876	1.153448	ppm Osol=	1223.672		
30	76.3834	R2 - SD Regression	0.997899	1.559221	mass (mg)	122.3672		
50	93.4798	Fstat - Degrees Freedom	1424.577	3		165.2918		
100	132.134	Sum Squares Regression/residual	3463.388	7.293508		0.165292		
					mass %	79.65871		
					% Recovery	124.079		
Hf								
Concentration (ppm)	Intensity				x-int	-1.16352		
1	0.082423	Slope - Intercept	0.038196	0.044442		1.163521		
2	0.121257	SD Slope - SD Intercept	0.000111	0.000586	ppm Osol=	23.27042		

3	0.158169	R2 - SD Regression	0.999975	0.000792	mass (mg)	2.327042		
5	0.236342	Fstat - Degrees Freedom	118206.4	3		2.744238		
10	0.426141	Sum Squares Regression/residual	0.074115	1.88E-06		0.002744		
					mass %	1.322524		
					% Recovery	100.9561		

Table 8-8:Initial standard addition result 2

Al					**x-int**	**-4.38867**	**Mass (g)**	**0.2044**
Concentration (ppm)	Intensity					4.388668		
1	0.306569	Slope / Intercept	0.081624	0.358219	ppm Osol=	87.77336		
2	0.502274	SD Slope / SD Intercept	0.018499	0.097539	mass (mg)	8.777336		
3	0.699487	R2 / SD Regression	0.866478	0.131852		16.58462		
5	0.901983	Fstat / Degrees Freedom	19.46813	3		0.016585		
10	1.09488	Sum Squares Regression/Residual	0.338451	0.052155	mass %	8.113805		
					% Recovery	922.0233		
Fe								
Concentration (ppm)	Intensity				x-int	-3.17719		
1	0.129069	Slope - Intercept	0.051641	0.164075		3.17719		
2	0.255618	SD Slope - SD Intercept	0.011926	0.062881	ppm Osol=	63.5438		
3	0.382295	R2 - SD Regression	0.862068	0.085002	mass (mg)	6.35438		
5	0.508415	Fstat - Degrees Freedom	18.74984	3		9.085244		
10	0.629446	Sum Squares Regression/residual	0.135475	0.021676		0.009085		
					mass %	4.444836		
					% Recovery	6349.765		
Zr								
Concentration (ppm)	Intensity				x-int	-161.396		
10	40.6591	Slope - Intercept	0.263641	42.55048		161.3958		
20	47.0552	SD Slope - SD Intercept	0.063086	3.32628	ppm Osol=	3227.915		
30	53.9528	R2 - SD Regression	0.853403	4.496434	mass (mg)	322.7915		
50	60.2211	Fstat - Degrees Freedom	17.46433	3		436.0219		
100	66.2287	Sum Squares Regression/residual	353.0923	60.65375		0.436022		
					mass %	213.318		
					% Recovery	332.271		
Hf								
Concentration (ppm)	Intensity				x-int	-5.66113		
1	0.070918	Slope - Intercept	0.013993	0.079218		5.661129		
2	0.104368	SD Slope - SD Intercept	0.00308	0.016239	ppm Osol=	113.2226		
3	0.136814	R2 - SD Regression	0.873116	0.021951	mass (mg)	11.32226		

5	0.171989	Fstat - Degrees Freedom	20.64372	3		13.35213		
10	0.205861	Sum Squares Regression/residual	0.009947	0.001446		0.013352		
					mass %	6.532354		
					% Recovery	498.653		

Table 8-9: Initial standard addition result 3

Al					**x-int**	**-4.29286**	**Mass (g)**	**0.2049**
Concentration (ppm)	Intensity					4.292859		
1	0.271213	Slope / Intercept	0.073062	0.313644	ppm Osol=	85.85718		
2	0.4554	SD Slope / SD Intercept	0.015432	0.081368	mass (mg)	8.585718		
3	0.603302	R2 / SD Regression	0.881955	0.109992		16.22256		
5	0.795164	Fstat / Degrees Freedom	22.41408	3		0.016223		
10	0.977436	Sum Squares Regression/Residual	0.271171	0.036295	mass %	7.917306		
					% Recovery	899.6938		
Fe								
Concentration (ppm)	Intensity				x-int	-3.10581		
1	0.123939	Slope - Intercept	0.048829	0.151654		3.105812		
2	0.247606	SD Slope - SD Intercept	0.010079	0.053143	ppm Osol=	62.11625		
3	0.345537	R2 - SD Regression	0.886665	0.071838	mass (mg)	6.211625		
5	0.469953	Fstat - Degrees Freedom	23.47009	3		8.881138		
10	0.596644	Sum Squares Regression/residual	0.121121	0.015482		0.008881		
					mass %	4.334377		
					% Recovery	6191.967		
Zr								
Concentration (ppm)	Intensity				x-int	-153.029		
10	47.6582	Slope - Intercept	0.326134	49.90795		153.0292		
20	56.5214	SD Slope - SD Intercept	0.070031	3.692432	ppm Osol=	3060.584		
30	63.2347	R2 - SD Regression	0.878481	4.991396	mass (mg)	306.0584		
50	71.0295	Fstat - Degrees Freedom	21.68756	3		413.419		
100	79.584	Sum Squares Regression/residual	540.3245	74.74209		0.413419		
					mass %	201.7662		
					% Recovery	314.2776		
Hf								
Concentration (ppm)	Intensity				x-int	-5.49701		
1	0.069481	Slope - Intercept	0.013987	0.076885		5.497013		
2	0.102906	SD Slope - SD Intercept	0.002886	0.015215	ppm Osol=	109.9403		
3	0.133678	R2 - SD Regression	0.886761	0.020567	mass (mg)	10.99403		
5	0.167678	Fstat - Degrees Freedom	23.49268	3		12.96505		

10	0.204401	Sum Squares Regression/residual	0.009938	0.001269		0.012965		
					mass %	6.327503		
					% Recovery	483.0155		

8.4.2 FIRST MODIFIED STANDARD ADDITION METHOD

Table 8-10: First modified standard addition 1

Al					**x-int**	**-0.49309**	**Mass (g)**	**0.1989**
Concentration (ppm)	Intensity					0.493085		
1	0.374176	Slope / Intercept	0.248916	0.122737	ppm Osol=	9.861708		
2	0.617041	SD Slope / SD Intercept	0.001622	0.005378	mass (mg)	0.986171		
3	0.872712	R2 / SD Regression	0.999873	0.005128		1.863352		
4	1.11243	Fstat / Degrees Freedom	23561.93	3		0.001863		
5	1.37106	Sum Squares Regression/Residual	0.61959	7.89E-05	mass %	0.936829		
					% Recovery	106.4578		
Fe								
Concentration (ppm)	Intensity				x-int	-0.01811		
1	0.65964	Slope - Intercept	0.648666	0.011746		0.018108		
2	1.32071	SD Slope - SD Intercept	0.003996	0.013253	ppm Osol=	0.362159		
3	1.9399	R2 - SD Regression	0.999886	0.012636	mass (mg)	0.036216		
4	2.61029	Fstat - Degrees Freedom	26353.04	3		0.05178		
5	3.25818	Sum Squares Regression/residual	4.207676	0.000479		5.18E-05		
					mass %	0.026033		
					% Recovery	37.19028		
Zr								
Concentration (ppm)	Intensity				x-int	-25.5819		
1	81.8001	Slope - Intercept	3.11221	79.61631		25.58192		
2	86.4348	SD Slope - SD Intercept	0.346574	1.149455	ppm Osol=	511.6384		
3	90.2864	R2 - SD Regression	0.964132	1.095963	mass (mg)	51.16384		
4	91.3297	Fstat - Degrees Freedom	80.63923	3		69.11134		
5	94.9137	Sum Squares Regression/residual	96.85851	3.603402		0.069111		
					mass %	34.74678		
					% Recovery	54.12271		
Hf								
Concentration (ppm)	Intensity				x-int	-2.3143		
1	0.171082	Slope - Intercept	0.051214	0.118526		2.314302		
2	0.21855	SD Slope - SD Intercept	0.000565	0.001874	ppm Osol=	46.28604		
3	0.272447	R2 - SD Regression	0.999635	0.001787	mass (mg)	4.628604		
4	0.324672	Fstat - Degrees Freedom	8217.902	3		5.458429		

5	0.374093	Sum Squares Regression/residual	0.026229	9.58E-06		0.005458		
					mass %	2.744308		
					% Recovery	209.4892		
Ti								
Concentration (ppm)	Intensity				x-int	-0.01186		
1	3.92286	Slope - Intercept	3.840917	0.045543		0.011857		
2	7.71171	SD Slope - SD Intercept	0.012628	0.041884	ppm Osol=	0.237146		
3	11.525	R2 - SD Regression	0.999968	0.039934	mass (mg)	0.023715		
4	15.3972	Fstat - Degrees Freedom	92507.12	3		0.031639		
5	19.2847	Sum Squares Regression/residual	147.5264	0.004784		3.16E-05		
					mass %	0.015907		
					% Recovery	12.23628		

Table 8-11: First modified standard addition 2

Al					**x-int**	**-0.24612**	**Mass (g)**	**0.1998**
Concentration (ppm)	Intensity					0.246124		
1	0.300479	Slope / Intercept	0.242642	0.05972	ppm Osol=	4.922478		
2	0.557132	SD Slope / SD Intercept	0.00384	0.012735	mass (mg)	0.492248		
3	0.778659	R2 / SD Regression	0.999249	0.012142		0.930093		
4	1.01941	Fstat / Degrees Freedom	3993.561	3		0.00093		
5	1.28255	Sum Squares Regression/Residual	0.588751	0.000442	mass %	0.465512		
					% Recovery	52.89911		
Fe								
Concentration (ppm)	Intensity				x-int	-0.08062		
1	0.649758	Slope - Intercept	0.609315	0.049123		0.080621		
2	1.2952	SD Slope - SD Intercept	0.007063	0.023424	ppm Osol=	1.612413		
3	1.86112	R2 - SD Regression	0.999597	0.022334	mass (mg)	0.161241		
4	2.47067	Fstat - Degrees Freedom	7443.274	3		0.230536		
5	3.1086	Sum Squares Regression/residual	3.712653	0.001496		0.000231		
					mass %	0.115384		
					% Recovery	164.8338		
Zr								
Concentration (ppm)	Intensity				x-int	-45.468		
1	85.5216	Slope - Intercept	1.87666	85.32792		45.46797		
2	91.9182	SD Slope - SD Intercept	0.642609	2.131294	ppm Osol=	909.3594		
3	90.6412	R2 - SD Regression	0.739777	2.032109	mass (mg)	90.93594		
4	91.689	Fstat - Degrees Freedom	8.528585	3		122.8349		
5	95.0195	Sum Squares Regression/residual	35.21853	12.38841		0.122835		

					mass %	61.47892		
					% Recovery	95.76157		
Hf								
Concentration (ppm)	Intensity				x-int	-2.78134		
1	0.186623	Slope - Intercept	0.049616	0.137999		2.781345		
2	0.243577	SD Slope - SD Intercept	0.001859	0.006166	ppm Osol=	55.62689		
3	0.28118	R2 - SD Regression	0.995805	0.005879	mass (mg)	5.562689		
4	0.332729	Fstat - Degrees Freedom	712.1757	3		6.559978		
5	0.390127	Sum Squares Regression/residual	0.024617	0.000104		0.00656		
					mass %	3.283272		
					% Recovery	250.6315		
Ti								
Concentration (ppm)	Intensity				x-int	-0.06857		
1	3.85805	Slope - Intercept	3.679296	0.25229		0.06857		
2	7.72404	SD Slope - SD Intercept	0.025739	0.085367	ppm Osol=	1.371404		
3	11.2878	R2 - SD Regression	0.999853	0.081395	mass (mg)	0.13714		
4	14.9289	Fstat - Degrees Freedom	20433.26	3		0.182968		
5	18.6521	Sum Squares Regression/residual	135.3722	0.019875		0.000183		
					mass %	0.091576		
					% Recovery	70.4429		

Table 8-12: First modified standard addition 3

Al					**x-int**	**-0.73447**	**Mass (g)**	**0.2225**
Concentration (ppm)	Intensity					0.734474		
1	0.419893	Slope / Intercept	0.238481	0.175158	ppm Osol=	14.68947		
2	0.645014	SD Slope / SD Intercept	0.002791	0.009258	mass (mg)	1.468947		
3	0.893328	R2 / SD Regression	0.999589	0.008827		2.775549		
4	1.11993	Fstat / Degrees Freedom	7298.979	3		0.002776		
5	1.37484	Sum Squares Regression/Residual	0.568732	0.000234	mass %	1.247438		
					% Recovery	141.7543		
Fe								
Concentration (ppm)	Intensity				x-int	-0.13493		
1	0.697025	Slope - Intercept	0.609327	0.082218		0.134932		
2	1.29964	SD Slope - SD Intercept	0.002253	0.007472	ppm Osol=	2.698649		
3	1.90011	R2 - SD Regression	0.999959	0.007124	mass (mg)	0.269865		
4	2.52148	Fstat - Degrees Freedom	73152.24	3		0.385842		
5	3.13274	Sum Squares Regression/residual	3.712794	0.000152		0.000386		
					mass %	0.173412		

					% Recovery	247.7319		
Zr								
Concentration (ppm)	Intensity				x-int	-110.955		
1	98.0925	Slope - Intercept	0.875712	97.16446		110.9549		
4	100.458	SD Slope - SD Intercept	0.090633	0.339117	ppm Osol=	2219.097		
5	101.7	R2 - SD Regression	0.989402	0.266816	mass (mg)	221.9097		
		Fstat - Degrees Freedom	93.35778	1		299.7523		
		Sum Squares Regression/residual	6.646213	0.071191		0.299752		
					mass %	134.7201		
					% Recovery	209.8445		
Hf								
Concentration (ppm)	Intensity				x-int	-3.3597		
1	0.205567	Slope - Intercept	0.047331	0.159019		3.359699		
2	0.249768	SD Slope - SD Intercept	0.001592	0.005279	ppm Osol=	67.19399		
3	0.307265	R2 - SD Regression	0.996619	0.005033	mass (mg)	6.719399		
4	0.350708	Fstat - Degrees Freedom	884.3978	3		7.924064		
5	0.391753	Sum Squares Regression/residual	0.022402	7.6E-05		0.007924		
					mass %	3.561377		
					% Recovery	271.8609		
Ti								
Concentration (ppm)	Intensity				x-int	-0.08686		
1	4.11115	Slope - Intercept	3.6881	0.32033		0.086855		
2	7.6161	SD Slope - SD Intercept	0.034192	0.113402	ppm Osol=	1.7371		
3	11.3378	R2 - SD Regression	0.999742	0.108125	mass (mg)	0.17371		
4	14.9968	Fstat - Degrees Freedom	11634.65	3		0.231759		
5	18.8613	Sum Squares Regression/residual	136.0208	0.035073		0.000232		
					mass %	0.104161		
					% Recovery	80.12394		

Table 8-13: First modified standard addition 4

Al					**x-int**	**-0.29404**	**Mass (g)**	**0.2094**
Concentration (ppm)	Intensity					0.294042		
1	0.300731	Slope / Intercept	0.236587	0.069567	ppm Osol=	5.880831		
2	0.539675	SD Slope / SD Intercept	0.005545	0.018391	mass (mg)	0.588083		
3	0.783286	R2 / SD Regression	0.998355	0.017535		1.111172		
4	1.03889	Fstat / Degrees Freedom	1820.41	3		0.001111		
5	1.23406	Sum Squares Regression/Residual	0.559736	0.000922	mass %	0.530646		
					% Recovery	60.30067		
Fe								
Concentration (ppm)	Intensity				x-int	-0.13579		
1	0.662133	Slope - Intercept	0.60263	0.081829		0.135787		
2	1.27645	SD Slope - SD Intercept	0.015589	0.051703	ppm Osol=	2.715741		
3	1.92475	R2 - SD Regression	0.997996	0.049297	mass (mg)	0.271574		
4	2.54352	Fstat - Degrees Freedom	1494.375	3		0.388286		
5	3.04175	Sum Squares Regression/residual	3.631634	0.007291		0.000388		
					mass %	0.185428		
					% Recovery	264.897		
Zr								
Concentration (ppm)	Intensity				x-int	-84.3084		
1	93.1459	Slope - Intercept	1.09414	92.24522		84.30842		
2	93.9975	SD Slope - SD Intercept	0.389343	1.291304	ppm Osol=	1686.168		
3	95.741	R2 - SD Regression	0.724704	1.231211	mass (mg)	168.6168		
4	98.2769	Fstat - Degrees Freedom	7.897346	3		227.7651		
5	96.4769	Sum Squares Regression/residual	11.97142	4.547638		0.227765		
					mass %	108.7703		
					% Recovery	169.4242		
Hf								
Concentration (ppm)	Intensity				x-int	-3.35179		
1	0.199825	Slope - Intercept	0.046487	0.155816		3.35179		
2	0.242325	SD Slope - SD Intercept	0.003461	0.011479	ppm Osol=	67.0358		
3	0.304853	R2 - SD Regression	0.983644	0.010945	mass (mg)	6.70358		
4	0.351927	Fstat - Degrees Freedom	180.417	3		7.905409		
5	0.377461	Sum Squares Regression/residual	0.021611	0.000359		0.007905		
					mass %	3.775267		
					% Recovery	288.1883		
Ti								

Concentration (ppm)	Intensity				x-int	-0.14527		
1	4.05061	Slope - Intercept	3.624945	0.526613		0.145275		
2	7.68773	SD Slope - SD Intercept	0.086721	0.287619	ppm Osol=	2.905495		
3	11.5893	R2 - SD Regression	0.998286	0.274234	mass (mg)	0.29055		
4	15.3208	Fstat - Degrees Freedom	1747.266	3		0.387642		
5	18.3588	Sum Squares Regression/residual	131.4023	0.225613		0.000388		
					mass %	0.18512		
					% Recovery	142.4003		

Table 8-14: First modified standard addition 5

Al					**x-int**	**-0.62073**	**Mass (g)**	**0.1999**
Concentration (ppm)	Intensity					0.620727		
1	0.38436	Slope / Intercept	0.240831	0.149491	ppm Osol=	12.41454		
2	0.629727	SD Slope / SD Intercept	0.003183	0.010557	mass (mg)	1.241454		
3	0.882465	R2 / SD Regression	0.999476	0.010066		2.345705		
4	1.11998	Fstat / Degrees Freedom	5724.54	3		0.002346		
5	1.34339	Sum Squares Regression/Residual	0.579997	0.000304	mass %	1.173439		
					% Recovery	133.3454		
Fe								
Concentration (ppm)	Intensity				x-int	-0.09227		
1	0.647013	Slope - Intercept	0.607921	0.056094		0.092272		
2	1.27772	SD Slope - SD Intercept	0.006346	0.021047	ppm Osol=	1.845449		
3	1.90663	R2 - SD Regression	0.999673	0.020067	mass (mg)	0.184545		
4	2.4849	Fstat - Degrees Freedom	9177.244	3		0.263855		
5	3.08303	Sum Squares Regression/residual	3.695684	0.001208		0.000264		
					mass %	0.131994		
					% Recovery	188.5622		
Zr								
Concentration (ppm)	Intensity				x-int	-46.548		
1	84.686	Slope - Intercept	1.79926	83.75194		46.54799		
2	87.9863	SD Slope - SD Intercept	0.278455	0.92353	ppm Osol=	930.9598		
3	90.1039	R2 - SD Regression	0.932964	0.880551	mass (mg)	93.09598		
4	90.5939	Fstat - Degrees Freedom	41.75211	3		125.7526		
5	92.3785	Sum Squares Regression/residual	32.37337	2.326112		0.125753		
					mass %	62.90778		
					% Recovery	97.98719		
Hf								
Concentration (ppm)	Intensity				x-int	-2.9018		

1	0.183654	Slope - Intercept	0.047557	0.138002		2.901803		
2	0.231046	SD Slope - SD Intercept	0.001556	0.005162	ppm Osol=	58.03605		
3	0.288276	R2 - SD Regression	0.996797	0.004922	mass (mg)	5.803605		
4	0.326859	Fstat - Degrees Freedom	933.6187	3		6.844086		
5	0.373534	Sum Squares Regression/residual	0.022617	7.27E-05		0.006844		
					mass %	3.423755		
					% Recovery	261.3553		
Ti								
Concentration (ppm)	Intensity				x-int	-0.09302		
1	3.92296	Slope - Intercept	3.671043	0.341493		0.093023		
2	7.68435	SD Slope - SD Intercept	0.040441	0.134129	ppm Osol=	1.860469		
3	11.5391	R2 - SD Regression	0.999636	0.127887	mass (mg)	0.186047		
4	15.0127	Fstat - Degrees Freedom	8239.974	3		0.248218		
5	18.614	Sum Squares Regression/residual	134.7656	0.049065		0.000248		
					mass %	0.124171		
					% Recovery	95.51618		

Table 8-15: First modified standard addition 6

Al					**x-int**	**-0.23545**	**Mass (g)**	**0.2032**
Concentration (ppm)	Intensity					0.235445		
1	0.297639	Slope / Intercept	0.245225	0.057737	ppm Osol=	4.708908		
2	0.540146	SD Slope / SD Intercept	0.005115	0.016964	mass (mg)	0.470891		
3	0.818339	R2 / SD Regression	0.998697	0.016175		0.88974		
4	1.03419	Fstat / Degrees Freedom	2298.608	3		0.00089		
5	1.27674	Sum Squares Regression/Residual	0.601351	0.000785	mass %	0.437864		
					% Recovery	49.75727		
Fe								
Concentration (ppm)	Intensity				x-int	-0.05348		
1	0.642854	Slope - Intercept	0.619021	0.033103		0.053477		
2	1.25368	SD Slope - SD Intercept	0.010671	0.035392	ppm Osol=	1.069534		
3	1.94213	R2 - SD Regression	0.999109	0.033745	mass (mg)	0.106953		
4	2.49474	Fstat - Degrees Freedom	3365.132	3		0.152918		
5	3.11743	Sum Squares Regression/residual	3.831872	0.003416		0.000153		
					mass %	0.075255		
					% Recovery	107.5069		
Zr								
Concentration (ppm)	Intensity				x-int	-54.6489		
1	90.3505	Slope - Intercept	1.62576	88.84602		54.64891		

2	92.2052	SD Slope - SD Intercept	0.061093	0.207176	ppm Osol=	1092.978		
4	95.5112	R2 - SD Regression	0.997184	0.193193	mass (mg)	109.2978		
5	96.8263	Fstat - Degrees Freedom	708.1578	2		147.6379		
		Sum Squares Regression/residual	26.43096	0.074647		0.147638		
					mass %	72.65643		
					% Recovery	113.172		
Hf								
Concentration (ppm)	Intensity				x-int	-3.07894		
1	0.192586	Slope - Intercept	0.048845	0.150392		3.078943		
2	0.25354	SD Slope - SD Intercept	0.001969	0.006531	ppm Osol=	61.57886		
3	0.30225	R2 - SD Regression	0.995147	0.006227	mass (mg)	6.157886		
4	0.345366	Fstat - Degrees Freedom	615.2286	3		7.261882		
5	0.3909	Sum Squares Regression/residual	0.023859	0.000116		0.007262		
					mass %	3.573761		
					% Recovery	272.8062		
Ti								
Concentration (ppm)	Intensity				x-int	-0.06879		
1	3.95918	Slope - Intercept	3.723492	0.256144		0.068791		
2	7.53642	SD Slope - SD Intercept	0.062966	0.208833	ppm Osol=	1.375827		
3	11.7001	R2 - SD Regression	0.999143	0.199115	mass (mg)	0.137583		
4	15.1851	Fstat - Degrees Freedom	3496.984	3		0.183559		
5	18.7523	Sum Squares Regression/residual	138.6439	0.11894		0.000184		
					mass %	0.090334		
					% Recovery	69.48762		

8.4.3 SECOND MODIFIED STANDARD ADDITION METHOD

Table 8-16: Second modified standard addition 1

Al					**x-int**	**-0.62608**	**Mass (g)**	**0.2059**
Concentration (ppm)	Intensity					0.626077		
1	0.185488	Slope / Intercept	0.114456	0.071658	ppm Osol=	12.52154		
2	0.300583	SD Slope / SD Intercept	0.000285	0.000946	mass (mg)	1.252154		
3	0.415976	R2 / SD Regression	0.999981	0.000902		2.365922		
4	0.530055	Fstat / Degrees Freedom	160943.4	3		0.002366		
5	0.643033	Sum Squares Regression/Residual	0.131002	2.44E-06	mass %	1.149064		
					% Recovery	130.5754		
Fe								
Concentration (ppm)	Intensity				x-int	-0.04583		
1	0.280132	Slope - Intercept	0.270674	0.012405		0.045831		
2	0.55613	SD Slope - SD Intercept	0.001737	0.005762	ppm Osol=	0.916617		
3	0.823298	R2 - SD Regression	0.999876	0.005494	mass (mg)	0.091662		
4	1.10201	Fstat - Degrees Freedom	24275.72	3		0.131054		
5	1.36056	Sum Squares Regression/residual	0.732642	9.05E-05		0.000131		
					mass %	0.063649		
					% Recovery	90.92785		
Zr								
Concentration (ppm)	Intensity				x-int	-48.2383		
1	36.6669	Slope - Intercept	0.74717	36.04219		48.23827		
2	37.628	SD Slope - SD Intercept	0.057848	0.191861	ppm Osol=	964.7654		
3	38.2865	R2 - SD Regression	0.982335	0.182932	mass (mg)	96.47654		
4	39.2407	Fstat - Degrees Freedom	166.8237	3		130.3191		
5	39.5964	Sum Squares Regression/residual	5.58263	0.100393		0.130319		
					mass %	63.2924		
					% Recovery	98.5863		
Hf								
Concentration (ppm)	Intensity				x-int	-1.41897		
1	0.118715	Slope - Intercept	0.049374	0.07006		1.418965		
2	0.169683	SD Slope - SD Intercept	0.000431	0.001428	ppm Osol=	28.37931		
3	0.217498	R2 - SD Regression	0.999772	0.001362	mass (mg)	2.837931		
4	0.269175	Fstat - Degrees Freedom	13149.1	3		3.34672		
5	0.315839	Sum Squares Regression/residual	0.024378	5.56E-06		0.003347		

					mass %	1.62541		
					% Recovery	124.0771		

Table 8-17: Second modified standard addition 2

Al					**x-int**	**-0.82797**	**Mass (g)**	**0.2059**
Concentration (ppm)	Intensity					0.82797		
1	1.3006	Slope / Intercept	0.712946	0.590298	ppm Osol=	16.5594		
2	2.02023	SD Slope / SD Intercept	0.005147	0.01707	mass (mg)	1.65594		
3	2.73993	R2 / SD Regression	0.999844	0.016275		3.128869		
4	3.41895	Fstat / Degrees Freedom	19189.53	3		0.003129		
5	4.16597	Sum Squares Regression/Residual	5.08292	0.000795	mass %	1.519606		
					% Recovery	172.6825		
Fe								
Concentration (ppm)	Intensity				x-int	-0.168		
1	2.18296	Slope - Intercept	1.888041	0.317197		0.168003		
2	4.11887	SD Slope - SD Intercept	0.019192	0.063653	ppm Osol=	3.360065		
3	6.0284	R2 - SD Regression	0.99969	0.060691	mass (mg)	0.336006		
4	7.78754	Fstat - Degrees Freedom	9677.801	3		0.480409		
5	9.78883	Sum Squares Regression/residual	35.64699	0.01105		0.00048		
					mass %	0.233321		
					% Recovery	333.3164		
Zr								
Concentration (ppm)	Intensity				x-int	-59.9079		
1	457.321	Slope - Intercept	7.5158	450.2556		59.90787		
2	464.512	SD Slope - SD Intercept	0.560309	1.858336	ppm Osol=	1198.157		
3	475.469	R2 - SD Regression	0.9836	1.771854	mass (mg)	119.8157		
4	479.114	Fstat - Degrees Freedom	179.9262	3		161.8453		
5	487.599	Sum Squares Regression/residual	564.8725	9.418402		0.161845		
					mass %	78.60384		
					% Recovery	122.4359		
Hf								
Concentration (ppm)	Intensity				x-int	-1.45459		
1	0.877096	Slope - Intercept	0.354164	0.515164		1.454592		
2	1.22221	SD Slope - SD Intercept	0.003538	0.011733	ppm Osol=	29.09184		
3	1.56887	R2 - SD Regression	0.999701	0.011187	mass (mg)	2.909184		
4	1.92216	Fstat - Degrees Freedom	10022.78	3		3.430747		
5	2.29794	Sum Squares Regression/residual	1.25432	0.000375		0.003431		
					mass %	1.66622		

					% Recovery	127.1924		
Ti								
Concentration (ppm)	Intensity				x-int	-0.1097		
1	19.243	Slope - Intercept	17.29287	1.89711		0.109705		
2	36.2518	SD Slope - SD Intercept	0.077594	0.257349	ppm Osol=	2.194095		
3	54.093	R2 - SD Regression	0.99994	0.245373	mass (mg)	0.21941		
4	70.9151	Fstat - Degrees Freedom	49668.44	3		0.292729		
5	88.3757	Sum Squares Regression/residual	2990.434	0.180624		0.000293		
					mass %	0.142171		
					% Recovery	109.362		
Si								
Concentration (ppm)	Intensity				x-int	-29.0798		
1	10.0562	Slope - Intercept	0.3343	9.72138		29.07981		
2	10.3265	SD Slope - SD Intercept	0.022198	0.073621	ppm Osol=	581.5962		
3	10.7918	R2 - SD Regression	0.986946	0.070195	mass (mg)	58.15962		
4	11.1119	Fstat - Degrees Freedom	226.8085	3		91.29192		
5	11.335	Sum Squares Regression/residual	1.117565	0.014782		0.091292		
					mass %	44.33799		
					% Recovery	135.1768		

Table 8-18: Second modified standard addition 3

Al					**x-int**	**-0.85401**	**Mass (g)**	**0.2042**
Concentration (ppm)	Intensity					0.854009		
1	1.30419	Slope / Intercept	0.713304	0.609168	ppm Osol=	17.08018		
2	2.04322	SD Slope / SD Intercept	0.007967	0.026422	mass (mg)	1.708018		
3	2.76205	R2 / SD Regression	0.999626	0.025193		3.227269		
4	3.48724	Fstat / Degrees Freedom	8016.686	3		0.003227		
5	4.1487	Sum Squares Regression/Residual	5.088026	0.001904	mass %	1.580445		
					% Recovery	179.596		
Fe								
Concentration (ppm)	Intensity				x-int	-0.11909		
1	2.13961	Slope - Intercept	1.97746	0.235494		0.119089		
2	4.2448	SD Slope - SD Intercept	0.023321	0.077348	ppm Osol=	2.381783		
3	6.21314	R2 - SD Regression	0.999583	0.073748	mass (mg)	0.238178		
4	8.18502	Fstat - Degrees Freedom	7189.736	3		0.340538		
5	10.0568	Sum Squares Regression/residual	39.10348	0.016316		0.000341		
					mass %	0.166767		
					% Recovery	238.2384		

Zr								
Concentration (ppm)	Intensity				x-int	-51.9306		
1	461.362	Slope - Intercept	8.7188	452.7722		51.93056		
2	470.707	SD Slope - SD Intercept	0.740229	2.455062	ppm Osol=	1038.611		
3	476.872	R2 - SD Regression	0.978834	2.340809	mass (mg)	103.8611		
4	490.785	Fstat - Degrees Freedom	138.7335	3		140.294		
5	494.917	Sum Squares Regression/residual	760.1747	16.43817		0.140294		
					mass %	68.70423		
					% Recovery	107.0159		
Hf								
Concentration (ppm)	Intensity				x-int	-1.39515		
1	0.910574	Slope - Intercept	0.371132	0.517786		1.395153		
2	1.22797	SD Slope - SD Intercept	0.007662	0.025412	ppm Osol=	27.90306		
3	1.6404	R2 - SD Regression	0.998723	0.02423	mass (mg)	2.790306		
4	1.9935	Fstat - Degrees Freedom	2346.163	3		3.290557		
5	2.38347	Sum Squares Regression/residual	1.377391	0.001761		0.003291		
					mass %	1.611438		
					% Recovery	123.0106		

Table 8-19: Second modified standard addition 4

Al					**x-int**	**-0.82964**	**Mass (g)**	**0.2042**
Concentration (ppm)	Intensity					0.829636		
1	1.31157	Slope / Intercept	0.719976	0.597318	ppm Osol=	16.59272		
2	2.03863	SD Slope / SD Intercept	0.002202	0.007304	mass (mg)	1.659272		
3	2.76606	R2 / SD Regression	0.999972	0.006964		3.135164		
4	3.47841	Fstat / Degrees Freedom	106880.4	3		0.003135		
5	4.19156	Sum Squares Regression/Residual	5.183654	0.000145	mass %	1.53534		
					% Recovery	174.4705		
Fe								
Concentration (ppm)	Intensity				x-int	-0.11277		
1	2.15203	Slope - Intercept	1.928291	0.217449		0.112768		
2	4.07256	SD Slope - SD Intercept	0.002986	0.009904	ppm Osol=	2.255355		
3	5.99665	R2 - SD Regression	0.999993	0.009443	mass (mg)	0.225535		
4	7.92121	Fstat - Degrees Freedom	417004	3		0.322462		
5	9.86916	Sum Squares Regression/residual	37.18306	0.000268		0.000322		
					mass %	0.157915		

					% Recovery	225.5924		
Zr								
Concentration (ppm)	Intensity				x-int	-49.8807		
1	455.733	Slope - Intercept	8.9788	447.8688		49.8807		
2	467.796	SD Slope - SD Intercept	0.432559	1.434636	ppm Osol=	997.6139		
3	474.114	R2 - SD Regression	0.993085	1.367871	mass (mg)	99.76139		
4	483.716	Fstat - Degrees Freedom	430.8698	3		134.7562		
5	492.667	Sum Squares Regression/residual	806.1885	5.613216		0.134756		
					mass %	65.99225		
					% Recovery	102.7917		
Hf								
Concentration (ppm)	Intensity				x-int	-1.7573		
1	0.865901	Slope - Intercept	0.323819	0.569046		1.757297		
2	1.23625	SD Slope - SD Intercept	0.0176	0.058372	ppm Osol=	35.14594		
3	1.59871	R2 - SD Regression	0.991216	0.055656	mass (mg)	3.514594		
4	1.79706	Fstat - Degrees Freedom	338.5198	3		4.144697		
5	2.20459	Sum Squares Regression/residual	1.048586	0.009293		0.004145		
					mass %	2.029724		
					% Recovery	154.9408		
Ti								
Concentration (ppm)	Intensity				x-int	-0.11454		
1	19.1027	Slope - Intercept	17.29292	1.9807		0.114538		
2	36.8719	SD Slope - SD Intercept	0.096639	0.320515	ppm Osol=	2.290764		
3	53.6092	R2 - SD Regression	0.999906	0.305599	mass (mg)	0.229076		
4	71.4205	Fstat - Degrees Freedom	32020.87	3		0.305627		
5	88.293	Sum Squares Regression/residual	2990.451	0.280172		0.000306		
					mass %	0.14967		
					% Recovery	115.1309		
Si								
Concentration (ppm)	Intensity				x-int	-29.5726		
1	10.0093	Slope - Intercept	0.3288	9.72346		29.57257		
2	10.4399	SD Slope - SD Intercept	0.016807	0.055742	ppm Osol=	591.4513		
3	10.7326	R2 - SD Regression	0.992223	0.053148	mass (mg)	59.14513		
4	10.9885	Fstat - Degrees Freedom	382.7329	3		92.83887		
5	11.379	Sum Squares Regression/residual	1.081094	0.008474		0.092839		
					mass %	45.46467		
					% Recovery	138.6118		

Table 8-20: Second modified standard addition 5

Al					**x-int**	**-0.74381**	**Mass (g)**	**0.2014**
Concentration (ppm)	Intensity					0.743814		
1	1.24876	Slope / Intercept	0.725535	0.539663	ppm Osol=	14.87628		
2	1.99595	SD Slope / SD Intercept	0.007169	0.023777	mass (mg)	1.487628		
3	2.73082	R2 / SD Regression	0.999707	0.022671		2.810846		
4	3.4628	Fstat / Degrees Freedom	10241.85	3		0.002811		
5	4.14301	Sum Squares Regression/Residual	5.26401	0.001542	mass %	1.395653		
					% Recovery	158.597		
Fe								
Concentration (ppm)	Intensity				x-int	-0.09759		
1	2.07064	Slope - Intercept	1.952467	0.190537		0.097588		
2	4.11931	SD Slope - SD Intercept	0.028557	0.094714	ppm Osol=	1.951756		
3	6.12458	R2 - SD Regression	0.999359	0.090306	mass (mg)	0.195176		
4	8.06506	Fstat - Degrees Freedom	4674.445	3		0.279055		
5	9.8601	Sum Squares Regression/residual	38.12127	0.024466		0.000279		
					mass %	0.138557		
					% Recovery	197.9391		
Zr								
Concentration (ppm)	Intensity				x-int	-46.9314		
1	446.851	Slope - Intercept	9.3608	439.3158		46.93144		
2	459.964	SD Slope - SD Intercept	0.609086	2.02011	ppm Osol=	938.6287		
3	468.855	R2 - SD Regression	0.987458	1.926099	mass (mg)	93.86287		
4	475.368	Fstat - Degrees Freedom	236.1939	3		126.7886		
5	485.953	Sum Squares Regression/residual	876.2458	11.12957		0.126789		
					mass %	62.9536		
					% Recovery	98.05857		
Hf								
Concentration (ppm)	Intensity				x-int	-1.42916		
1	0.865131	Slope - Intercept	0.355452	0.507999		1.429164		
2	1.24658	SD Slope - SD Intercept	0.016936	0.056171	ppm Osol=	28.58327		
3	1.56526	R2 - SD Regression	0.993235	0.053557	mass (mg)	2.858327		
4	1.85824	Fstat - Degrees Freedom	440.4762	3		3.370773		
5	2.33656	Sum Squares Regression/residual	1.26346	0.008605		0.003371		
					mass %	1.673671		

					% Recovery	127.7611		

Table 8-21: Second modified standard addition 6

Al					**x-int**	**-0.74632**	**Mass (g)**	**0.2014**
Concentration (ppm)	Intensity					0.746325		
1	1.25235	Slope / Intercept	0.720063	0.537401	ppm Osol=	14.9265		
2	1.98226	SD Slope / SD Intercept	0.003982	0.013207	mass (mg)	1.49265		
3	2.70892	R2 / SD Regression	0.999908	0.012593		2.820335		
4	3.40125	Fstat / Degrees Freedom	32696.69	3		0.00282		
5	4.14317	Sum Squares Regression/Residual	5.184907	0.000476	mass %	1.400365		
					% Recovery	159.1324		
Fe								
Concentration (ppm)	Intensity				x-int	-0.08179		
1	2.06353	Slope - Intercept	1.917112	0.156794		0.081787		
2	3.99408	SD Slope - SD Intercept	0.011723	0.038881	ppm Osol=	1.635731		
3	5.94782	R2 - SD Regression	0.999888	0.037071	mass (mg)	0.163573		
4	7.77818	Fstat - Degrees Freedom	26743.57	3		0.23387		
5	9.75704	Sum Squares Regression/residual	36.75318	0.004123		0.000234		
					mass %	0.116122		
					% Recovery	165.8891		
Zr								
Concentration (ppm)	Intensity				x-int	-61.7743		
1	440.401	Slope - Intercept	7.0748	437.0406		61.77427		
2	452.387	SD Slope - SD Intercept	1.720572	5.706492	ppm Osol=	1235.485		
3	461.127	R2 - SD Regression	0.849304	5.440926	mass (mg)	123.5485		
4	470.883	Fstat - Degrees Freedom	16.90763	3		166.8875		
5	466.527	Sum Squares Regression/residual	500.528	88.81104		0.166887		
					mass %	82.8637		
					% Recovery	129.0712		
Hf								
Concentration (ppm)	Intensity				x-int	-1.59438		
1	0.837074	Slope - Intercept	0.333609	0.531901		1.594384		
2	1.21124	SD Slope - SD Intercept	0.015272	0.05065	ppm Osol=	31.88768		
3	1.5426	R2 - SD Regression	0.993753	0.048293	mass (mg)	3.188768		
4	1.92398	Fstat - Degrees Freedom	477.2021	3		3.760456		
5	2.14875	Sum Squares Regression/residual	1.112951	0.006997		0.00376		
					mass %	1.867158		

					% Recovery	142.5311		
Ti								
Concentration (ppm)	Intensity				x-int	-0.12644		
1	18.7651	Slope - Intercept	16.92948	2.14058		0.126441		
2	36.2066	SD Slope - SD Intercept	0.101517	0.336693	ppm Osol=	2.52882		
3	53.1257	R2 - SD Regression	0.999892	0.321025	mass (mg)	0.252882		
4	70.0638	Fstat - Degrees Freedom	27810.63	3		0.337387		
5	86.4839	Sum Squares Regression/residual	2866.073	0.30917		0.000337		
					mass %	0.167521		
					% Recovery	128.8623		
Si								
Concentration (ppm)	Intensity				x-int	-36.7622		
1	9.71653	Slope - Intercept	0.259234	9.530024		36.76225		
2	10.1005	SD Slope - SD Intercept	0.02219	0.073595	ppm Osol=	735.2449		
3	10.3673	R2 - SD Regression	0.978492	0.07017	mass (mg)	73.52449		
4	10.5827	Fstat - Degrees Freedom	136.4836	3		115.4098		
5	10.7716	Sum Squares Regression/residual	0.672023	0.014772		0.11541		
					mass %	57.30379		
					% Recovery	174.7067		

Table 8-22: Second modified standard addition 7

Al					**x-int**	**-0.77301**	**Mass (g)**	**0.2005**
Concentration (ppm)	Intensity					0.773009		
1	1.28766	Slope / Intercept	0.724268	0.559866	ppm Osol=	15.46019		
2	2.00416	SD Slope / SD Intercept	0.005135	0.017031	mass (mg)	1.546019		
3	2.72062	R2 / SD Regression	0.999849	0.016238		2.921175		
4	3.47966	Fstat / Degrees Freedom	19893.94	3		0.002921		
5	4.17125	Sum Squares Regression/Residual	5.245641	0.000791	mass %	1.456945		
					% Recovery	165.5619		
Fe								
Concentration (ppm)	Intensity				x-int	-0.10847		
1	2.23129	Slope - Intercept	2.024075	0.219547		0.108468		
2	4.25015	SD Slope - SD Intercept	0.016506	0.054746	ppm Osol=	2.169356		
3	6.30944	R2 - SD Regression	0.999801	0.052198	mass (mg)	0.216936		
4	8.38248	Fstat - Degrees Freedom	15036.55	3		0.310166		
5	10.2855	Sum Squares Regression/residual	40.9688	0.008174		0.00031		
					mass %	0.154696		
					% Recovery	220.9947		

Zr								
Concentration (ppm)	Intensity				x-int	-46.5379		
1	468.212	Slope - Intercept	9.882	459.8878		46.53792		
2	481.264	SD Slope - SD Intercept	0.673377	2.283534	ppm Osol=	930.7584		
4	500.81	R2 - SD Regression	0.990799	2.129407	mass (mg)	93.07584		
5	507.849	Fstat - Degrees Freedom	215.3637	2		125.7254		
		Sum Squares Regression/residual	976.5392	9.068745		0.125725		
					mass %	62.70596		
					% Recovery	97.67283		
Hf								
Concentration (ppm)	Intensity				x-int	-1.30272		
1	0.934826	Slope - Intercept	0.412055	0.536791		1.302717		
2	1.36669	SD Slope - SD Intercept	0.006791	0.022523	ppm Osol=	26.05434		
3	1.7804	R2 - SD Regression	0.999186	0.021475	mass (mg)	2.605434		
4	2.20883	Fstat - Degrees Freedom	3681.763	3		3.072541		
5	2.57403	Sum Squares Regression/residual	1.697892	0.001383		0.003073		
					mass %	1.532439		
					% Recovery	116.9801		
Ti								
Concentration (ppm)	Intensity				x-int	-0.11812		
1	20.4374	Slope - Intercept	18.37232	2.1702		0.118123		
2	38.9148	SD Slope - SD Intercept	0.089137	0.295635	ppm Osol=	2.362467		
3	57.3097	R2 - SD Regression	0.999929	0.281877	mass (mg)	0.236247		
4	76.035	Fstat - Degrees Freedom	42482.37	3		0.315193		
5	93.7389	Sum Squares Regression/residual	3375.421	0.238364		0.000315		
					mass %	0.157203		
					% Recovery	120.9258		
Si								
Concentration (ppm)	Intensity				x-int	-17.2912		
1	9.93198	Slope - Intercept	0.538254	9.307074		17.29123		
2	10.384	SD Slope - SD Intercept	0.046049	0.152728	ppm Osol=	345.8246		
3	10.7053	R2 - SD Regression	0.978514	0.14562	mass (mg)	34.58246		
4	11.5453	Fstat - Degrees Freedom	136.6249	3		54.28336		
5	12.0426	Sum Squares Regression/residual	2.897174	0.063616		0.054283		
					mass %	27.07399		
					% Recovery	82.54266		

8.5. ANALYTICAL LINES USED

Table 8-23: Table showing the three most important emission lines for each analysed element

Line order	Zr (nm)	Hf (nm)	Al (nm)	Fe (nm)	Si (nm)	Ti (nm)
1	343.823	277.336	396.153	259.94	251.612	334.941
2	339.198	273.876	394.403	239.562	212.415	336.121
3	349.621	264.141	167.079	238.204	288.16	337.28

8.6. RECOVERIES FOR FLUX VARIATION

Table 8-24: Table of recoveries when varying amounts of flux are added

Mass Flux	Zr (% recovery)	Hf (% recovery)	Al (% recovery)	Fe (% recovery)
0	120.63	115.38	112.72	114.25
0.1007	112.01	110.17	122.69	105.95
0.5046	104.62	104.73	126.89	96.36
1.0065	99.17	100.33	136.17	90.12
2.0005	90.97	90.68	147.48	82.88

8.7. SPECTRUM OF STANDARD ADDITION SAMPLE

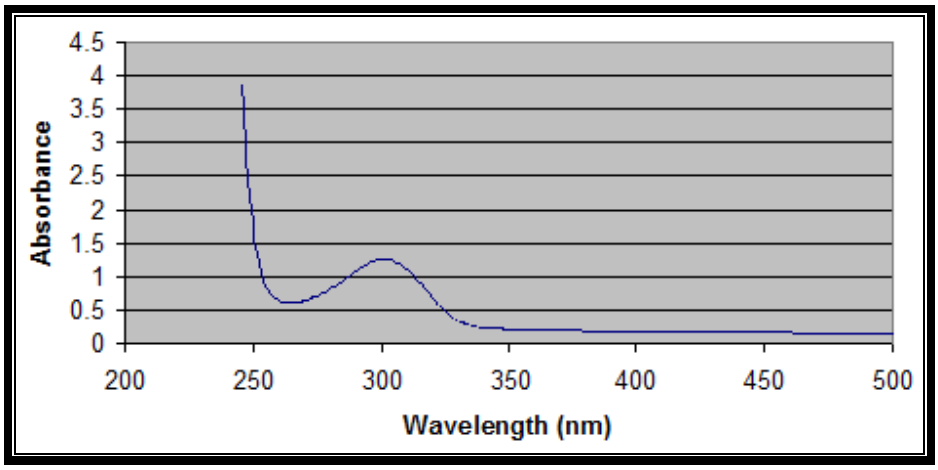

Figure 8-1: Spectrum of yellow coloured solution obtained in standard addition method – 5ml HNO_3, 10ppm Zr, Hf, Merck XVI multi-standard, 4X diluted, cell path length of 0.5cm, quartz cuvette

Bibliography

1. Gambogi , J., U.S. Geological Survey, Mineral Commodity Summaries, January 2008
2. Zircon: Zircon Mineral information and data, http://www.mindat.org/min-4421.html, accessed 21/04/2008
3. Chambers, I, The Dubbo Zirconia Project, June 2007
4. Markoff, J., http://www.nytimes.com, Intel says chips will run faster, use less power, January 7, 2007
5. http://chemistry.about.com/od/periodictableelements/ig/Element-Photo-Gallery.--98/Zirconium.htm accessed on 09/15/2008
6. Standard Specification for Zirconium and Zirconium Alloy Ingots for Nuclear Application, B350/B 350M, ASTM International, 2006
7. http://en.wikipedia.org/wiki/ Image:ZirconiumOutput.svg accessed on 16/05/2008
8. Blumenthal, W., B., The Chemical Behaviour of Zirconium, 1958
9. http://www.orleansjewels.com/cubic_zirconia_loose_stones.html accessed on 09/05/2008
10. Wilkinson, G., Gillard, R.D., McClevery, J.A., Comprehensive Coordination Chemistry, Volume 3, 1987, pp. 364-440
11. Cotton, F. A., Wilkinson, G., Advanced Inorganic Chemistry, 5th edition, 1988, pp. 776-787
12. Monnahela, O. S., Advanced Metals Initiative (AMI) Project Literature Survey, Delta-F Department (Necsa), 22-11-2006
13. McCleverty, J. A., meyer, T. J., Wedd, A. G., Comprehensive Coordination Chemistry II, Volume 4, 2004, pp. 105- 175

14. United States Patent 5176878

15. Mellor, J. W., A Comprehensive Treatise on Inorganic and Theoretical Chemistry, Volume VII, pp.106-109

16. The Economics of Zirconium, Roskill Information Services Ltd., ISBN 978 0 86214 538 5

17. Kaiser, A., Lobert, M., Telle, R., Thermal stability of zircon ($ZrSiO_4$), Journal of the European Ceramic Society, Volume 28, 2008, pp. 2199–2211

18. Xiaoguo Ma, Yibing Li, Determination of trace impurities in high-purity zirconium dioxide by inductively coupled plasma atomic emission spectrometry using microwave-assisted digestion and wavelet transform-based correction procedure, Analytica Chimica Acta, 579, 2006, 47–52

19. Nikitina, Z. A., Kuznetsova, N. M., Zharkova, I. P., Monakhova, N. G., Journal of Analytical Chemistry, Volume 50, No. 1, 1995, pp. 90-92

20. Dalawat, D. S., Chauhan, R. S., Goswami, A. K., Review of Spectrophotometric Methods for Determination of Zirconium, Reviews in Analytical Chemistry, Volume 24, No. 2, 2005, pp. 75-102

21. Kania, K., Buhl, F., Spectrophotometric Method for the Determination of Zirconium using 2,3,7-trihydroxyphenylfluorone and lauryldimethylammonium bromide, Chemia Analityczna, Volume 37, Issue 6, 1992, pp. 691-698

22. Lei, L., Xiao, G., *Kuangye Gongcheng*, 11(1), 63, 1991

23. Cheng, L., Luo, Q., Yu, X., Zeng, Y., *Huaxue Shiji*, 14(6), 325, 1992

24. Yang, H., Zhang, H., *Yejin Fenxi*, 13,(2), 26, 1993

25. Sun, J., Ma, J., Zhu, X., Yuan, R., Lihua, J., *Huaxue Fence*, 30(2), 95, 1994

26. Yin, J.J., Gansu, G., *Daxue Xuebao*, 23(4), 102, 1997

27. Hao, T., Hao., P., Tang, N., Liu, Z., *Yejin Fenxi*, 20(4), 44, 2000

28. Li, X., Jia, Z., Chen, Y., Lihua, J., *Huaxue Fence*, 37(9), 409, 2001

29. Yang, D., Lu, H., Liang, L., Zhang, Y., *Yejin Fenxi*, 16(5), 1, 1996

30. Li, X., Hung, Y.P., Zhang, H., *Fenxi Shiyanshi*, 12(6), 10, 1993

31. Okai, T., *Geostandards Newsletter*, Volume 15, No. 2, 1991, pp. 187-189

32. Nijhawan, M., Kakkar, L.R., *Chem. Anal. (Warsaw)*, 44(4), 711, 1999

33. Sharma, V., Nijhawan, M., Malik, A. K., Rao, A. L. J., 3-Hydroxy-2-(2'-thienyl)-4H-Chromon-4-one as a Spectro-photometric reagent for the Trace Determination of Zirconium in Aqueous Phase, Journal of Analytical Chemistry, Volume 56, No. 9, 2001, pp. 830-832

34. Jaganathan, J., Ewing, K. J., Buckley, E. A., Quantitative determination of Nickel and Copper in Zirconium Fluoride Using Graphite Furnace Atomic Absorption Spectroscopy, Microchemical Journal, Volume 41, 1990, pp. 106-112

35. Shariati, S., Yamini, Y., Cloud point extraction and simultaneous determination of zirconium and hafnium using ICP-OES, Journal of Colloid and Interface Science, 298, 2006, pp. 419–425

36. Boss, C. B., Fredeen, K. J., Concepts, Instrumentation and Techniques in Inductively Coupled Plasma Optical Emission Spectrometry, 2004

37. Skoog, D. A., Holler, F. J., Crouch, S. R., Fundamentals of Analytical Chemistry, 8th Edition, 2004, pp. 839-865

38. Xiaoguo Ma, Yibing Li, Determination of trace impurities in high-purity zirconium dioxide by inductively coupled plasma atomic emission spectrometry using microwave-assisted digestion and wavelet transform-based correction procedure, Analytica Chimica Acta, 579, 2006, 47–52

39. Skoog, D. A., Holler, F. J., Nieman, T. A., Principles of Instrumental Analysis 5th Edition, 1998. pp. 206-225

40. Skoog, D. A., Holler, F. J., Nieman, T. A., Principles of Instrumental Analysis 5th Edition, 1998, pp. 300-322

41. Skoog, D. A., Holler, F. J., Nieman, T. A., Principles of Instrumental Analysis 5th Edition, 1998. pp. 272-296

42. Jeffery, G.H., Bassett, J., Mendham, J., Denney, R.C., Vogel's Textbook of Quantitative Chemical Analysis 5th Edition,1991,pp. 112-113

43. Skoog, D. A., West, D, M., Holler, F. J., Crouch, S. R., Fundamentals of Analytical Chemistry, 8th Edition, 2004, pp. 1049-1051

44. Kingston, H. M., Jassie, L. B., Introduction to Microwave Sample Preparation Theory and Practice, 1988

45. http://en.wikipedia.org/wiki/Microwave retrieved on 15/05/2008

46. Arain, M. B., Kazi, T. G., Jamali, M. K., Speciation of heavy metals in sediment by conventional, ultrasound and microwave assisted single extraction methods: A comparison with modified sequential extraction procedure, Journal of Hazardous Materials, 154, 2008, pp. 998–1006

47. http://www.fap.pdx.edu/safety/hydrofluoric_acid/ accessed on 19/05/2008

48. Skoog, D. A., West, D, M., Holler, F. J., Crouch, S. R., Fundamentals of Analytical Chemistry, 8th Edition, 2004, p 1044

49. Winge, R. K., Fassel, V. A., Peterson, V. J., Floyd, M. A., Inductively Coupled Plasma-Atomic Emission Spectroscopy – An Atlas of Spectral Information, 6th Impression, 1993

50. Chan, C. C., Lee, Y. C., Zhang, X-M, Analytical Method Validation and Instrument Performance Verification, Wiley-Interscience, 2004

51. Afanasev Y. A., Ryabinin A. I., Eremin V. P., Synthesis and Investigation of zirconium tetraborate, Doklady AkademiiI NAUK SSSR, Volume 215, 1974, pp. 97-100

52. United States Patent 3804649

53. Latastea, E., Erauwb, J. P., Olagnona, C., Fantozzia, G., Microstructural and mechanical consequences of thermal cycles on a high zirconia fuse-cast refractory, Journal of the European Ceramic Society, 2008, pp. 1-8

54. Opeka, M. M., Talmy, I. G., Wuchina, E. J., Mechanical, Thermal, and Oxidation Properties of Refractory Hafnium and Zirconium Compounds, Journal of the European Ceramic Society, 19, 1999, pp. 2405-2414

55. Skoog, D. A., West, D. M., Holler, F. J., Crouch, S. R., Fundamentals of Analytical Chemistry, 8th Edition, 2004, pp. 196-197